Electronic Supplementary Material (ESI) for Chemical Science.

Electronic Supplementary Information

Heterologous biosynthesis of elsinochrome A sheds light on the formation of the photosensitive perylenequinone system

Jinyu Hu,[a] Farzaneh Sarrami,[a] Hang Li,[a] Guozhi Zhang,[a,b] Keith A. Stubbs,[a] Ernest Lacey,[c,d] Scott G. Stewart,[a] Amir Karton,[a] Andrew M. Piggott,[d] Yit-Heng Chooi [a]*

[a]School of Molecular Sciences, University of Western Australia, Perth, WA 6009, Australia.

[b]Research School of Biology, Australian National University, Canberra, ACT, Australia.

[c]Microbial Screening Technologies, Smithfield, NSW 2109, Australia.

[d]Department of Molecular Sciences, Macquarie University, Sydney, NSW 2109, Australia.

Corresponding Author: Yit-Heng Chooi,

Email: yitheng.chooi@uwa.edu.au.

Table of Contents

Experimental procedures section

Strains and culture conditions

The wild-type *P. nodorum* strain SN15 was from the Department of Agriculture and Food Western Australia (DAFWA). The *A. nidulans* LO7890 (a gift from Prof. Berl Oakley, University of Kansas) was used as the heterologous host for expression experiments in this work. The characteristics of *A. nidulans* LO7890 was as described previously.[1,2] *Saccharomyces cerevisiae* strain BJ5464 was used for yeast-mediated homologous recombination and targeted disruption of *elcE*.

Defined minimal medium (30 g Sucrose, 2g $NaNO_3$,1g K_2HPO_4, 0.5 g KCl, 0.5 g $MgSO_4{\cdot}7H_2O$, 0.01 g $ZnSO_4{\cdot}7H_2O$, 0.01 g $FeSO_4{\cdot}7H_2O$, 2.5 mg $CuSO_4{\cdot}5H_2O$ in 1 L, adjusted to pH 6) was used for culturing purpose of *P. nodorum*. The standard growth condition for *P. nodorum* strains was at 20 °C under a 12h dark/near-UV light regime. Glucose minimal medium (GMM, 10 g Glucose, 6g $NaNO_3$, 1.52 g K_2HPO_4, 0.52 g KCl, 0.52 g $MgSO_4{\cdot}7H_2O$, 22 mg $ZnSO_4{\cdot}7H_2O$, 11 mg H_3BO_3, 5 mg $MnCl_2{\cdot}4H2O$, 1.6 mg $FeSO_4{\cdot}7H2O$, 1.6 mg $CoCl_2{\cdot}5H_2O$, 1.6 mg $CuSO_4{\cdot}5H_2O$, 1.1 mg $(NH_4)_6Mo_7O_{24}{\cdot}4H_2O$, 50 mg Na_4EDTA in 1L, adjusted to pH 6.5) was used for culturing of *A. nidulans*. Uracil/Uridine, riboflavin and pyridoxine with suggested concentration are supplemented if necessary. In terms of *A. nidulans* protoplast transformation, Stabilised minimal medium (SMM, GMM supplemented with 1.2 M sorbitol) was used.

For small-scale metabolic profile analysis, spores with a concentration of ~10^8/L were inoculated into 50ml GMM media. Cultures were grown at 37°C/180rpm for 18h. 2.5ml/L of cyclopentanone was added to induce the expression of P_{alc} promoters.[3] Cultures were incubated at 25 °C/180rpm for another 4 days for the accumulation of secondary metabolites. For each combination, three separate transformants were peaked as replicates. For isolation of target compounds, scaled-up cultures were performed under the same conditions. For **12** and **13**, a longer induction period (5 days induction at 25 °C/180rpm plus an extra 3-days stationary culture) was performed.

Bioinformatics

Primer design and sequence analysis were performed using Geneious version 8.1 (http://www.geneious.com).[4] Conserved Domain identification and protein similarity comparison were performed on NCBI (National Center for Biotechnology Information) website. SignalP 4.1 was used for prediction of signal peptides. Phyre2 was used to predict protein modelling.[5] Sequences of *Cz_CTB11* and *Cz_CTB12* was acquired from orcAE (http://bioinformatics.psb.ugent.be/orcae).

YFACs construction and *A. nidulans* transformation

Yeast fungal artificial chromosomes (YFACs) used in this work were derived from pYFAC (renamed as pYFAC1 in this work)[2] or pKW20088 (a gift from Prof Kenji Watanabe, University of Shizuoka).[6] Yeast homologous recombination was used for the construction of YFACs in this work. Yeast miniprep of corrected transformants was performed with Zymoprep™ Yeast Plasmid Miniprep I Kit. 1 ul from the miniprep was used for *E. coli* NEB10-beta® electroporation. Samples with correct digestion pattern were used for *A. nidulans* transformation

pYFAC-*riboB* was modified from pKW-20088. pKW-20088 was first digested with *Not*I and *Msc*I to release *pyrG* coding region. The 2.4 kb fragment containing *riboB* open reading frame (ORF) flanked by its own promoter and terminator region was amplified from *Aspergillus fumigatus*

genomic DNA and cloned into *Not*I/*Msc*I digested pKW-20088. pYFAC-*pyroA* was constructed in a similar way. pYFAC-CH5 was constructed by cloning $P_{alcS/M}$ directly into *Not*I site of pYFAC-*riboB*. For the construction of pYFAC-CH3 and pYFAC-CH4, bi-directional *alcS/M* promoter region ($P_{alcS/M}$), *aldA* promoter region (P_{aldA}), two terminator regions (T1 and T2) were amplified from *A. nidulans* genomic DNA and cloned into *Pac*I digested pYFAC-CH1. The P_{alcA}-T1-$P_{alcS/M}$-T2-P_{aldA} expression cassette was then amplified with pKW-F as the forward primer and either ribo-P_{aldA}-R or pyro-P_{aldA}-R as reverse primer. Fragments with corresponding homologue arms were cloned into *Not*I site of pYFAC-*riboB* and pYFAC-*pyroA*, resulted in pYFAC-CH-3 and pYFAC-CH4, respectively. Genes from *elc* cluster were amplified with primers specified in Table S1 and introduced under control of a specific promoter, resulted in pYFAC-CH10-26.

For the construction of pYFAC-CH6, the 27-kb fragment containing *elcR-elcG* was amplified as four fragments and assembled into pYFAC-CH1. The direction of elc-fragment1 was inverted during yeast homologous recombination in order to put *elcR* under control of P_{alcA}. Elc-gBlock1-3 were used as homology arms for ease of construction. pYFAC-CH7 was constructed in a similar way.

For the construction of pYFAC-CH27, the 2.4-kb fragment covering *elcH* and its promoter and terminator region was amplified and cloned into *Sma*I site of pYFAC-CH1. *elc* cluster was then cloned into the resulting YFAC in a similar way as that of pYFAC-CH6. For the construction of pYFAC-CH-28, *elcB* was first cloned into pBG under control of $P_{gpdA.}$ The $P_{gpdA.}$-*elcB*-T*trpC* fragment was then amplified and cloned into *Asc*I site of pYFAC-CH21 together with *elcE.* The 27-kb fragment containing *elcR-elcG* was amplified as 4 fragments and assembled into pYFAC-CH1 by yeast homologous recombination, gBlocks were synthesized as homology arms (Table S2). pYFAC-*ribo* and pYFAC-*pyroA* were modified from pKW-20088 by replacing *pyrG* with *riboB* and *pyroA*, respectively. Alcohol-inducible promoter regions P_{alcA}, $P_{alcS/M}$, P_{aldA} and two terminator regions (*T1* and *T2*) were amplified from *A. nidulan*s genomic DNA and cloned into pYFAC-*riboB* and pYFAC-*pyroA*, resulted in pYFAC-CH3 and pYFAC-CH4, respectively (Figure S1).

Protoplast preparation and polyethylene glycol transformation of *A nidulans* LO7890 was done as described previously.[7]

CRISPR-Cas9 mediated disruption of *elcE*

Targeted disruption of *elcE* was performed in *S. cerevisiae*. sgRNA-frag1-F/ElcE-sgRNA-R and ElcE-sgRNA-F/sgRNA-frag2-R were used to amplify the sgRNA expression cassette from p426-SNR52p-gRNA.CAN1.Y-SUP4t (Addgene plasmid #43803[8], yeast single-guide RNA (sgRNA) expression plasmid). The protospacer sequence for targeting of *elcE* was designed in the overlapping region of ElcE-sgRNA -F/R. Geneticin antibiotic marker *apt1* was amplified from pINT1-HIS3NB with primer pair kanMX-F/R and assembled with *elcE*-targeted sgRNA expression cassette via yeast homologous recombination, resulted in pCH-1. Transformants were selected with Geneticine resistance.

kan marker offering kanamycin resistance was amplified from pET-28(a), *leu2* offering leucine auxotrophic completion in *S. cerevisiae* BJ5464-NpgA was amplified from pBG-CA-ADH2-leu2. The two selective markers were fused together by fusion PCR before transformation.

For targeted disruption of *elcE*, pYFAC-CH6 and p414-TEF1p-Cas9-CYC1t (Addgene plasmid #43802,[8] Yeast Cas9 expression plasmid) were first introduced into *S. cerevisiae* to allow replication of pYFAC-CH6 as well as expression of Cas9. Linearized pCH-1 and *kan-leu2* insertion marker were then co-transformed into the strain containing pYFAC-CH6 and p414-TEF1p-Cas9-CYC1t.

Transformants were selected for both Uracil and leucine auxotrophy. Constructs with correct digestion pattern were sent out for Sanger sequencing.

Metabolic profile analysis of *A. nidulans* strains

Extracts from both mycelium and media were analysed. Mycelium was collected by filtration and extracted with acetone. Media was extracted with either ethyl acetate/methanol/acetic acid (89:10:1) or a modified QuEChERS method. For QuEChERS extraction, 10 ml media was first mixed with equal volume of acetonitrile (w/ 0.1% acetic acid). 4g of MgSO4 anhydrous plus 1g of NaCl was then added. The mixture was gently mixed for 1 min and then centrifuged. The top acetonitrile layer was collected. Crude extracts were dried down and redissolved in methanol for LC-DAD-MS analysis. Standards of **1**-**3** were acquired from Microbial Screening Technologies (BioAustralis) and **6** was from Abcam.

LC-DAD-MS analysis was performed with Agilent 1260 liquid chromatography (LC) system coupled to a diode array detector (DAD) and an Agilent 6130 quadrupole mass spectrum (MS) with an ESI source. For analytical purpose, a Kinetex C18 column (2.6 µm, 2.1 mm i.d. x 100 mm; Phenomenex) was used. The mobile phase gradient of eluent B (acetonitrile with 0.1% formic acid) started at 5% and gradually increased to 95% over 10 mins at a flow rate of 0.75 ml/min.

Compound isolation and structure characterisation.

Diaion® HP-20 from Sigma was used for extraction of **13**, **14** and **16**. Dried Diaion® HP-20 was equilibrated with MQ water and then loaded into a funnel to form a column. The medium was separated from mycelium and directly go through the column. The column was flushed with MQ water and then eluted with methanol. Coloured fraction (purple for **13** and **14**, red for **16**) was collected and evaporated with Heidolph® evaporator.

Ethyl acetate/methanol/acetic acid (89:10:1) extraction method was used for isolation of **8** from the medium. **12**/**6** and **19**/**20** were extracted with acetone from mycelium.

Crude extracts from scaled-up cultures were first loaded on a Sephadex LH-20 (GE Healthcare®) column and eluted with methanol. Fractions containing the target compounds were combined and further purified by HPLC Semiprep. An Agilent C18 Preparative Cartridge (5 µm, 21.2 mm i.d. x 150 mm; Agilent) was used at a flow rate of 5 $mlmin^{-1}$, with the mobile phase eluent B set as isocratic at a specific percentage, according to the property of different target compounds

1 was isolated from 20L of *A. nidulans* pYFAC-CH26 culture as bright red pigment, with a titre of 0.075 mg/L. **12** and **6** were isolated from 30 L of *A. nidulans* pYFAC-CH10/28 culture as deep red pigments, with a titre of 0.01 mg/L and 0.003 mg/L. **13** was isolated from 30 L of *A. nidulans* pYFAC-CH10/13 culture as a deep-purple water-soluble pigment, with a titre of 0.3 mg/L. **14** was isolated from 30 L of *A. nidulans* pYFAC-CH10/29 culture as a deep-purple pigment, with a titre of 0.2 mg/L. **16** was isolated from 30 L of *A. nidulans* pYFAC-CH10/13/16 culture as a deep-red water-soluble pigment, with a titre of 1 mg/L. **19** and **20** were isolated from 30 L of *A. nidulans* pYFAC-CH10/24/25 culture as purple-red pigments, with a titre of 0.003 mg/L.

For structural characterisation, nuclear magnetic resonance (NMR) spectra were collected on Bruker Avance IIIHD 500MHz/600MHz NMR spectrometer. chloroform-*d*, DMSO-d_6, deuterium oxide and were used as solvents. Electronic circular dichroism (ECD) spectra were recorded on a JASCO J-810 spectropolarimeter, with acetonitrile as solvent. High-resolution mass spectra were acquired on Thermo Orbitrap Fusion™ Tribrid™ Mass Spectrometer.

Theoretical calculation of NMR shielding tensors to support structure elucidation

Structures were initially subjected to a LowModeMD conformational search using the Molecular Operating Environment 2016.08 package. The lowest energy geometry for each molecule was further optimized at the B3LYP-D3/def-TZVP level of theory using the Turbomole 7.1 package[9] NMR shielding tensors for each carbon atom were calculated at the B3LYP/def-TZVP level of theory using the gauge-including atomic orbital (GIAO) method and were plotted against the corresponding experimentally-determined ^{13}C NMR chemical shifts. The resulting data were analyzed by linear regression to determine the residuals for each nucleus and the overall goodness of fit.

Theoretical calculation for the formation of (*P*) hypocrellins

The geometries of all structures were optimized at the B3LYP-D3/6-31G(2df,p) level of theory[10-12] using the Gaussian 09 program package.[13] Empirical D3 dispersion corrections were included using the Becke–Johnson[14] damping potential as recommended in ref. 15[15] (denoted by the suffix-D3). Double-hybrid density functional theory (DHDFT) calculations[16] were performed in order to obtain accurate electronic energies for the equilibrium and transition structures located along the uncatalysed and catalysed reaction pathways considered in the present work. DHDFT has been found to produce thermochemical properties (such as reaction energies and barrier heights) with mean absolute deviations (MADs) approaching the threshold of 'chemical accuracy' (arbitrarily defined as 1 kcal mol^{-1} ≈ 4.2 kJ mol^{-1}) from a wide range of accurate thermochemical determinations.[16-23] In the present work, we used the spin-component-scaled DSD-PBEP86-D3 DHDFT functional of Kozuch and Martin[17, 18] in conjunction with the Def2-TZVPP basis set of Weigend and Ahlrichs.[24] These single-point energy calculations were carried out on top of the B3LYP-D3/6-31G(2df,p) optimised geometries. The DSD-PBEP86-D3 electronic energies were converted to Gibbs-free energies at 298K (ΔG_{298}) using zero-point vibrational energy, thermal, and entropic corrections obtained at the B3LYP-D3/6-31G(2df,p) level of theory. Corrections for bulk solvent effects in aqueous solution were added to the gas-phase ΔG_{298} values using the SMD model at the M05-2X/6-31G(d) level of theory[25] as recommended by Marenich, Cramer, and Truhlar.[26]

Supplementary Tables

Table S1. List of primers used in this work.

Primer name	Sequence (5'-3')	Discription
P_{alcA}-T1-F	ATTAGAACTCTTCCAATCCTATCACCTCGCCTTAATTAAGCGGAACAAATTGAAGCGAGT	Amplify T1, with homologue arm to P_{alcA}
T1-R	CCTGAATACGGCCTGAAT	
T1-P_{alcSM}-F	AAGGTCTACAATCAATTCAGGCCGTATTCAGGGCGGCCGCTTCTGCTGTTTCTGGGCTCA	Amplify $P_{alcS/M}$ with homologue arm to T1 and T2
T2-P_{alcSM}-R	TTCGATCTCAACTAAATTATCTCCTCCCGCGATCGCTCTGCTGGAGATATATGGTTTAAT	
T2-F	GGGAGGAGATAATTTAGTTGAGATCGA	Amplify *T2,* with homologue arm to P_{aldA}
P_{aldA}-T2-R	CTCTCCCAAGATACCCATATTTCCCGCTCACCGGCGCGCCTCGTTCCCAGAAGTAAGTAG	
P_{aldA}-F	GGTGAGCGGGAAATATGGGT	Amplify P_{aldA} for construction of pYFAC-CH3
ribo-P_{aldA}-R	ACACAGTGGAGGACATACCCGTAATTTTCTGGGCTTAATTGATCTTCTCATCACGCCTCT	
pyrO-P_{aldA}-R	TAGGAGTGATGAGACCCAACAACCATGATACCAGGGGGCTGATCTTCTCATCACGCCTCT	For construction of pYFAC-CH4
pKW-F	CACTGAGAACCATGGCACCGAAG	
elcClus-frag1-F	ATGGCTACACAATTGCCTTCTC	Amplify *elc* cluster fragment 1
elcClus-frag1-R	ACAAAAGATGATGCCGTTGCA	
elcClus-frag2-F	CAGGGCTCATGTGCTGTCG	Amplify *elc* cluster fragment 2
elcClus-frag2-R	CGCCGATGGAACGAGGTCT	
elcClus-frag3-F	GGAGTCATTACAGTCTTGCCGT	Amplify *elc* cluster fragment 3
elcClus-frag3-R	GTGCCCTCTAGAGTGGTACG	

elcClus-frag4-F	GCCAGCCTATGCTTGGGATC	Amplify *elc* cluster fragment 4 for construction of pYFAC-CH6
elcClus-frag4-R	GAAAGATTGAGGCAATCTTGGTGA	
elcClusT-frag4-R	GTTGCGATAACATGTGTGTAATGC	For construction of pYFAC-CH7
sgRNA-frag1-F	TCTAAAACTGCGCTCGAGAATCTCATCGGATCATTTATCTTTCACTGCGG	Synthesis of sgRNA for disruption of *elcE*
ElcE-sgRNA-R	TAGATCAGTTAGAAAGCTTGCGGCCGCCTCGTGATACGCCTATTTTTAT	
ElcE-sgRNA-F	AATGATCCGATGAGATTCTCGAGCGCAGTTTTAGAGCTAGAAATAGCAA	Synthesis of sgRNA for disruption of *elcE*
sgRNA-frag2-R	GATGCTCGATGAGTTTTTCTAAGCGGCCGCGTAAATGCATGTATACTAAACTCAC	
KanMX-F	GCATTTACGCGGCCGCTTAGAAAAACTCATCGAGCA	Amplify *apt1* marker from pINT1-HIS3NB
KanMX-R	ATCACGAGGCGGCCGCAAGCTTTCTAACTGATCTATCCA	
ElcE-leu-F	TTAATGAAGTGGGCGTATTTGTCATAAGGTACGGCGGATTTTCTTAACTTCTTCGGCGA	Amplify *elcE*-targeted *kan-leu* insertion marker
ElcE-kan-R	AGACTTTCCACCCAATCAGCACGCGTAAAGACCACTTTTGCCGATTTCGGCCTAT	
kan-F	GTATCTCAGTTCGGTGTAGGTC	Amplify *kan* marker
kan-Leu-R	CGACCTACACCGAACTGAGATACTAACCATTATTTTTTTCCTCAACATAAC	*kan-leu* fusion PCR
pKW-P_{alcSM}-F	ACCTCGCGGGTGTTCTTGACGATGGCATCCTGCGGCCGCTTCTGCTGTTTCTGGGCTCA	Amplify $P_{alcS/M}$ for construction of pYFAC-CH5
ribo-P_{alcSM}-R	TGCTAAAGGGTATCATCGAAAGGGAGTCATCCAGCGATCGCTTTGTAGAAGACACGACTT	
P_{alcSM}-ElcB-F	GATATAGGAACGATCGGCCATGAAGTCGTGTCTTCTACAAAATGGCAGCTTCAACAGGCC	Cloning *elcB* under control of P_{alcM}
ribo-ElcB-R	CTTCTGCTAAAGGGTATCATCGAAAGGGAGTCATCCAGCCTAGAGCTCGGCAACATCAAG	
ribo-ElcBMO-R	ACTTCTGCTAAAGGGTATCATCGAAAGGGAGTCATCCAGCGGCCGCCTTCAAGTCCGTGG	Cloning of *elcB*MO
P_{alcSM}-ElcE-F	CTTTGAGATACCAAAGCATTGAGCCCAGAAACAGCAGAAATGTTCATCCAGCGATTGAGG	Cloning *elcE* under control of P_{alcS}
pKW-ElcE-R	AGTAACCTCGCGGGTGTTCTTGACGATGGCATCCTGCTGGATCTATGTTACGGGAAATGA	

T1-ElcD-F	AGTCTAAAGGTCTACAATCAATTCAGGCCGTATTCAGGGCTTATGCTTCGTCCACGTTCG	Cloning *elcD* under control of P_{alcS}
P_{alcSM}-ElcD-R	TCCTTTGAGATACCAAAGCATTGAGCCCAGAAACAGCAGAAATGTCTCTTCTACAGTTGA	
P_{alcSM}-ElcF-F	GGAACGATCGGCCATGAAGTCGTGTCTTCTACAAAGCGATATGAAACTCTTCACACTCCT	Cloning *elcF* under control of P_{alcM}
T2_ElcF-R	AGCCAACTTCGATCTCAACTAAATTATCTCCTCCCGCGATTCATCTCAAAGGCTTCTGGG	
P_{alcA}-ElcG-F	TTAATTAGAACTCTTCCAATCCTATCACCTCGCCTTAAAATGGCCTGCAACATTCTCAAC	Cloning *elcG* under control of P_{alcA}
T1-ElcG-R	TCGCGCTCCACGGGGACTCGCTTCAATTTGTTCCGCTTAATCTACACCGGCGCTTCGAAA	
P_{alcA}-ElcH-F	TTAATTAGAACTCTTCCAATCCTATCACCTCGCCTTAATATGTTCACACTACGTTCCTTG	Cloning *elcH* under control of P_{alcA}
T1-ElcH-R	CGCGCTCCACGGGGACTCGCTTCAATTTGTTCCGCTTAATTGAATGTCCTGTCCCACGAT	
P_{aldA}-SN_8592-F	TCTCCTCTCCCAAGATACCCATATTTCCCGCTCACCGGATGCGATTGAACTCAGAAAATC	Cloning *SNOG_08592* under control of P_{aldA}
T2-SN_8592-R	TTAGGGAGCGGCGGATGCCTACTTACTTCTGGGAACGAGGAGTGCGAAGTTACTGCTATG	
T2-P_{gpdA}-F	TAGGGAGCGGCGGATGCCTACTTACTTCTGGGAACGAGGCATGCGGAGAGACGGACGGTC	Amplify P_{gpdA}-*elcB*-*TtrpC* fragment
T_{trpC}-R	TCATAAATAACGTCATGCATTGC	
P_{gpdA}-ElcB-F	ATCTTCAGTATATTCATCTTCCCATCCAAGAACCTTTAATAATGGCAGCTTCAACAGGCC	Cloning *elcB* under control of P_{gpdA}, for construction of pYFAC-CH-28
T_{trpC}-ElcB-R	ACGAGTGATCCTCTAGAGTCGAGGTCGACGGTATCGATACTAGAGCTCGGCAACATCAAG	
P_{aldA}-ElcE-F	CTCTCCTCTCCCAAGATACCCATATTTCCCGCTCACCGGATGTTCATCCAGCGATTGAGG	Cloning *elcE* under control of P_{aldA}, for construction of pYFAC-CH-28
T_{trpC}-ElcE-R	GTTTACCTCTTCCAGATACAGCTCATCTGCAATGCATTGGATCTATGTTACGGGAAATGA	
CEN/ARS-ElcH-F	CGAGGCGCGTGTAAGTTACGAATTCGAGCTCGGTACCCGTCTAAAAAGACGGACCAGAAA	Cloning of fragment covering *elcH* with its promoter and terminator, for construction of pYFAC-CH-27
URA3-ElcH-R	TAACTTCGTATAGCATACATTATACGAAGTTATCCCTCCAATTTCCTCTACCCATGATG	

Table S2. List of gBlocks used in this work.

Elc-gBlock1	ACCCCCAAGGTTCTCAGTCTCACCAACATCATCAACCAACAATCAACAGTTCTCTACTCAGTTAATTAGAACTCTTC CAATCCTATCACCTCGCCTTAATATGGCTACACAATTGCCTTCTCCTACTGCAACAACCTCACACAGCGGCAACGAG CCACGGCGCGTCATCCGTGAATCGTGTAACAACTGCAGTGCGCAAG
Elc-gBlock2	TTCACGGGATTTCCAAGACTTTCGTGTCGGCGTAAAATGATTACGTCTTGCCTGACATTATCCACAACGGTTACCGA TTTGCAACGGCATCATCTTTTGTCAGGGCTCATGTGCTGTCGCTTCATTAGGCATATGTCGTAGGCTCTCGCGTCAG CATTCGGGCTAGGCCGTGTCCAGACTTGTGATCAGTCCAGAACTAT
Elc-gBlock3	GTACAATTCAAAAATACTTTCTTCTCTCATAAGGAAACGAGCCCAGGACGCAACTTCCGATGAACTCACCATCAAC TCACCAAGATTGCCTCAATCTTTCATTAAGCCCAGAAAATTACGGGTATGTCCTCCACTGTGTTGAAGTCAGAAAA ACAATCGATAATTTGAAGCTCATTAAAATGCCAGTTCCGTCGTCGCCG
Elc-gBlock4	ATCTCGCTGGTGGGATGGGCGTTGTGATCTTAGATGGTGTTGATGAGTGGCCAGAGTTGCCGGAGGCGTATGCA GAATGGAATGGTTTCGAAGCGCCGGTGCATCACCATCACCACCATCACTAGTATTTGTACATCAGTGAATTGCAGA TTTGGAGGCGGTTCGGTCGCAGCCTAATAGTTCGCTTGTCGTCCGAACTCAAAGTCCTGAATGTCCAGGAGCTAT GAA
CTB5-gBlock	TTTAGTCTAAAGGTCTACAATCAATTCAGGCCGTATTCAGGGCTCAAATCTGCGGCAACTTGAAGCCACCCGGCAC CTGCTTCTGGAAAACCTGTAGGGGATCATACTTCTTGCTCGTAGCAACCAGCTCCTCAATCGTGCTCTTGCTTCTGT AATCAAAGGGGCTCTGCCAGCTGTCTGCATAGGTAGGTTGGATGAAATGCCTGTAGATACCCAGCTCTTTGGCCTT AGTGTTGGCAGCATGGAACAAGTCCTGGACGCTCTTGGTGATAGCATCGTCGAATTGGGCCTCGGACTCATCGTA GCTGACAGCCCAGTGTACGAAGACGACGTTGCCTTCAGTTTGAATTGGGCCCAAAGAGTCAACTGCTCCATTACG TTCCAGCTGAACGGTTGGTGCGGGTTGGTAGTTGAGGATGAGCTTGAAGCCTGGCAGTTTCACGTATTGTTGCAT GGCGTCGTTGGCCATTTGGAAGAATGTCTCCATGAAGTCTGCATCGGGAGCGAAGCTGATGCAGGCGAATTGCC ACCGTTGAGGGTATAAAGTGTTTGCTGCGTACTCGCGAGAGAACGAGGTGACGTTGTCCACTCGAAGAGTGTCTT CAGGCAGTCCAGGGAAAATTGGGGTTCGTTCAGTCTTGAGGAACGGCTTGAATACTTCTGGCTCTGCCACTGGC GGGTCGCTCTTGGTGTACTGGATGCTATTGCCGATGAACCAATGACCTCCGTTTGCCAAGACCAGAGTATTGATGT AGTGGGCGTATGGATCGTAGGGATGCGCTGAGGCAAGTTTTGCGTGATTCTTGAAGTGTTCTTGGCGGGTCTCGA TAGAGTGGAATGTTTGACCGCCCCAGAAGGGGCCTTGTTCGAACGCCTTCAAAGTAACAGCGGTGACGATGCCA AAGTTGTTGATTCCACCTCGCAGCGCTTTCCAGAGATCGGCATTTTCGTTTGCGTTGGCATTGACGATATCACCGG TGGCGAGAACGACTTCCCAATTCTCTACCATGTCGCAAATGTATCCATAGCGAGGGGAGAAATATGAGACTCCGCA GCTCGTCGATGCTCCTCCGACACCAATACCGGCGACTTTGGTTCCAAGTGTGCTTCGGTTGTGAGCATCGAGAAC TTCGTATACCAAATCCCATGTCGTACTGGGCGACACTGTGATGGTCTCGTAGTCAGGCGAAATGCCCGCGGACGGC ATGTGCAGGAGATCGAGCACAATCCCGTTGTCGGTGCTTGCGGCTCCTTTGAAGGGTGTATGACCACCACCTCGT ACGCCGAATTGGCATTGCCCTTCCCATTTGTGAGCGCCAAGGGACAGCGTTCGCACTGCTTTCGAGACCTCTTCT GCTGATCGTGGAAGTGCTATACAACTGGGATGAAGGTCGCTGTTCTTCAAGCTGAAGTATGAGCCCATGGATTGG GAGTAGGCCGCATCATATGGGAACACCACTGAGTTCTTGCCCAGGCTTTTGATCAAGGCATCGCAACAAGATTTT GACGCCGCCACTGAAGCCCATGCACTGCTGTCTGACCCATGTTGATATGAGCCTACACCACTGACGATGCTGGATA TCGTAGGAACATTGGAGAGGACCTGCTGTAAATTAAGCCCCAACATGCTTCTGCTGTTTCTGGGCTCAATGCTTTG GTATCTCAAAGGAGAGGAGA
Cz_CTB12-gBlock	TACTCAGTTAATTAGAACTCTTCCAATCCTATCACCTCGCCTTAATATGAGGCCTGTTCGATACTTCCCCTTGGCACTA AGCCTACTGCTCCAATGCGTCGTTCCGACCGTGGGTCGTCCTTCAGGATGCGTGGACGATGTCGAAGATGGTCAC CAAAAGGAAACGCAAGGATCGCCAGCTTCTGTGCTTCGCTTCGAAATCGAACTGACAACACAGTCGATCGACGC AGCTGGAATAGGCTCGCGGGAAGCGATATTCATCAACGACGCCTTCATCGGACCTACCCTCCACGCCAGACAAGG CGATAGAATCGAATTCGTCGTTCACAATTACATGAATCAAGACACGAGCATTCACTTCCACGGCATCGACCAGCGA TCGACGCCGTGGTCGGACGGAGTACCAGGTTTGACCCAAACGCAAATCAGACCTGGGGCGTCTTTCCTGTACAAT

	TGGACCGCTCACGAAGCCGGAACATACTTTTACCACTCACACGCCAGATCTCAAATGATGGACGGCCTATACGGC GCGGTCGTCATTGCACCGAACGATGAGACTCCACGGCCATTCCATCTTGTCAGCAGCGATGAGGCTGACCACGCA GCGATGCTCGCAGCGGAGAAGTTGATGCGACCCATTTTCGTCAGTGACTGGTCCCAGTACACATCCGCAGAATAC CAGGGGATACAGCGCGCCGCGAATATTGATTTCTCCTGCATGGACTCAATTCTCATCAACGGCGTCGGATCGCAAT ACTGCCTGTCCGAAGAAGAGCTAGACGACATGACGAACCCCATCGTGTTGCAGCTTTTGAAAGAGCTCGCAGGG GGGCATATGACACCCAAAGGATGCATTCCTCCCTTGCAAATGTTCAACGGAGATTTTGAGTTACATCTCGAGAATG TGCCAGAGCTTGCATACAACAAGTGCAATGGGGGACAAAGCTCGAAGGGCAACTACACGATTGATGTTGACTCC TCGCTTGGCTGGACGGCCTTGACATTCGTCAACCCAGGAGGCCTGTACCCTCTGCAACTGTCGATTGACAATCATG AACTGTGGGTATACGCCGTGGACGGGCAGTACGTGCAGCCCATCGTTGCGGATCGCATCCTGGTCAACACTGGCA GCCGTATCTCCGTGATGATCAAGCTCGATCAAGAGAGAGCCAAATATGTCGTGCGAGTAGCCAACGACTACCTGA ACCAGATCCTGGGCGGCTTCGCCGAGTTGTCGTACGATGGCGCGACACATGCTCCCACACGCCCGCACGAAAAG ACAAACTACGGAGGCAAGCCCACCAGCAGCGATGTTGTGTCGTTCGTCCCTGAGGATAGCAGCCCGTACCCAGC CTTGCGACCTGCGCAGAATGCGGATACCACCTTCAAATTGCGGCTGAAGAAGTTGGGGCAGCCTTACGGAGCTTA TGAGTGGACTCAGACTGGCAACTTGGGGTACAACATCAGCCACGAGCATGATAATCCGCCGTTGCTACTTCAGGA CGTAGAGCACATCCCCAGCACTGAGCTCAGGCTGAAGACACAGCTCGGGGATTGGATTGACCTCGTTCTCGTGAC AGCTGGTCCCTTTGCCCAAGCGCATCCAATGCACAAGCACGGCAATAAGGTTTTCCTCATTGGTTCGGGCTCAGG AAACTTCCCGTGGGAGAGCGTGGAAGAGGCGATCCCACATTTGCCTGAAGGCACATTCAACTTCCAAGATCCGC CGTATCTCGATACTTTCAACACCGTGGAAATGGAGGGACAAGCCAACGATACTTGGACGGCAGTCAGATATCAAG CAGAATATGCAGGTGCATGGCTGTTCCACTGCCACGTACAAACGCATCTTTCCGGCGGGATGGGCATGGTCGTCC TCGACGGCGTGGATGCATGGCCAGAAGTGCCCTTGGCTTATCAAGAGTGGAATGGATTCGAGCCGCCGGCTTGA ATTAAGCGGAACAAATTGAAGCGAGTCCCCGTGGAGCGCGAGCCCGCG

Table S3. List of constructs in this work.

Construct Name	Description	Source
pYFAC	*AMA1; CEN/ARS; ColE1 ori; pyrG; URA3; Amp^R*	[2]
pKW-20088	*AMA1; 2μ replicon; pyrG; URA3; Amp^R*	[6]
pYFAC-*riboB*	Modified from pKW-20088 by replacing *pyrG* with *riboB*	This work
pYFAC-*pyroA*	Modified from pKW-20088 by replacing *pyrG* with *pyroA*	This work
pCH-1	*elcE*-targeted sgRNA expression plasmid	This work
-	p426-SNR52p-gRNA.CAN1.Y-SUP4t	[27]
-	p414-TEF1p-Cas9-CYC1t	[27]
-	pINT1-HIS3NB	[28]
-	pXP741	[29]
pYFAC-CH1	pYFAC carrying P_{alcA}; unique restriction site: *Pac*I	[2]
pYFAC-CH2	pYFAC carrying *P_{alcA}-T1-$P_{alcS/M}$-T2-P_{aldA}* expression cassette; unique restriction site: *Pac*I for P_{alcA}, *Not*I for P_{alcS}, *AsiS*I for P_{alcM}, *Asc*I for P_{aldA}	This work
pYFAC-CH3	pYFAC-*riboB* carrying *P_{alcA}-T1-$P_{alcS/M}$-T2-P_{aldA}* expression cassette	This work
pYFAC-CH4	pYFAC-*pyroA* carrying *P_{alcA}-T1-$P_{alcS/M}$-T2-P_{aldA}* expression cassette	This work
pYFAC-CH5	pYFAC-*riboB* carrying *$P_{alcS/M}$*; cloning cut sites: *Not*I for P_{alcS}, *AsiS*I for P_{alcM}	This work
pYFAC-CH6	pYFAC-CH1 carrying *elc* cluster, with *elcR* under control of P_{alcA}	This work
pYFAC-CH7	pYFAC-CH6with *elcG* coding region removed	This work
pYFAC-CH9	pYFAC-CH6 with *elcE* disrupted.	This work
pYFAC-CH10	pYFAC-CH1 expressing *elcA*(P_{alcA})	This work
pYFAC-CH11	pYFAC-CH5 expressing *elcB*(P_{alcS}) and *elcE*(P_{alcM})	This work
pYFAC-CH12	pYFAC-CH4 expressing *elcD*(P_{alcS}), *elcF*(P_{alcM}) and *elcG*(P_{alcA})	This work
pYFAC-CH13	pYFAC-CH5 expressing *elcB*(*P_{alcM}*)	This work
pYFAC-CH14	pYFAC-CH5 expressing *elcB-MT*(P_{alcM})	This work
pYFAC-CH15	pYFAC-CH5 expressing *elcE*(P_{alcS})	This work
pYFAC-CH16	pYFAC-CH4 expressing *elcD*(P_{alcS})	This work
pYFAC-CH17	pYFAC-CH4 expressing *elcF*(P_{alcM})	This work
pYFAC-CH18	pYFAC-CH4 expressing *elcG*(P_{alcA})	This work
pYFAC-CH19	pYFAC-CH5 expressing *elcE*(P_{alcS}) and *elcB-MT*(P_{alcM})	This work
pYFAC-CH20	pYFAC-CH4 expressing *elcD*(P_{alcS}) and *elcF*(P_{alcM})	This work
pYFAC-CH21	pYFAC-CH4 expressing *elcF*(P_{alcM}) and *elcG*(P_{alcA})	This work
pYFAC-CH22	pYFAC-CH4 expressing *elcD*(P_{alcS})and *elcG*(P_{alcA})	This work
pYFAC-CH23	pYFAC-CH3 expressing *elcH*(P_{alcA})	This work
pYFAC-CH24	pYFAC-CH5 expressing *elcB*(P_{alcM}) and *CTB5*(P_{alcS})	This work
pYFAC-CH25	pYFAC-CH4 expressing *elcD*(P_{alcS}), *elcF*(P_{alcM}) and *Cz_CTB12*(P_{alcA})	This work

pYFAC-CH26	pYFAC-CH6 with fragment containing *elcH* and flanked by its promoter and terminator region inserted between *CEN/ARS* and *URA3* marker	This work
pYFAC-CH27	pYFAC-CH-4 expressing *elcD*(P_{alcS}), *elcF*(P_{alcM}), *elcG*(P_{alcA}), *elcE*(P_{aldA}), and fragment containing P_{gpdA}-*elcB*-*TtrpC* inserted between *T2* and *elcE*	This work

Table S4. Comparison of *CTB*, *HYP* and *elc* cluster

elc* cluster** ***P. nodorum	***HYP* cluster** ***Shiraia sp.* Slf14** (protein identity%)	***CTB* cluster** ***C. nicotianae*** (protein identity%)	**putative function**
SNOG_04778	HYP11(83%)	-	major facilitator superfamily (MFS) transporter
SNOG_04781	HYP12(80%)	-	NADPH-dependent oxidoreductase
-	HYP10	-	hypothetical protein
-	HYP9	-	hypothetical protein
SNOG_08601 (ElcH)	HYP7(51%)	-	FAD-dependent monooxygenase
SNOG_08608 (ElcE)	HYP8(77%)	CTB5(58%)	FAD/FMN-dependent oxidoreductase/berberine bridge enzyme-like oxidase
SNOG_08609 (ElcR)	HYP6(65%)	CTB8(31%)	zinc-finger transcription factor
-	HYP5	-	hypothetical protein
SNOG_08610 (ElcD)	HYP4(79%)	CTB2(58%)	*O*-methyltransferase
SNOG_08611 (ElcC)	HYP3(72%)	-	major facilitator superfamily (MFS) transporter
SNOG_08612 (ElcB)	HYP2(66%)	CTB3(49%)	*O*-methyltransferase/FAD-dependent monooxygenase
SNOG_08614 (ElcA)	HYP1(73%)	CTB1(56%)	polyketide synthase
SNOG_08615 (ElcF)	ORF2(60%)	Cz_CTB11(40%)	fasciclin
SNOG_08616 (ElcG)	ORF1(76%)	Cz_CTB12 (51%)	laccase
-	-	CTB4	major facilitator superfamily (MFS) transporter
SNOG_11921	-	CTB6(40%)	NADPH-dependent reductase
-	-	CTB7	flavin-dependent oxidoreductase
-	-	CTB9	alpha-ketoglutarate-dependent dioxygenase
-	-	CTB10	dehydratase

Table S5. NMR data of 12 in $CDCl_3$-*d*

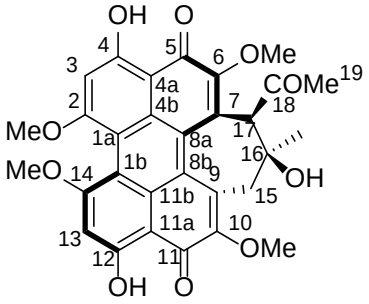

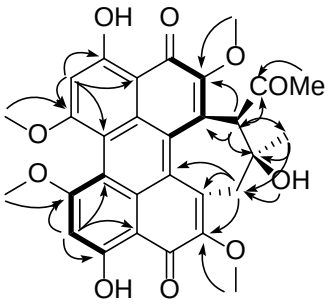

Carbon No.	^{13}C NMR	^{1}H NMR (ppm, multi, *J*)	HMBC
1a	117.6	-	-
1b	118.1	-	-
2	167.4	-	-
2-OMe	56.6	4.08 (3H, s)	2
3	101.9	6.57 (1H, s)	1a, 2, 4, 4a
4	179.8	-	-
4a	106.8	-	-
4b	124.6	-	-
5	171.8	-	-
6	149.3	-	-
6-OMe	61.3	4.27 (3H, s)	6
7	131.3	-	-
8a	128.0	-	-
8b	128.4	-	-
9	135.2	-	-
10	152.0	-	-
10-OMe	62.0	4.18 (3H, s)	10
11	171.9	-	-
11a	107.2	-	-
11b	125.5	-	-
12	180.2	-	-
13	102.2	6.56 (1H, s)	1b, 11a, 12, 14
14	167.8	-	-
14-OMe	56.7	4.08 (3H, s)	14
15	42.6	3.67 (1H, d, 13.8) 2.34 (1H, d, 13.8)	8b, 9, 10
16	78.7	-	-
16-OH	-	3.80 (1H, s)	15
16-Me	24.9	1.78 (3H, s)	15, 16, 17
17	64.4	3.72 (1H, s)	6, 7, 16, 16-Me, 18
18	206.8	-	-
19	28.6	1.83 (3H, s)	18

Table S6. 1-D NOE interaction data of 12 and hypocrellin A standard in $CDCl_3$-*d*

12	hypocrellin A standard	3-D NOE data of hypocrellin A (from reference)[30]
15-Ha ····16- H_3	-	15-Ha ···· 16-OH
15-Ha ···· 15-Hb	-	-
15-Hb ···· 10-OMe	-	15-Hb ···· 10-OMe
15-Hb ····16- H_3	-	-
15-Hb ···· 15-Ha	-	15-Hb ···· 15-Ha
16-OH···· 19-H_3	-	-
16-OH···· 16-H_3	-	-
16-H_3 ···· 16-OH	-	16-H_3 ···· 16-OH
16-H_3 ···· 6-OMe	-	-
16-H_3 ···· 15-Ha	-	-
16-H_3 ···· 15-Hb	16-H_3 ···· 15-Hb	16-H_3 ···· 15-Hb
16-H_3 ···· 17-H	-	16-H_3 ···· 17-H
17-H ···· 15-Ha	-	17-H ···· 16-OH
17-H ···· 19- H_3	17-H ···· 19-H_3	17-H ···· 19-H_3
17-H ···· 16- H_3	17-H ···· 16- H_3	-
19-H_3 ···· 17-H	-	19-H_3 ···· 6-OMe
19-H_3 ···· 6-OMe	-	-

Table S7. ^{1}H NMR spectrum comparison of 6 and hypocrellin A

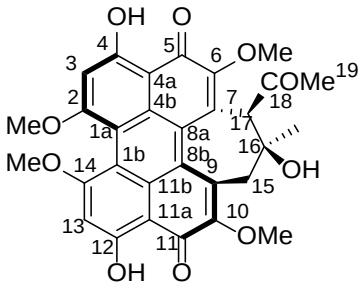

Carbon No.	^{1}H NMR (ppm, multi, *J*)		
	6	hypocrellin A Standard	data from reference[30]
2-OMe	4.07 (6H, s)	4.07 (6H, s)	4.06
3	6.56 (1H, s)	6.56 (1H, s)	6.56
4-OH	15.91 (1H, s)	15.90 (1H, s)	15.89
6-OMe	4.11 (6H, s)	4.11 (6H, s)	4.10
10-OMe	4.11 (6H, s)	4.11 (6H, s)	4.08
12-OH	15.96 (1H, s)	15.95 (1H, s)	15.94
13	6.55 (1H, s)	6.55 (1H, s)	6.55
14-OMe	4.07 (6H, s)	4.07 (6H, s)	4.06
15	3.51(1H, d, 12.2) 2.63 (1H, d, 12.0)	3.51 (1H, d, 12.2) 2.63 (1H, d, 12.1)	3.50, 2.61
16-OH	4.90 (1H, s)	4.89 (1H, s)	4.88
16-Me	1.70 (3H, s)	1.70 (3H, s)	1.69
17	3.44 (1H, s)	3.44 (1H, s)	3.43
19	1.89 (3H, s)	1.89 (3H, s)	1.87

Table S8. NMR data of elsinochrome A (1) in $CDCl_3$-*d*

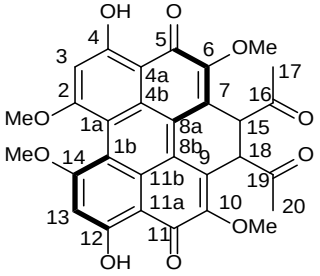

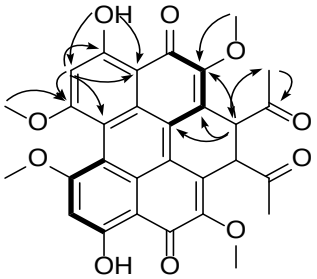

Carbon No.	^{13}C NMR	^{1}H NMR	HMBC
1a (1b)	118.8	-	-
2 (14)	167.6	-	-
2-OMe (14-OMe)	56.7	4.08	2 (14)
3 (13)	102.6	6.62	4a (11a), 1a (1b), 2 (14), 4 (12)
4 (12)	180.0	-	-
4-OH (12-OH)	-	16.1	4a (11a), 3 (13)
4a (11a)	107.9	-	-
4b (11b)	122.9	-	-
5 (11)	172.1	-	-
6 (10)	150.3	-	-
6-OMe (10-OMe)	61.3	4.36	6 (10)
7 (9)	130.4	-	-
8a (8b)	121.8	-	-
15 (18)	48.8	5.19	8a (8b), 7 (9), 6 (10), 16 (19)
16 (19)	205.0	-	-
17 (20)	28.2	2.03	15 (18), 16 (19)

Table S9. NMR data of compound 13 in D_2O

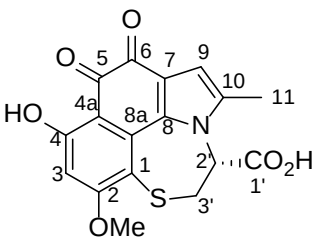

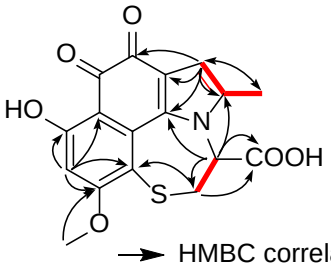

HMBC correlation

gCOSY correlation

Carbon No.	^{13}C NMR	^{1}H NMR (ppm, multi, *J*)	gCOSY	HMBC
1	122.9	-	-	-
2	165.1	-	-	-
2-OMe	57.1	3.85 (3H, s)	-	2
3	98.8	6.13 (1H, s)	-	1, 2, 4, 4a
4	169.7	-	-	-
4a	108.4	-	-	-
5	181.5	-	-	-
6	174.6	-	-	-
7	123.0	-	-	-
8	136.9	-	-	-
8a	127.5	-	-	-
9	107.9	6.37 (1H, s)	11	6, 7, 8, 10, 11
10	139.8	-	-	-
11	12.9	2.16 (3H, s)	9	9
1′	174.4	-	-	
2′	65.9	5.3 (1H, d, 5.0)	3′	8, 10, 1′, 3′
3′	30.7	3.5 (1H, dd, 5.4, 14.5) 2.9 (1H, d, 14.6)	2′	1, 1′

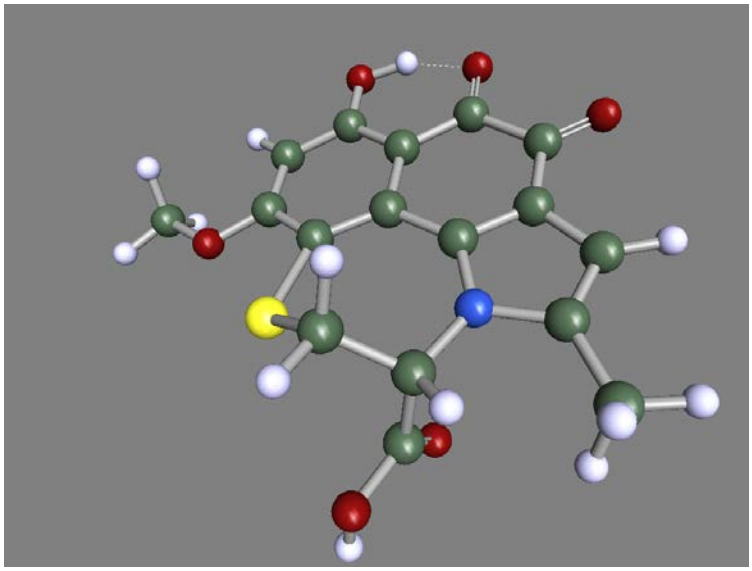

DFT (B3LYP-D3/def-TZVP) optimized structure of **13**

Table S10. DFT-calculated chemical shifts based on proposed structure of 13

Carbon No.	Calculated shielding tensor	Experimental chemical shift	Predicted chemical shift	Residual error (ppm)
1	55.98	122.9	123.4	0.5
2	13.48	165.1	164.8	–0.3
2-OMe	127.88	57.1	53.3	–3.8
3	84.11	98.8	96.0	–2.8
4	5.42	169.7	172.6	2.9
4a	69.27	108.4	110.4	2.0
5	–3.68	181.5	181.5	0.0
6	3.48	174.6	174.5	-0.1
7	51.74	123	127.5	4.5
8	43.37	136.9	135.6	–1.3
8a	48.50	127.5	130.6	3.1
9	69.03	107.9	110.6	2.7
10	41.73	139.8	137.2	-2.6
11	169.37	12.9	12.9	0.0
1'	9.40	174.4	168.7	–5.7
2'	117.70	65.9	63.2	–2.7
3'	147.66	30.7	34.1	3.4

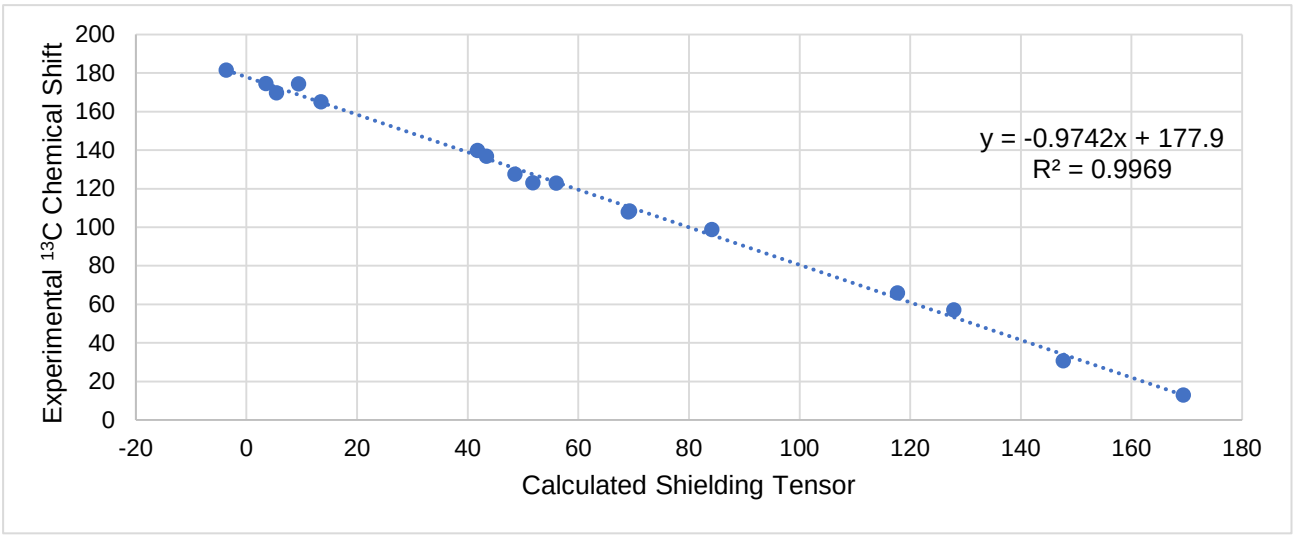

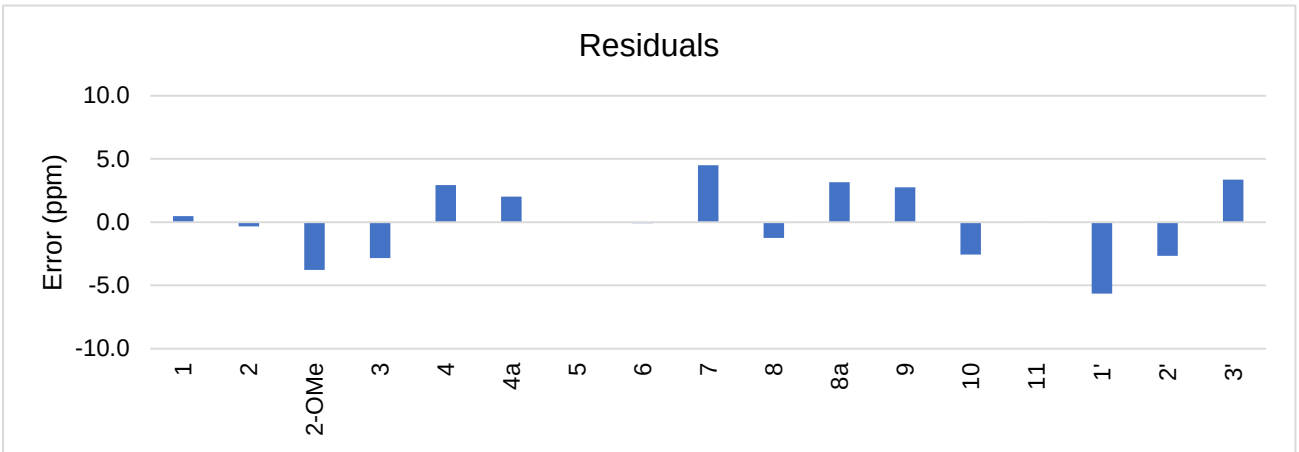

Table S11. NMR data of compound 14 in DMSO-d_6

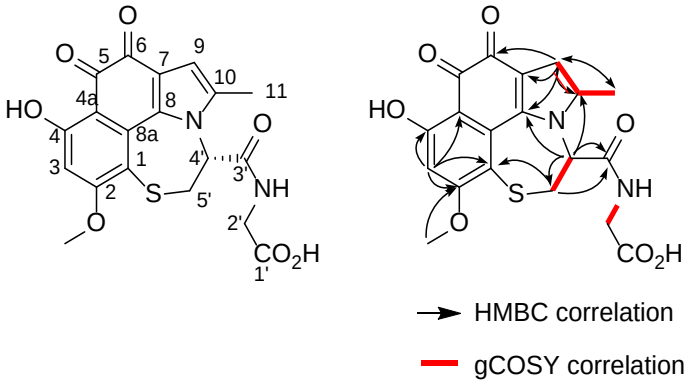

Carbon No.	^{13}C NMR	^{1}H NMR (ppm, multi, *J*)	gCOSY	HMBC
1	121.5	-	-	-
2	164.7	-	-	-
2-OMe	57.5	3.93 (1H, s)		2
3	98.6	6.48 (1H, s)	-	1, 2, 4, 4a
4	170.3	-	-	-
4a	108.9	-	-	-
5	182.0	-	-	-
6	174.0	-	-	-
7	123.5	-	-	-
8	135.6	-	-	-
8a	127.7	-	-	-
9	107.5	6.47 (1H, s)	11	6, 7, 8, 10, 11
10	139.8	-	-	-
11	13.3	2.2 (3H, s)	9	10
1′	170.8			
2′	42.8	3.51 (2H, s)	2′-NH-3′	
2′-NH-3′		7.92	2′	
3′	167.0	-	-	
4′	63.9	5.6 (1H, d, 4.8)	5′	8, 10, 3′, 5′
5′	31.2	3.6 (1H, m) 3.2 (1H, d, 14.8)	4′	1, 3′

Table S12. NMR data of compound 16

HMBC NMR correlations

DMSO-d_6 | D_2O

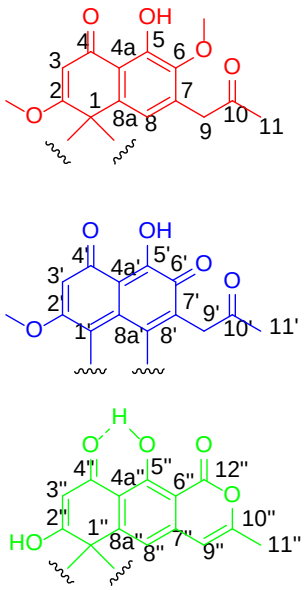

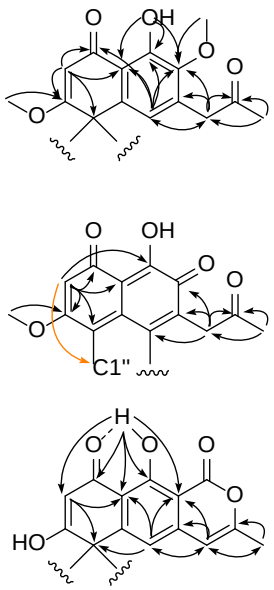

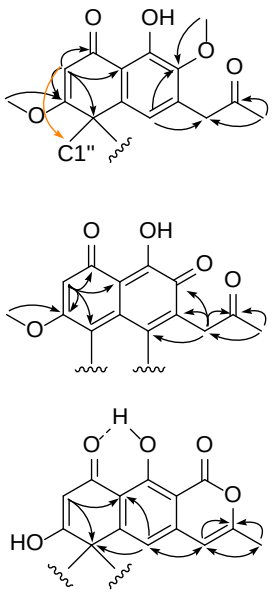

Key long-range HMBC correlations

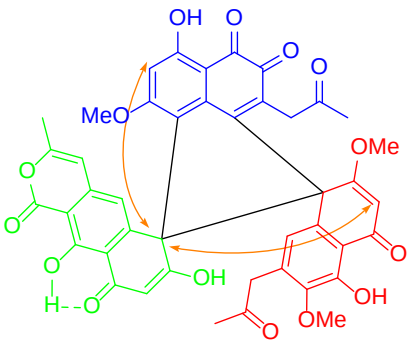

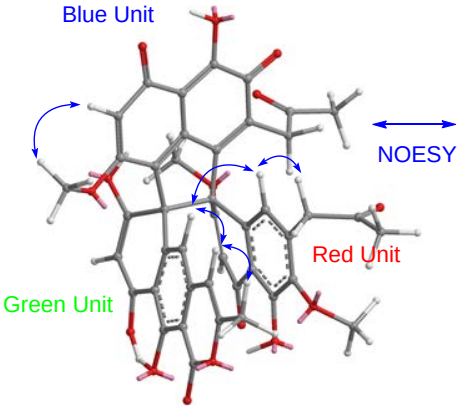

Table S12-1. NMR data of compound 16 in DMSO-d_6

Carbon No.	^{13}C NMR	^{1}H NMR (ppm, multi, *J*)	gCOSY	HMBC
1	67.90	-	-	-
2	177.43	-	-	-
2-OMe	56.67	3.5 (3H, s)	-	2
3	102.16	5.6 (1H, s)		1, 2, 4, 4a
4	190.5	-	-	-
4a	114.75	-	-	-
5	152.78	-	-	-
5-OH	-	13.08 (1H, s)		4a, 6, 5
6	144.62	-	-	-
6-OMe	59.36	3.55 (3H, s)	-	6
7	130.94	-	-	-
8	122.05	5.78 (1H, s)	-	1, 4, 4a, 5, 6, 9
8a	143.3[†]	-	-	-
9	44.32	2.85 (1H, d, 16.4) 3.2 (1H. d, 16.3)	-	6, 7, 8, 10
10	204.07	-	-	-
11	29.11	1.88 (3H, s)	-	9,10
1′	126.8	-	-	-
2′	162.2	-	-	-

2′-OMe	55.04	3.4 (3H, s)	-	2′
3′	109.0	5.84 (1H, s)	-	1′, 2′, 4′, 4a′ ,5′, 1′′
4′	170.6	-	-	-
4a′	109.8	-	-	-
5′	181.5	-	-	-
6′	185.98	-	-	-
7′	128.4	-	-	-
8′	156.2	-	-	-
8a′	134.16[†]	-	-	-
9′	41.7	2.78 (2H, d, 14.5)	-	6′, 7′, 8′, 10′
10′	203.5	-	-	-
11′	28.95	1.7 (3H, s)	-	9′, 10′
1′′	75.11	-	-	-
2′′	165.9[†]	8.51 (1H, s)	-	-
3′′	99.05	4.59 (1H,s)	-	1′′, 4a′′
4′′	180.68	-	-	-
4a′′	114.27	-	-	-
5′′	167.19	-	-	-
5′′-OH	-	18.85 (1H, s)	-	3′′, 4′′, 4a′′, 5′′, 6′′
6′′	105.42	-	-	-
7′′	138.77	-	-	-
8′′	112.16	5.55 (1H, s)	-	1′′, 4a′′, 6′′, 9′′
8a′′	150.2[†]	-	-	-
9′′	103.92	6.06 (1H, s)	2.06	6′′, 8′′, 7′′, 10′′, 11′′
10′′	158.7	-	-	-
11′′	18.79	2.06 (3H, s)	6.06	9′′, 10′′
12′′	154.8[†]	-	-	-

[†] indicates carbons that lack 2D NMR correlation. The chemical shifts were assigned to each carbon based on prediction and list of unassigned carbon signals from **16**.

Table S12-2. NMR data of compound 16 in D_2O

Carbon No.	^{13}C NMR (DMSO-d_6)	^{13}C NMR (D_2O)	^{1}H NMR (ppm, multi, *J*)	HMBC
1	67.90	69.18	-	-
2	177.43	177.29	-	-
2-OMe	56.67	57.1	3.68 (3H, s)	2
3	102.16	102.44	5.71 (1H, s)	1, 2, 4, 4a, 1′′
4	190.5	191.42	-	-
4a	114.75	114.98	-	-
5	152.78	152.6[§]	-	-
5-OH	-	-	-	-
6	144.62	145.04	-	-
6-OMe	59.36	60.39	3.59 (3H, s)	6
7	130.94	131.81[§]	-	-

8	122.05	122.68	5.73 (1H, s)	9, 6
8a	143.3	143.95[§]	-	-
9	44.32	43.34	2.9 (s)	-
10	204.07	209.71	-	-
11	29.11	29.01	2.0 (3H, s)	9, 10
1′	126.8	126.1	-	-
2′	162.2	163.25	-	-
2′-OMe	55.04	55.8	3.62 (3H, s)	2′
3′	109.3	108.7	6.25 (1H, s)	1′, 2′, 4′, 4a′
4′	170.6	172.57	-	-
4a′	109.8	109.85	-	-
5′	181.5	181.93[§]	-	-
6′	185.98	185.97	-	-
7′	128.4	129.0	-	-
8′	156.2	158.0	-	-
8a′	134.16	133.86[§]	-	-
9′	41.7	41.1	3.0 (1H, d, 18.2) 3.2 (1H, d, 18.1)	6′, 7′, 8′, 10′
10′	203.5	210.32/210.26	-	-
11′	28.95	28.99	1.85 (3H, s)	9′, 10′
1″	75.11	75.0	-	-
2″	165.9	192.2[§]	-	-
3″	99.05	102.01	5.09 (1H, s)	1″, 4a″
4″	180.68	185.17[§]	-	-
4a″	114.27	113.6	-	-
5″	167.19	162.81[§]	-	-
5″-OH	-	-	-	-
6″	105.42	105.45[§]	-	-
7″	138.77	140.7[§]	-	-
8″	112.16	115.25	5.83 (1H, s)	1″, 4a″, 9″
8a″	150.2	150.7[§]		
9″	103.92	104.05	5.86 (1H, s)	8″, 10″, 11″
10″	158.7	157.1	-	-
11″	18.79	18.28	1.98 (3H, s)	9″, 10″
12″	154.8	161.5[§]	-	-

[§] indicates carbons that lack 2D NMR correlations. ^{13}C NMR data of **16** in DMSO-d_6 is added for comparison.

Table S13. DFT-calculated chemical shifts based on proposed structure of 16

Carbon No.	Calculated shielding tensor	Exp. chemical shift DMSO-d_6	Predicted chemical shift	Residual error DMSO-d_6 (ppm)
1	104.9	67.9	75.8	–8.3
2	3.5	177.4	172.8	4.5
2-OMe	128.5	56.5	53.3	2.8
3	74.2	102.0	105.2	–3.5
4	–10.4	190.5	186.1	4.2
4a	66.8	114.8	112.3	2.2
5	23.4	152.8	153.7	–1.1
5-OH	29.9	144.6	147.6	–3.2
6	123.0	59.2	58.5	0.3
6-OMe	49.8	130.9	128.5	2.1
7	53.8	121.9	124.7	-3.0
8	35.0	143.4	142.7	0.4
8a	139.3	44.2	43.0	0.8
9	–33.9	204.1	208.5	–4.6
10	153.4	29.1	29.5	-0.9
11	57.4	126.7	121.2	5.2
1′	12.6	162.2	164.1	–2.1
2′	128.3	55.0	53.5	1.0
2′-OMe	81.1	109.0	98.6	10.1
3′	6.7	170.6	169.8	0.7
4′	72.6	109.9	106.8	2.8
4a′	–4.2	181.6	180.2	1.3
5′	–11.1	186.0	186.8	–0.9
6′	44.5	128.5	133.6	–5.4
7′	18.7	156.2	158.3	–2.3
8′	49.1	134.1	129.2	4.7
8a′	141.1	41.5	41.2	–0.1
9′	–28.0	203.5	202.9	0.5
10′	154.3	28.8	28.6	–0.3
11′	106.1	75.1	74.7	0.1
1″	3.9	165.9	172.4	–6.6
2″	76.2	99.0	103.3	–4.6
3″	0.4	180.6	175.8	4.7
4″	67.5	114.3	111.6	2.4
4a″	9.6	167.2	167.0	0.0
5″	73.5	105.5	105.9	-0.7
5″-OH	36.8	138.8	141.0	–2.5
6″	64.2	112.2	114.8	–2.9
7″	31.3	150.1	146.2	3.7
8″	76.5	103.8	103.1	0.5
8a″	16.3	158.7	160.6	–2.1
9″	163.5	18.6	19.8	–1.7
10″	24.2	154.9	153.0	1.6
11″	104.9	67.9	75.8	–8.3
12″	3.5	177.4	172.8	4.5

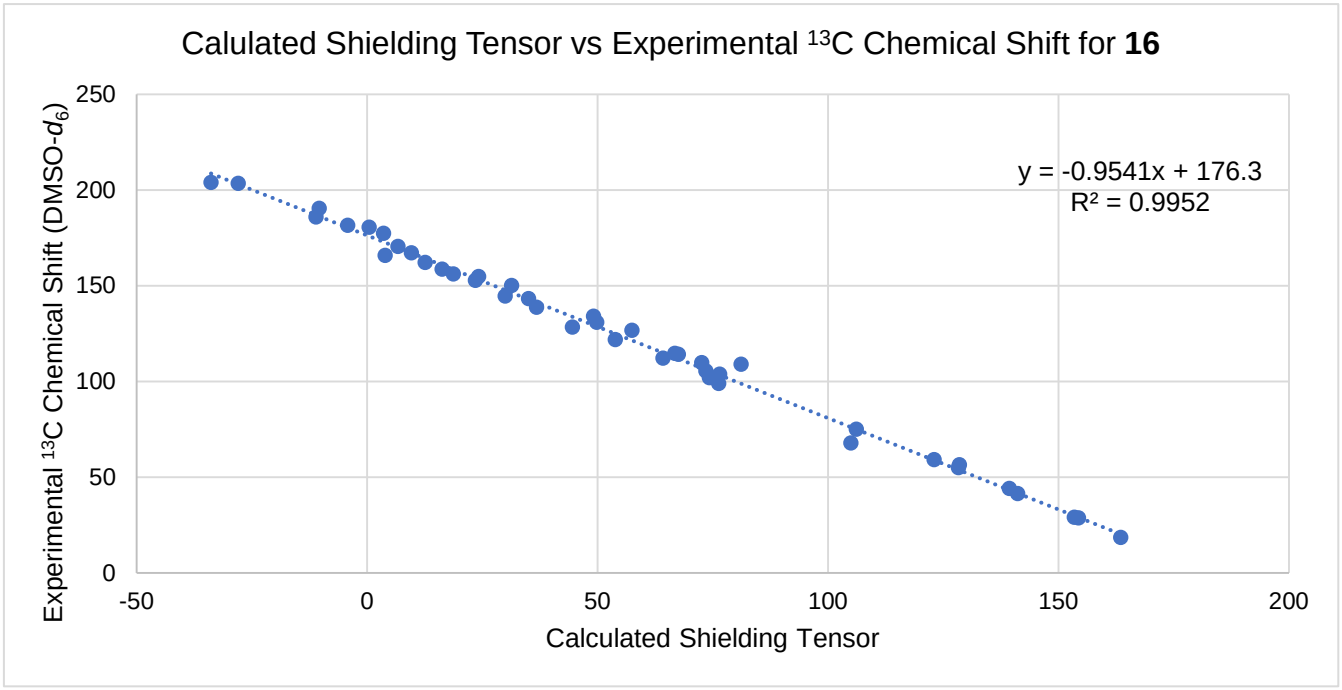
Calulated Shielding Tensor vs Experimental 13C Chemical Shift for 16
Experimental 13C Chemical Shift (DMSO-d6)
Calculated Shielding Tensor
y = -0.9541x + 176.3
R² = 0.9952
250
200
150
100
50
0
-50
0
50
100
150
200

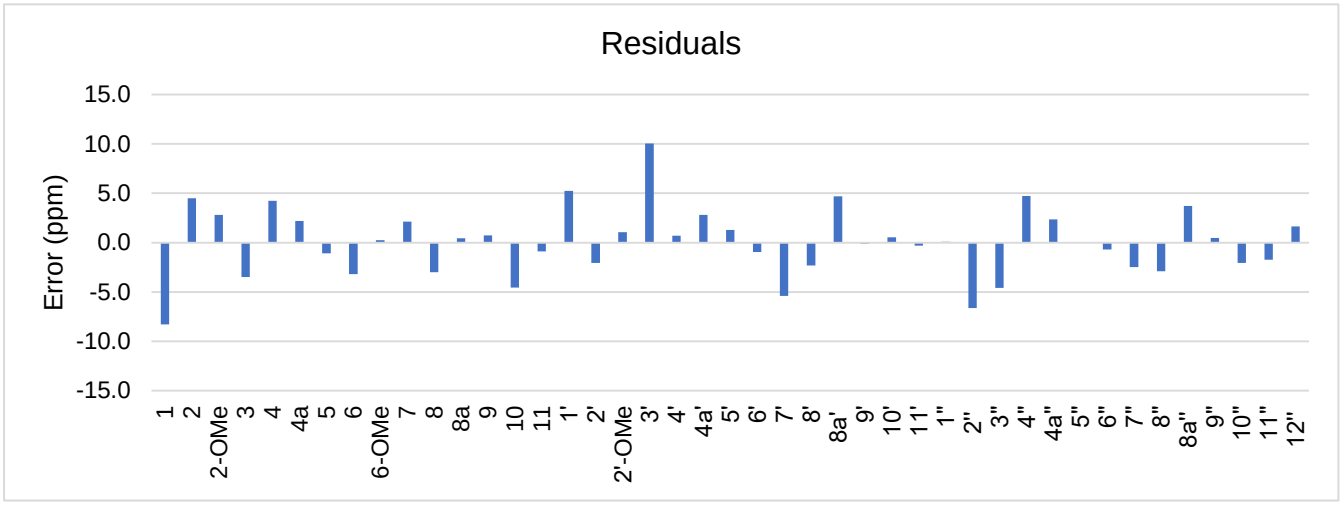
Residuals
Error (ppm)
15.0
10.0
5.0
0.0
-5.0
-10.0
-15.0
1
2
2-OMe
3
4
4a
5
6
6-OMe
7
8
8a
9
10
11
1'
2'
2'-OMe
3'
4'
4a'
5'
6'
7'
8'
8a'
9'
10'
11'
1"
2"
3"
4"
4a"
5"
6"
7"
8"
8a"
9"
10"
11"
12"

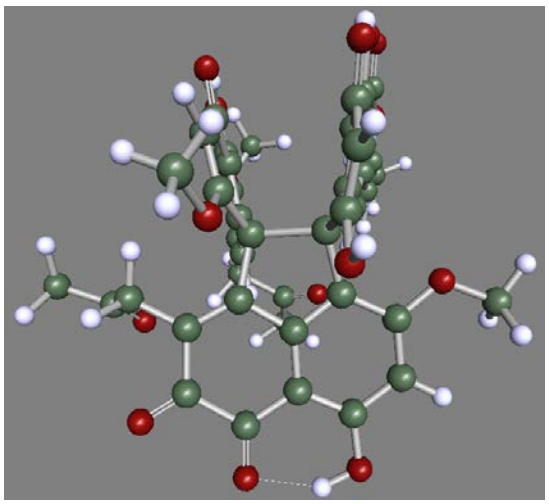

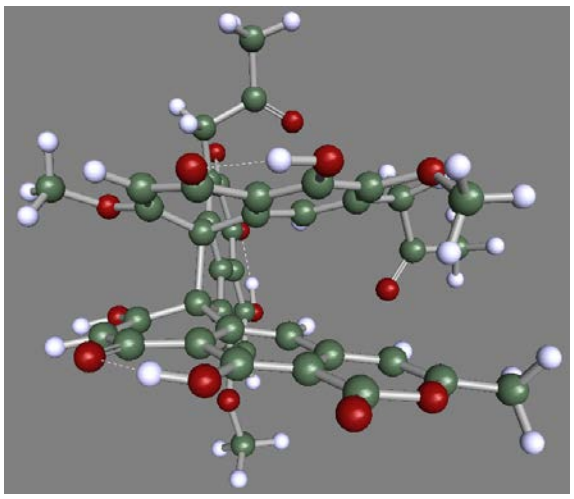

DFT (B3LYP-D3/def-TZVP) optimized structure of **16**

Table S14. Comparison of 12/19/20 NMR data

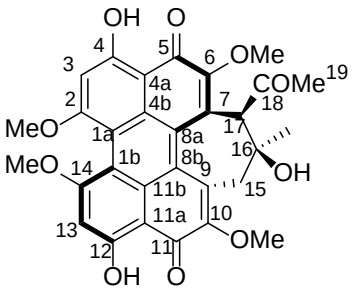

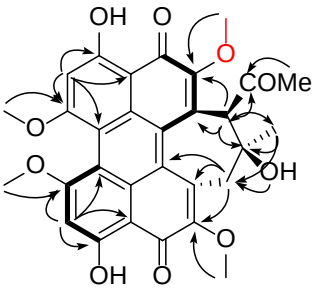

12

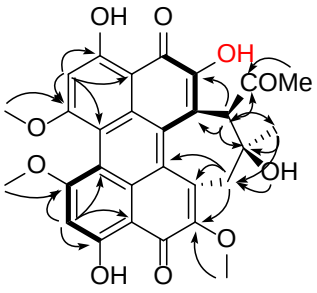

19

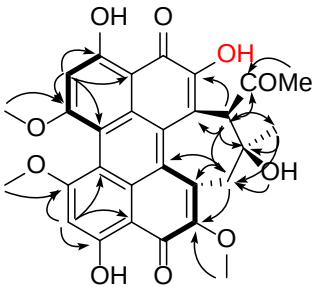

20

	12		**19**		**20**	
Carbon No.	^{1}H NMR (ppm, multi, *J*)	HMBC	^{1}H NMR (ppm, multi, *J*)	HMBC	^{1}H NMR (ppm, multi, *J*)	HMBC
2-OMe	4.08 (3H, s)	167.4	4.13 (3H, s)	167.8	4.11 (3H, s)	167.8
3	6.57 (1H, s)	106.8, 117.6, 167.4, 179.8	6.75 (1H, s)	103.9, 114.9, 167.8, 171.6	6.74 (1H, s)	104.3, 115.1, 167.8, 172.7
6-OMe	4.27 (3H, s)	149.3	-	-	-	-
10-OMe	4.18 (3H, s)	152.0	4.19 (3H, s)	152.8	4.22 (3H, s)	151.7
13	6.56 (1H, s)	107.2, 118.1, 167.8, 180.2	6.72 (1H, s)	105.9, 114.4, 166.3, 173.9	6.67 (1H, s)	105.8, 115.0, 165.6, 175.0
14-OMe	4.08 (3H, s)	167.8	4.10 (3H, s)	166.3	4.08 (3H, s)	165.6
15	3.67 (1H, d, 13.8) 2.34 (1H, d, 13.8)	128.4, 135.2, 152.0	3.6 (1H, d, 13.8) 2.6 (1H, dd, 2.0, 13.9)	64.1, 77.8, 129.7, 134.9, 152.8	3.7 (1H, d, 13.7) 2.6 (1H, d, 13.8)	59.4, 79.0, 129.4, 136.2, 151.7
16-OH	3.80 (1H, s)	42.6	3.8 (1H, d, 1.56)	42.6	-	-
16-Me	1.78 (3H, s)	42.6, 64.4, 78.7	1.77 (3H, s)	42.6, 64.1, 77.8,	1.62 (3H, s)	43.0, 59.4, 79.0
17	3.72 (1H, s)	24.9, 78.7, 131.3, 149.3, 206.8	3.76, (1H, s)	24.9, 77.8, 120.5, 130.2, 147.3, 207.6	4.66 (1H, s)	29.8, 43.0, 79.0, 120.8, 127.0, 149.7, 209.7
19	1.83 (3H, s)	206.8	1.92 (3H, s)	207.6	1.33 (3H, s)	209.7

Table S15. B3LYP/6-31G(2df,p) optimized geometries (Å) for the species considered for the aldol reaction and atropisomerisation steps in the present study.

Reac *(M)*-**11**			
C	3.242362	1.434015	0.853838
C	2.155403	0.703601	0.245346
C	0.937909	1.395854	0.058256
C	0.926118	2.815515	0.130645
C	2.106584	3.560964	0.525657
C	3.239903	2.803227	0.944463
C	-0.283409	0.684758	-0.219896
C	-0.209646	3.537029	-0.263527
H	4.059218	3.356773	1.380269
C	-1.354045	2.830431	-0.729403
C	-1.408483	1.448075	-0.703109
O	2.101683	4.831060	0.557370
O	-0.190315	4.858678	-0.284879
O	-2.385323	3.484456	-1.349781
C	-2.923340	4.661351	-0.753742
H	-2.964068	4.571719	0.336250
H	-2.337649	5.543961	-1.014983
H	-3.941051	4.752562	-1.142068
C	3.392535	-1.346547	-0.581888
C	2.210444	-0.664406	-0.145295
C	0.982539	-1.392457	-0.195334
C	0.981058	-2.787887	-0.444137
C	2.183603	-3.443398	-0.732092
C	3.380755	-2.699431	-0.833256
C	-0.267724	-0.725785	-0.037903
C	-0.251433	-3.566500	-0.392575
H	4.262299	-3.230206	-1.164083
C	-1.422954	-2.904210	0.028417
C	-1.464058	-1.522684	0.305006
O	2.217825	-4.748236	-0.969123
O	-0.202913	-4.829394	-0.596142
O	-2.511072	-3.683979	0.357639
C	-2.309748	-4.489476	1.511306
H	-1.528182	-5.234877	1.334170
H	-2.044235	-3.868921	2.377538
H	-3.261618	-4.990079	1.711672
H	0.760607	5.098448	0.067969
H	1.217741	-5.027862	-0.856854
O	4.478211	-0.565850	-0.834166
O	4.207981	0.665713	1.400453

C	5.675669	-1.194704	-1.222020
H	6.413212	-0.397879	-1.338036
H	6.024857	-1.906651	-0.462396
H	5.566932	-1.727123	-2.176420
C	5.368309	1.293755	1.898050
H	6.028470	0.489843	2.228187
H	5.867761	1.883946	1.119794
H	5.140973	1.949071	2.748385
C	-2.470878	-0.867811	1.036847
H	-2.155825	0.036390	1.546979
C	-2.577914	0.831033	-1.426210
H	-2.632171	1.296140	-2.418287
H	-2.433924	-0.234683	-1.584797
C	-3.833008	-1.222017	1.364224
O	-4.382630	-0.707960	2.349419
C	-4.696821	-2.056923	0.426192
H	-4.940416	-3.016683	0.889637
H	-5.626520	-1.500846	0.277546
H	-4.232357	-2.251669	-0.537936
C	-3.995306	1.015828	-0.854272
C	-4.240684	1.811287	0.412284
H	-4.769190	1.179173	1.129442
H	-3.324771	2.169506	0.878530
H	-4.881960	2.661924	0.162211
O	-4.922268	0.538399	-1.471785

TS *(M)*-**6**			
C	-2.969101	-1.698945	0.721840
C	-1.968246	-0.846632	0.113530
C	-0.717247	-1.436544	-0.175594
C	-0.586030	-2.851171	-0.181472
C	-1.684574	-3.710670	0.210977
C	-2.859557	-3.063625	0.716902
C	0.435242	-0.622499	-0.442660
C	0.609758	-3.440265	-0.616672
H	-3.609410	-3.705850	1.156316
C	1.692880	-2.619711	-1.057677
C	1.623605	-1.246271	-0.966819
O	-1.582111	-4.970996	0.179568
O	0.731840	-4.752911	-0.687132
O	2.737041	-3.237879	-1.678812
C	3.700182	-3.836013	-0.794687
H	4.155287	-3.051394	-0.182318
H	3.222264	-4.602708	-0.175119

H	4.441842	-4.309772	-1.442847
C	-3.383835	1.168436	-0.490246
C	-2.132179	0.541007	-0.164892
C	-0.963393	1.354169	-0.236465
C	-1.068930	2.757343	-0.415686
C	-2.329747	3.344208	-0.589437
C	-3.482685	2.532159	-0.648258
C	0.336800	0.764800	-0.184516
C	0.111366	3.602910	-0.472540
H	-4.416131	3.017248	-0.894807
C	1.370060	2.980770	-0.202608
C	1.489163	1.624564	0.087594
O	-2.460781	4.651511	-0.771693
O	-0.001951	4.857024	-0.640497
O	2.471157	3.797234	-0.111927
C	2.525802	4.576734	1.081139
H	1.638188	5.210985	1.169081
H	2.620415	3.925903	1.960050
H	3.417451	5.203899	1.001444
H	-0.167532	-5.107924	-0.348005
H	-1.489913	4.995973	-0.746469
O	-4.422322	0.333407	-0.737302
O	-3.954857	-1.042657	1.372139
C	-5.686877	0.892611	-1.006199
H	-6.369183	0.049909	-1.132086
H	-6.034051	1.523217	-0.177598
H	-5.679132	1.492170	-1.925839
C	-5.012881	-1.794946	1.922725
H	-5.704495	-1.070607	2.356491
H	-5.529640	-2.381757	1.152994
H	-4.658909	-2.475281	2.707460
C	2.718821	1.151368	0.714425
C	2.770231	-0.433728	-1.462869
H	3.329903	-1.026518	-2.190858
H	2.412460	0.477566	-1.948119
C	3.775032	-0.065337	-0.321518
C	4.823798	0.936588	-0.849150
H	4.375172	1.828594	-1.295737
H	5.474425	1.233061	-0.022946
H	5.437211	0.425247	-1.602388
O	4.214805	-1.019927	0.387656
H	3.397795	1.989824	0.813488
C	2.664068	0.537172	2.082770
O	3.324279	1.046732	2.972309

C	1.887988	-0.731886	2.343423
H	2.017114	-1.010841	3.390490
H	0.825756	-0.615056	2.119585
H	2.299218	-1.507771	1.691086

TS *(M)*-12			
C	3.413921	0.778735	0.844916
C	2.197958	0.303081	0.219064
C	1.173683	1.239790	-0.042883
C	1.522715	2.619912	-0.063037
C	2.837736	3.082903	0.329805
C	3.742885	2.102656	0.859444
C	-0.180182	0.808540	-0.300920
C	0.600927	3.562031	-0.543378
H	4.651586	2.476229	1.309542
C	-0.683424	3.129814	-0.939898
C	-1.106317	1.819802	-0.764556
O	3.155362	4.305796	0.279351
O	0.915209	4.843311	-0.647270
O	-1.493706	4.067542	-1.526970
C	-2.256268	4.881188	-0.636048
H	-3.090562	4.316663	-0.204434
H	-1.622555	5.288673	0.159526
H	-2.648370	5.705689	-1.236741
C	3.007212	-1.953080	-0.514860
C	1.955495	-1.045432	-0.126961
C	0.609360	-1.497735	-0.208700
C	0.381534	-2.888108	-0.396136
C	1.452237	-3.777715	-0.610408
C	2.771156	-3.291402	-0.706128
C	-0.502369	-0.580911	-0.113950
C	-0.943307	-3.435115	-0.340575
H	3.544353	-3.987976	-0.994864
C	-2.000721	-2.520715	0.013768
C	-1.836071	-1.152672	0.150627
O	1.239872	-5.069167	-0.786934
O	-1.157146	-4.675938	-0.481153
O	-3.202494	-3.112598	0.279068
C	-3.254964	-3.830018	1.502420
H	-2.532519	-4.652828	1.513792
H	-3.071224	-3.158418	2.352045
H	-4.267865	-4.231747	1.578647
H	1.870869	4.894584	-0.293724
H	0.211975	-5.164421	-0.701449

O	4.203311	-1.382389	-0.779754
O	4.128578	-0.175046	1.487340
C	5.294638	-2.218484	-1.094485
H	6.152255	-1.556929	-1.227073
H	5.501326	-2.929945	-0.285142
H	5.120957	-2.777399	-2.022679
C	5.382990	0.183896	2.022319
H	5.806557	-0.730252	2.442128
H	6.050653	0.576833	1.245177
H	5.283989	0.935655	2.815519
C	-3.029179	-0.441728	0.716335
C	-2.547636	1.573566	-0.962179
H	-2.972705	2.370523	-1.570192
H	-2.797286	0.626215	-1.439514
C	-4.292595	-0.758785	0.078052
O	-4.387533	-0.948708	-1.135090
C	-5.535483	-0.665394	0.943584
H	-5.683819	0.396882	1.173766
H	-6.396549	-1.045302	0.389767
H	-5.418165	-1.217226	1.882728
C	-3.273612	1.654547	0.437904
C	-2.460095	2.079701	1.672443
H	-3.080219	1.880408	2.549788
H	-1.503239	1.568444	1.785664
H	-2.269870	3.160328	1.642768
O	-4.459561	2.039241	0.408346
H	-3.028085	-0.458221	1.805986

(M)-**6**			
C	-2.912040	-1.789531	0.679710
C	-1.928993	-0.926370	0.058651
C	-0.654453	-1.485008	-0.192174
C	-0.466007	-2.891508	-0.126862
C	-1.533112	-3.771434	0.294435
C	-2.744172	-3.145966	0.744295
C	0.469093	-0.641660	-0.488213
C	0.764084	-3.453417	-0.516454
H	-3.476794	-3.797541	1.198917
C	1.808769	-2.617303	-1.001376
C	1.678938	-1.241542	-0.987322
O	-1.384930	-5.027348	0.333989
O	0.940137	-4.761721	-0.506165
O	2.876469	-3.227683	-1.588734
C	3.941687	-3.580566	-0.688337

H	4.358917	-2.664362	-0.248600
H	3.568282	-4.258349	0.089351
H	4.680307	-4.109332	-1.297094
C	-3.393437	1.038763	-0.583459
C	-2.126265	0.451794	-0.244498
C	-0.984208	1.300824	-0.300695
C	-1.146591	2.706295	-0.420820
C	-2.431292	3.252655	-0.587671
C	-3.548627	2.402843	-0.701728
C	0.334942	0.751802	-0.266118
C	-0.011361	3.599736	-0.389403
H	-4.497088	2.857301	-0.948645
C	1.279415	3.004372	-0.127822
C	1.457859	1.643429	-0.003184
O	-2.608622	4.560651	-0.708947
O	-0.157549	4.851961	-0.491191
O	2.330476	3.863298	0.037977
C	2.333311	4.559405	1.287919
H	1.422921	5.156984	1.397419
H	2.429594	3.843165	2.112396
H	3.202967	5.220617	1.266381
H	0.052282	-5.134157	-0.161950
H	-1.660703	4.945166	-0.641815
O	-4.386703	0.169884	-0.877432
O	-3.944541	-1.147546	1.274381
C	-5.681679	0.676096	-1.108951
H	-6.322525	-0.193824	-1.262841
H	-6.046914	1.253005	-0.249982
H	-5.715185	1.312300	-2.002783
C	-4.965255	-1.921829	1.862580
H	-5.696614	-1.211451	2.252323
H	-5.446740	-2.578017	1.126440
H	-4.581563	-2.537583	2.685825
C	2.755639	1.151284	0.575331
C	2.776392	-0.398179	-1.503561
H	3.432590	-0.995221	-2.136125
H	2.367735	0.431920	-2.087577
C	3.693429	0.197744	-0.335583
C	4.656915	1.188306	-1.061990
H	4.128921	2.017664	-1.547810
H	5.350832	1.595130	-0.320762
H	5.236964	0.637067	-1.809125
O	4.349300	-0.711154	0.347495
H	3.348888	2.044335	0.753656

C	2.501793	0.647622	2.013538
O	2.577955	1.450711	2.924253
C	2.198489	-0.803428	2.271312
H	2.240434	-0.992539	3.345768
H	1.203489	-1.060405	1.899413
H	2.943483	-1.381677	1.712929

(M)-**12**			
C	3.540598	0.503004	0.669811
C	2.256739	0.158251	0.100193
C	1.312500	1.193452	-0.085336
C	1.758899	2.544302	-0.030901
C	3.114863	2.878849	0.329086
C	3.965818	1.797595	0.740141
C	-0.078328	0.886120	-0.318681
C	0.878299	3.595675	-0.367800
H	4.923815	2.075094	1.156615
C	-0.437588	3.290918	-0.749568
C	-0.925109	1.988942	-0.708527
O	3.529974	4.076294	0.356118
O	1.288548	4.853591	-0.365328
O	-1.217385	4.321632	-1.213989
C	-2.013640	4.980721	-0.228806
H	-2.850139	4.349374	0.097864
H	-1.402315	5.269820	0.634855
H	-2.403318	5.883639	-0.706757
C	2.790992	-2.177446	-0.626135
C	1.859115	-1.163622	-0.213073
C	0.474178	-1.492205	-0.185450
C	0.127964	-2.872425	-0.213684
C	1.107743	-3.868244	-0.423756
C	2.439716	-3.505684	-0.683765
C	-0.540618	-0.464572	-0.126423
C	-1.221478	-3.299895	-0.005192
H	3.129474	-4.283539	-0.976540
C	-2.181056	-2.258147	0.236537
C	-1.916218	-0.906442	0.148088
O	0.780759	-5.149407	-0.446237
O	-1.549998	-4.525007	0.002541
O	-3.462668	-2.667491	0.500924
C	-3.644888	-3.364453	1.727076
H	-3.074644	-4.296525	1.736040
H	-3.348433	-2.736362	2.578334
H	-4.713304	-3.580683	1.798481

H	2.266708	4.797306	-0.073976
H	-0.235166	-5.152145	-0.270579
O	3.992941	-1.724732	-1.044277
O	4.227507	-0.534252	1.213879
C	5.013235	-2.662936	-1.303935
H	5.903577	-2.080871	-1.547571
H	5.212306	-3.289415	-0.425579
H	4.761956	-3.310722	-2.153390
C	5.511157	-0.277780	1.735062
H	5.892232	-1.237674	2.088982
H	6.184513	0.124069	0.966964
H	5.473934	0.429399	2.573628
C	-3.168443	-0.082001	0.463785
C	-2.342821	1.788655	-0.950880
H	-2.810955	2.675199	-1.361124
H	-2.554796	0.943672	-1.603958
C	-4.315630	-0.447867	-0.490459
O	-4.127664	-0.663484	-1.669253
C	-5.691651	-0.439202	0.126915
H	-5.819677	0.563741	0.549266
H	-6.445121	-0.656568	-0.632740
H	-5.748931	-1.176878	0.933499
C	-3.095349	1.494171	0.479685
C	-2.265710	1.914421	1.725360
H	-2.908989	1.728273	2.591458
H	-1.323978	1.375659	1.867882
H	-2.046820	2.983905	1.699549
O	-4.268599	2.086564	0.464856
H	-3.488974	-0.380353	1.468720

(P)-**6**			
C	-2.856007	-2.203801	-0.536249
C	-1.936659	-1.175540	-0.155566
C	-0.557938	-1.493697	-0.221621
C	-0.127195	-2.829203	-0.417702
C	-1.080045	-3.838593	-0.649049
C	-2.442213	-3.508857	-0.729406
C	0.436922	-0.458441	-0.172540
C	1.279771	-3.174827	-0.411183
H	-3.128086	-4.294360	-1.011170
C	2.219887	-2.122754	-0.059502
C	1.820877	-0.818099	0.086247
O	-0.715267	-5.100518	-0.857065
O	1.656597	-4.359002	-0.627992

O	3.525922	-2.448777	0.146951
O	-4.124925	-1.808535	-0.792294
C	3.800093	-3.459047	1.122704
H	3.468162	-3.120648	2.109989
H	3.327261	-4.403409	0.852470
H	4.886320	-3.570084	1.127228
C	-3.525562	0.572031	0.802479
C	-2.303607	0.176872	0.175342
C	-1.350918	1.196897	-0.068040
C	-1.699512	2.564979	0.052106
C	-2.986871	2.910784	0.503012
C	-3.875056	1.904634	0.918570
C	0.010317	0.864546	-0.378633
C	-0.769137	3.620915	-0.307473
H	-4.805624	2.218285	1.369100
C	0.527572	3.220759	-0.796660
C	0.898591	1.894483	-0.884934
O	-3.365469	4.181666	0.607030
O	-1.128187	4.834926	-0.264522
O	1.353418	4.162336	-1.350690
O	-4.267178	-0.419959	1.351074
C	1.702342	5.278836	-0.540057
H	0.871236	5.980737	-0.452145
H	2.008131	4.955176	0.462099
H	2.557357	5.751317	-1.030671
C	-5.092548	-2.787561	-1.092550
H	-6.036592	-2.252254	-1.210069
H	-4.859623	-3.317732	-2.025115
H	-5.188032	-3.522495	-0.283120
C	-5.528867	-0.100459	1.889427
H	-5.445562	0.580667	2.746369
H	-6.184503	0.357577	1.137636
H	-5.963196	-1.044787	2.223122
C	2.762917	0.238258	0.583698
C	2.146661	1.478186	-1.563582
H	2.503095	2.257085	-2.234579
H	1.973275	0.564921	-2.133209
C	3.749296	-0.338396	1.615306
C	3.415854	1.091805	-0.620571
C	5.236941	-0.341352	1.333351
H	5.415109	-0.314815	0.256707
H	5.674094	0.557236	1.787071
H	5.685469	-1.205514	1.829488
O	4.311501	0.470158	-1.325286

O	3.314703	-0.737540	2.680111
H	0.297858	-5.075769	-0.811767
H	-2.557240	4.704608	0.275817
H	2.146365	0.929226	1.168740
C	3.911464	2.433832	0.002841
H	4.269523	3.076275	-0.805806
H	3.124048	2.959116	0.553241
H	4.748021	2.248472	0.681443

(P)-**12**			
C	3.454290	1.000536	-0.554803
C	2.194881	0.425495	-0.204628
C	1.071668	1.291490	-0.193959
C	1.243237	2.696486	-0.273742
C	2.531538	3.231141	-0.462517
C	3.627020	2.370661	-0.633721
C	-0.261769	0.758145	-0.176264
C	0.112924	3.599620	-0.186838
H	4.577609	2.817568	-0.886485
C	-1.173771	3.010968	0.080471
C	-1.373370	1.645981	0.141456
O	2.726520	4.544564	-0.546874
O	0.272274	4.854297	-0.261960
O	-2.233774	3.857378	0.296732
O	4.435829	0.131308	-0.897160
C	-2.138211	4.665877	1.463397
H	-2.075983	4.039091	2.363792
H	-1.270160	5.328219	1.412637
H	-3.056321	5.257417	1.503871
C	2.916624	-1.871946	0.626014
C	1.966376	-0.973820	0.042305
C	0.673520	-1.487805	-0.210140
C	0.414809	-2.878451	-0.128428
C	1.430997	-3.749146	0.299709
C	2.671444	-3.229375	0.706300
C	-0.428937	-0.602516	-0.465986
C	-0.879184	-3.426916	-0.483055
H	3.384566	-3.919283	1.133428
C	-1.874691	-2.495662	-0.997181
C	-1.666972	-1.144816	-0.994653
O	1.225791	-5.060168	0.388847
O	-1.105641	-4.661689	-0.424154
O	-2.971132	-3.043485	-1.587487
O	4.015773	-1.305540	1.177359

C	-4.020673	-3.394404	-0.670381
H	-3.651284	-4.117998	0.064992
H	-4.392496	-2.478485	-0.195847
H	-4.801520	-3.862807	-1.275690
C	5.733116	0.630851	-1.121727
H	6.364559	-0.240095	-1.307933
H	5.769523	1.294984	-1.995299
H	6.112315	1.176800	-0.248358
C	5.006753	-2.144423	1.723543
H	4.622388	-2.731709	2.567496
H	5.413862	-2.832553	0.971410
H	5.800229	-1.483284	2.077081
C	-2.669509	1.121555	0.625738
C	-2.667182	-0.226624	-1.607784
H	-3.282865	-0.784787	-2.314450
H	-2.137275	0.566574	-2.143793
C	-3.681274	0.429275	-0.590269
H	1.792106	4.938064	-0.447595
H	0.263636	-5.181423	0.089932
H	-3.273610	1.962871	0.957985
C	-4.297650	1.668700	-1.295470
H	-4.817087	1.330146	-2.199298
H	-5.037494	2.117509	-0.626905
H	-3.557759	2.427665	-1.567536
C	-2.601929	0.139813	1.778498
C	-3.852431	0.156981	2.629091
H	-3.994951	1.143581	3.084765
H	-4.680417	-0.031334	1.931277
H	-3.789741	-0.609059	3.404136
O	-1.680127	-0.614993	2.016551
O	-4.566976	-0.380884	-0.104788

	M		
C	1.431125	-2.411901	0.623424
C	0.715383	-1.301948	0.152388
C	1.435577	-0.081230	0.017356
C	2.865906	-0.063891	0.034609
C	3.553703	-1.267103	0.356772
C	2.834224	-2.393444	0.693786
C	0.718305	1.144557	-0.136073
C	3.515799	1.156116	-0.261334
H	3.392524	-3.264128	1.006401
C	2.796367	2.281904	-0.596299

C	1.392006	2.299217	-0.556585
O	4.904658	-1.358701	0.380916
O	4.885411	1.220316	-0.242806
O	3.559700	3.376716	-0.983752
C	-1.433119	-2.410739	-0.624841
C	-0.716401	-1.301371	-0.154007
C	-1.435643	-0.080146	-0.018535
C	-2.865978	-0.061832	-0.035021
C	-3.554795	-1.264565	-0.356939
C	-2.836259	-2.391351	-0.694451
C	-0.717423	1.145063	0.134973
C	-3.514858	1.158503	0.261759
H	-3.395281	-3.261616	-1.007016
C	-2.794462	2.283648	0.596808
C	-1.390141	2.300041	0.556222
O	-4.905821	-1.355254	-0.380354
O	-4.884438	1.223729	0.244119
O	-3.556935	3.378641	0.985436
H	5.280447	-0.492424	0.166060
H	-5.280917	-0.488730	-0.165284
O	-0.719164	-3.475889	-1.064075
O	0.716204	-3.476685	1.061948
C	-1.383307	-4.700478	-1.289830
H	-0.603285	-5.428020	-1.521151
H	-1.935452	-5.029201	-0.400843
H	-2.076543	-4.641356	-2.138621
C	1.380091	-4.700506	1.292601
H	0.599670	-5.427527	1.524199
H	1.934326	-5.031693	0.405822
H	2.071414	-4.638929	2.142785
C	-0.634079	3.498932	1.079354
C	0.636992	3.498683	-1.079978
C	0.001330	4.386642	-0.000449
H	0.179356	3.114448	1.704739
H	-0.176236	3.114741	-1.705960
H	1.285324	4.088623	-1.734609
H	-5.122221	2.130864	0.482608
H	5.124014	2.127444	-0.480503
H	3.184835	4.175717	-0.600620
H	-0.741808	5.042278	-0.472443
H	0.744237	5.042736	0.471278
H	-1.281627	4.089177	1.734497
H	-3.181769	4.177796	0.602942

TS OMe-flip			
C	1.629341	-2.513507	0.173927
C	0.751180	-1.393135	0.078853
C	1.444004	-0.119204	0.049886
C	2.882469	-0.005645	0.118962
C	3.651732	-1.167238	0.379876
C	3.009668	-2.377499	0.405969
C	0.717503	1.104032	-0.112832
C	3.498758	1.249550	-0.109314
H	3.627633	-3.250667	0.555785
C	2.761851	2.345168	-0.487284
C	1.362067	2.284644	-0.529329
O	4.995512	-1.172302	0.566314
O	4.866497	1.375441	-0.008633
O	3.500094	3.473837	-0.836792
C	-1.630191	-2.512850	-0.174293
C	-0.751520	-1.392862	-0.079441
C	-1.443867	-0.118686	-0.050515
C	-2.882270	-0.004564	-0.119911
C	-3.651865	-1.165771	-0.381603
C	-3.010280	-2.376282	-0.407467
C	-0.716996	1.104220	0.112768
C	-3.498199	1.250687	0.109033
H	-3.628409	-3.249228	-0.557851
C	-2.760971	2.345830	0.487778
C	-1.361195	2.284805	0.529866
O	-4.995519	-1.170187	-0.568929
O	-4.865900	1.376998	0.008335
O	-3.498877	3.474506	0.838097
H	5.335023	-0.265236	0.454584
H	-5.334704	-0.263061	-0.456713
O	-1.165945	-3.773977	-0.020052
O	1.164200	-3.774470	0.021007
C	-2.045054	-4.876829	0.026676
H	-1.412699	-5.736037	0.261388
H	-2.807101	-4.763105	0.808643
H	-2.542072	-5.053536	-0.936691
C	2.042392	-4.878107	-0.023916
H	1.409266	-5.737280	-0.256655
H	2.804199	-4.766531	-0.806430
H	2.539664	-5.053284	0.939593
C	-0.599285	3.466836	1.085064
C	0.600572	3.467128	-1.084120
C	0.000627	4.373765	0.000582

H	0.228890	3.076670	1.686797
H	-0.227502	3.077551	-1.686344
H	1.246957	4.035172	-1.762188
H	-5.073636	2.301875	0.237481
H	5.074472	2.300394	-0.237232
H	3.059164	4.261649	-0.483812
H	-0.756805	5.031011	-0.450505
H	0.758046	5.030940	0.451817
H	-1.245342	4.034683	1.763586
H	-3.058360	4.262358	0.484676

INT			
C	1.501195	-2.449756	-0.333468
C	0.731013	-1.316502	-0.014860
C	1.439859	-0.084114	0.114982
C	2.871333	-0.072400	0.200318
C	3.574308	-1.308127	0.164825
C	2.891392	-2.460794	-0.151279
C	0.730914	1.157942	0.000851
C	3.533371	1.176989	0.208107
H	3.473826	-3.357421	-0.305911
C	2.846599	2.332525	-0.074791
C	1.455507	2.333619	-0.264089
O	4.914065	-1.404569	0.333708
O	4.890425	1.234016	0.397309
O	3.634665	3.464535	-0.245472
C	-1.502003	-2.449314	0.332692
C	-0.731407	-1.316261	0.014239
C	-1.439795	-0.083585	-0.115321
C	-2.871278	-0.071279	-0.200514
C	-3.574724	-1.306718	-0.165131
C	-2.892228	-2.459717	0.150690
C	-0.730373	1.158206	-0.001015
C	-3.532842	1.178365	-0.208071
H	-3.475040	-3.356133	0.305073
C	-2.845611	2.333594	0.074928
C	-1.454504	2.334114	0.264149
O	-4.914534	-1.402629	-0.333888
O	-4.889888	1.235923	-0.397160
O	-3.633222	3.465892	0.245817
H	5.280730	-0.514527	0.440732
H	-5.280864	-0.512433	-0.440791
O	-0.866523	-3.502905	0.900746
O	0.865396	-3.502853	-0.902038

C	-1.548247	-4.731354	1.027391
H	-0.819072	-5.440364	1.423369
H	-2.392712	-4.662246	1.724887
H	-1.915040	-5.091649	0.058227
C	1.545298	-4.732659	-1.025328
H	0.815474	-5.441375	-1.420647
H	2.390643	-4.666404	-1.722041
H	1.910431	-5.091417	-0.054977
C	-0.817955	3.534143	0.928918
C	0.819432	3.533992	-0.928687
C	0.000898	4.434954	0.000183
H	-0.131410	3.145043	1.689551
H	0.132759	3.145271	-1.689397
H	1.588742	4.105999	-1.454640
H	-5.147929	2.160464	-0.275324
H	5.148825	2.158474	0.275616
H	3.199926	4.217613	0.166440
H	-0.639827	5.090887	-0.603553
H	0.641856	5.090565	0.604021
H	-1.587041	4.106354	1.454976
H	-3.198256	4.218836	-0.166100

TS ring-flip			
C	1.453049	-2.424446	-0.413844
C	0.712280	-1.283158	-0.059084
C	1.435261	-0.065050	0.112625
C	2.860211	-0.126579	0.261800
C	3.529359	-1.383038	0.210739
C	2.833001	-2.498215	-0.190876
C	0.757444	1.209489	-0.003549
C	3.570934	1.086667	0.314654
H	3.391262	-3.406204	-0.366651
C	2.940702	2.269004	0.025581
C	1.547442	2.365463	-0.199431
O	4.855192	-1.527107	0.440157
O	4.919773	1.092723	0.538683
O	3.801777	3.371610	-0.021406
C	-1.497588	-2.425817	0.301742
C	-0.741392	-1.280233	-0.003463
C	-1.438971	-0.040908	-0.090840
C	-2.873008	-0.039415	-0.139455
C	-3.564313	-1.281177	-0.165782
C	-2.887068	-2.441287	0.121053
C	-0.723537	1.210225	0.012286

C	-3.547587	1.196795	-0.060252
H	-3.464306	-3.348947	0.221894
C	-2.865759	2.363595	0.156761
C	-1.458215	2.373535	0.267678
O	-4.904479	-1.371070	-0.382935
O	-4.954374	1.287176	-0.126270
O	-3.550097	3.536944	0.300689
H	5.244580	-0.653746	0.594437
H	-5.229782	-0.483636	-0.593894
O	-0.848808	-3.493856	0.832892
O	0.793992	-3.423240	-1.049374
C	-1.552614	-4.702693	1.010089
H	-0.830558	-5.414618	1.413678
H	-2.382343	-4.593894	1.720288
H	-1.945921	-5.086581	0.060104
C	1.391243	-4.699923	-1.119972
H	0.638777	-5.362082	-1.551990
H	2.278554	-4.703002	-1.765733
H	1.671531	-5.067221	-0.125304
C	-0.846051	3.688299	0.647368
C	1.168498	3.708326	-0.820113
C	-0.215476	4.322203	-0.588351
H	-0.073158	3.537214	1.410587
H	1.362614	3.624442	-1.899669
H	1.899215	4.425545	-0.441584
H	-5.306686	1.141083	0.761898
H	5.200951	2.014448	0.428681
H	3.788347	3.749036	-0.907559
H	-0.874097	4.160233	-1.445636
H	-0.111645	5.406043	-0.471149
H	-1.614226	4.334130	1.070276
H	-4.473983	3.332336	0.103629

P

C	1.425074	-2.403269	-0.646258
C	0.714005	-1.295659	-0.163434
C	1.434702	-0.075522	-0.031076
C	2.863586	-0.056317	-0.064803
C	3.549390	-1.256057	-0.402992
C	2.827301	-2.381922	-0.736727
C	0.718127	1.148994	0.139478
C	3.513674	1.154420	0.267955
H	3.382797	-3.250566	-1.059868
C	2.795975	2.274366	0.626233

C	1.390342	2.298275	0.572028
O	4.900101	-1.344755	-0.442947
O	4.882674	1.213491	0.269168
O	0.705612	-3.469299	-1.074487
C	-1.425017	-2.403341	0.645987
C	-0.713972	-1.295688	0.163199
C	-1.434685	-0.075554	0.030940
C	-2.863568	-0.056353	0.064729
C	-3.549347	-1.256107	0.402897
C	-2.827237	-2.381989	0.736538
C	-0.718128	1.148989	-0.139543
C	-3.513680	1.154397	-0.267948
H	-3.382736	-3.250650	1.059625
C	-2.796001	2.274365	-0.626191
C	-1.390366	2.298287	-0.572007
O	-4.900054	-1.344820	0.442913
O	-4.882679	1.213451	-0.269115
O	-0.705532	-3.469426	1.074051
C	1.369168	-4.690381	-1.320141
H	0.587100	-5.418958	-1.541054
H	2.046089	-4.623843	-2.181441
H	1.939123	-5.022835	-0.443848
C	-1.369255	-4.690188	1.320819
H	-2.045828	-4.622887	2.182332
H	-1.939625	-5.023158	0.444988
H	-0.587250	-5.418770	1.541935
C	0.626660	3.496318	1.085552
C	-0.626714	3.496381	-1.085457
H	-1.261017	4.111945	-1.730794
H	0.186337	3.115487	-1.713501
C	-0.000031	4.380498	0.000076
H	5.276303	-0.481674	-0.215897
H	-5.276275	-0.481734	0.215909
H	-0.186389	3.115363	1.713560
H	0.755100	5.028016	-0.459160
H	-0.755168	5.027980	0.459351
H	1.260935	4.111853	1.730947
H	-5.115672	2.105486	-0.565765
H	5.115653	2.105499	0.565904
O	-3.563933	3.387591	-0.960948
H	-3.284889	3.720646	-1.820066
O	3.563895	3.387572	0.961066
H	3.284701	3.720702	1.820106

Supplementary Figures

Figure S1. Map of pYFAC-CH3-7

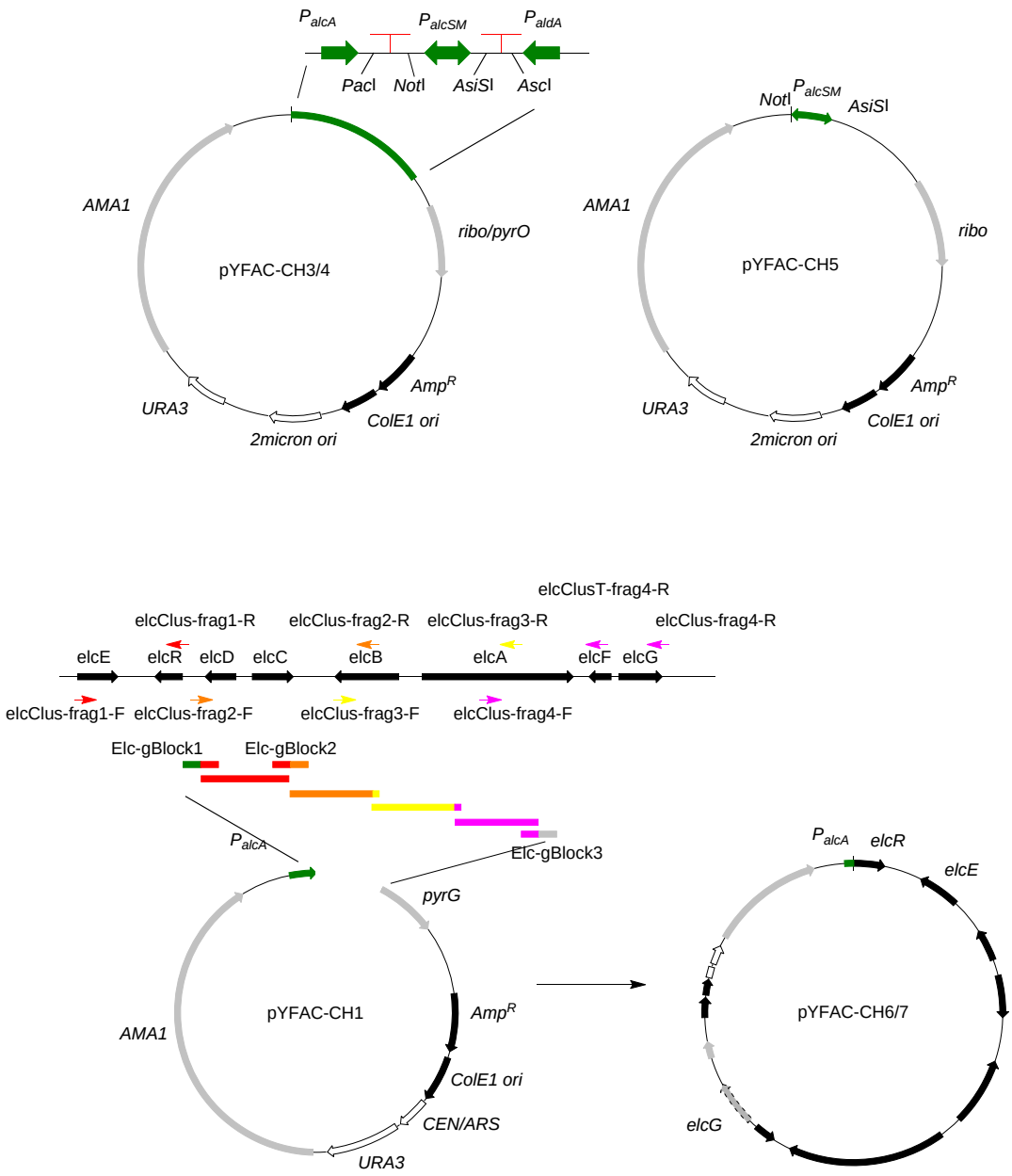

Figure S2. Comparison of 12/6 to known elsinochromes and hypocrellin A

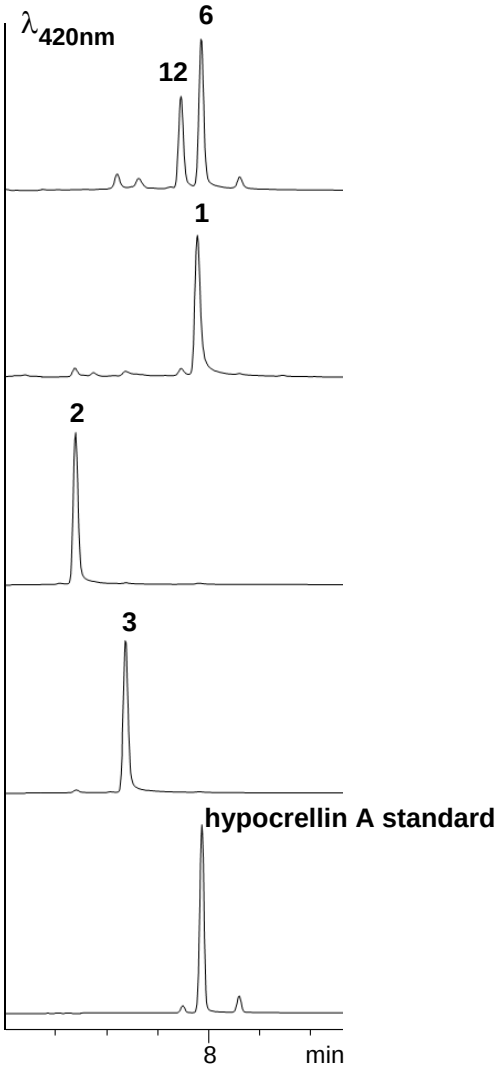

Figure S3. ECD-spectra of elsinochrome C (3), elsinochrome A (1) and 12/6

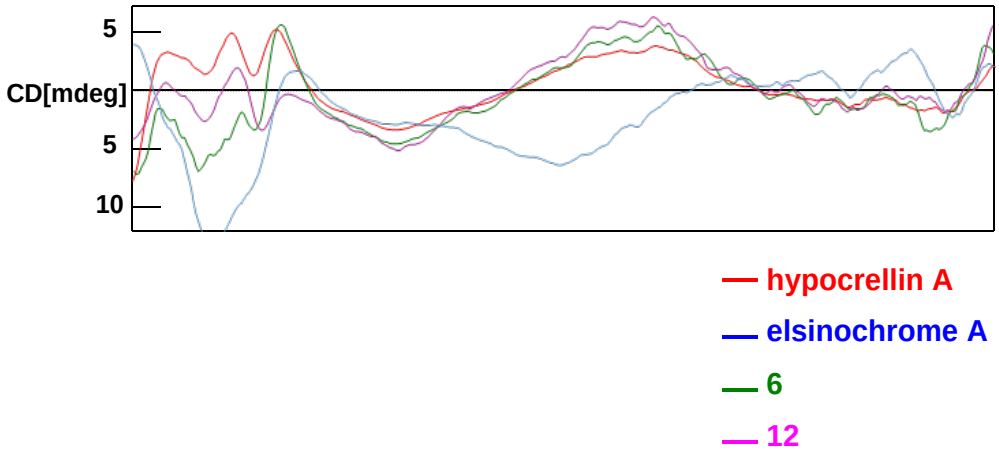

Figure S4. Key NOE interactions for 12 and 6 for determination of stereochemistry
C15-Ha chemical shift value: 2.34 ppm, C15-Hb chemical shift value: 3.67 ppm.

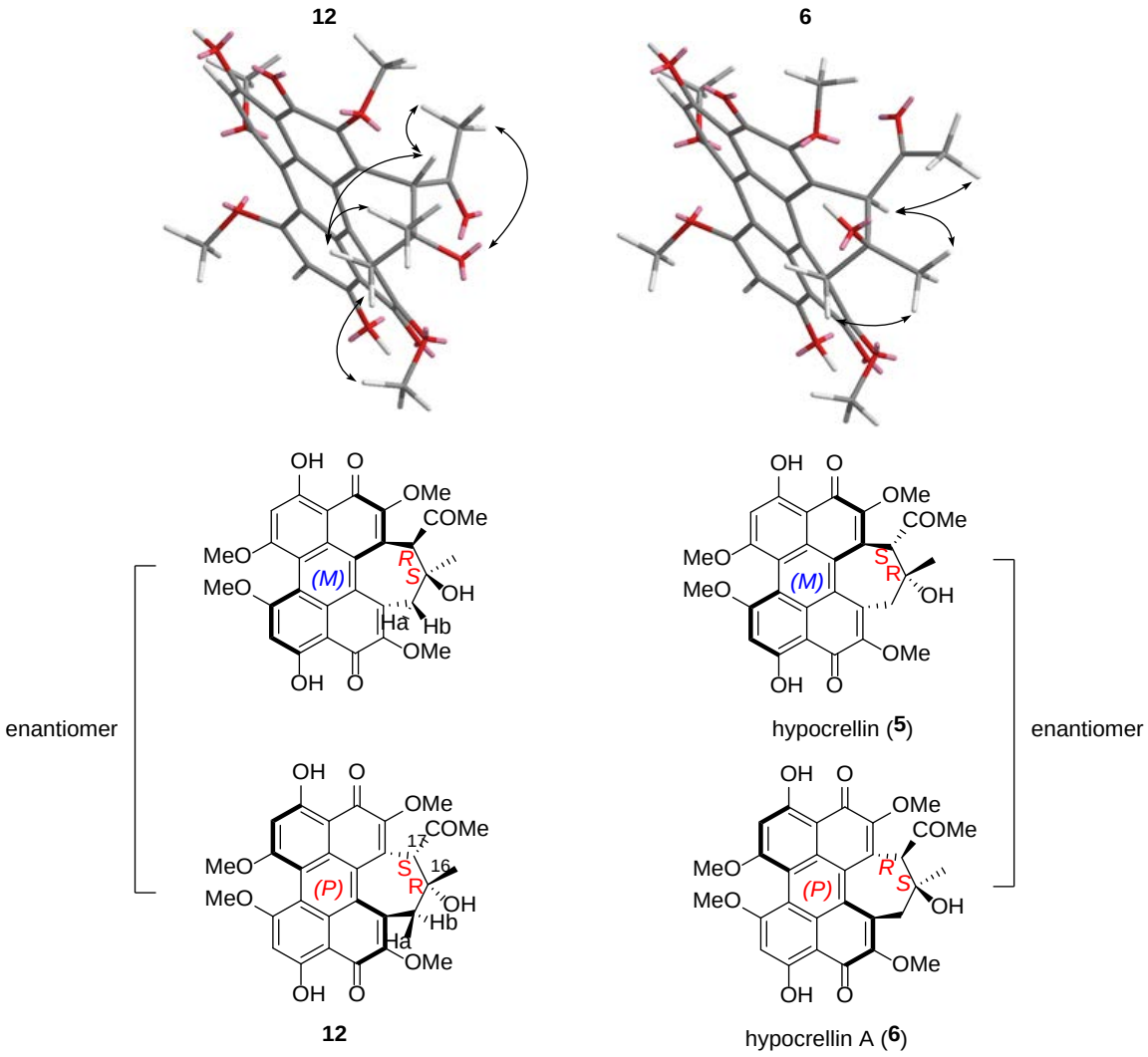

The NOE interaction data showed that the purified **12** could correspond to a pair of enantiomer where the compound either adopt a (*M*) helicity with the stereochemistry at C16-17 is *S*,*R* or adopt a (*P*) helicity where C16-17 is *R*,*S*. Likewise, **6** could adopt a (*M*) helicity where the stereochemistry at C16-17 is *R*,*S* or adopt a (*P*) helicity where C16-17 is *S*,*R*.

Figure S5. In planta transcriptomic data of elc cluster and genes surrounding it

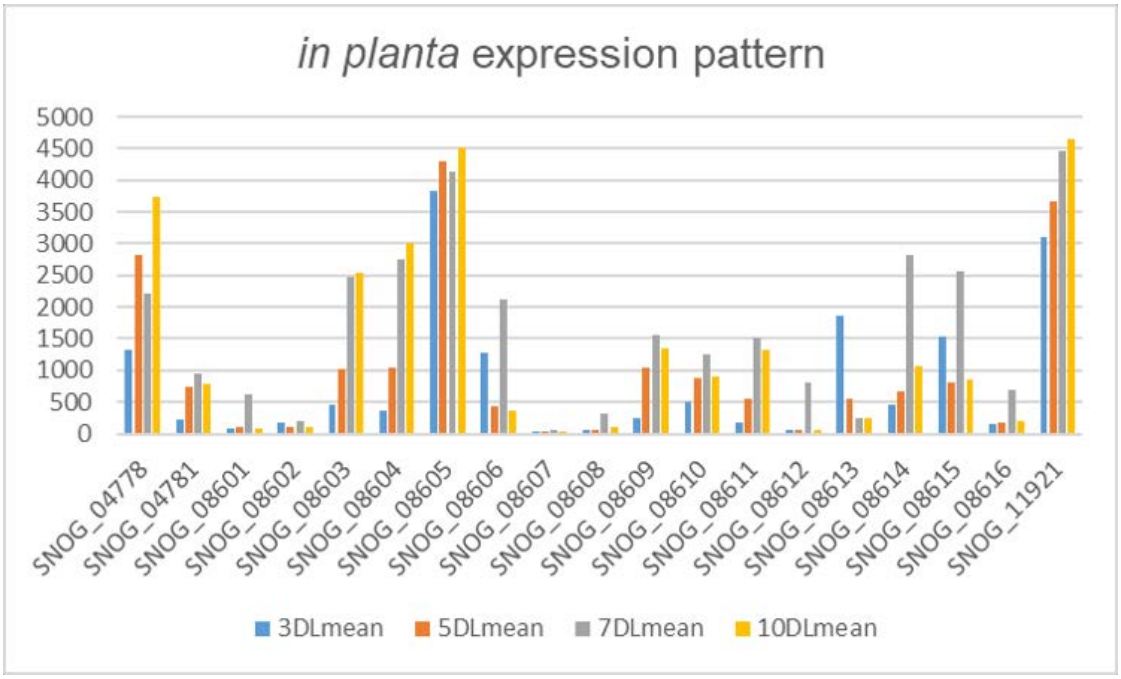

DLmean – mean expression value at No. of days post inoculation

Figure S6. CRISPR-Cas9 targeted-disruption of *elcE* and *elcB*

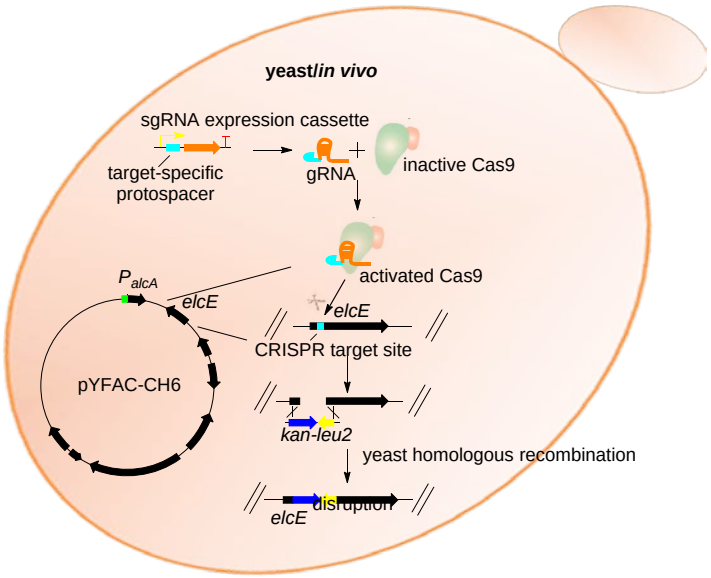

Figure S7. Phyre2 modeling of ElcE.

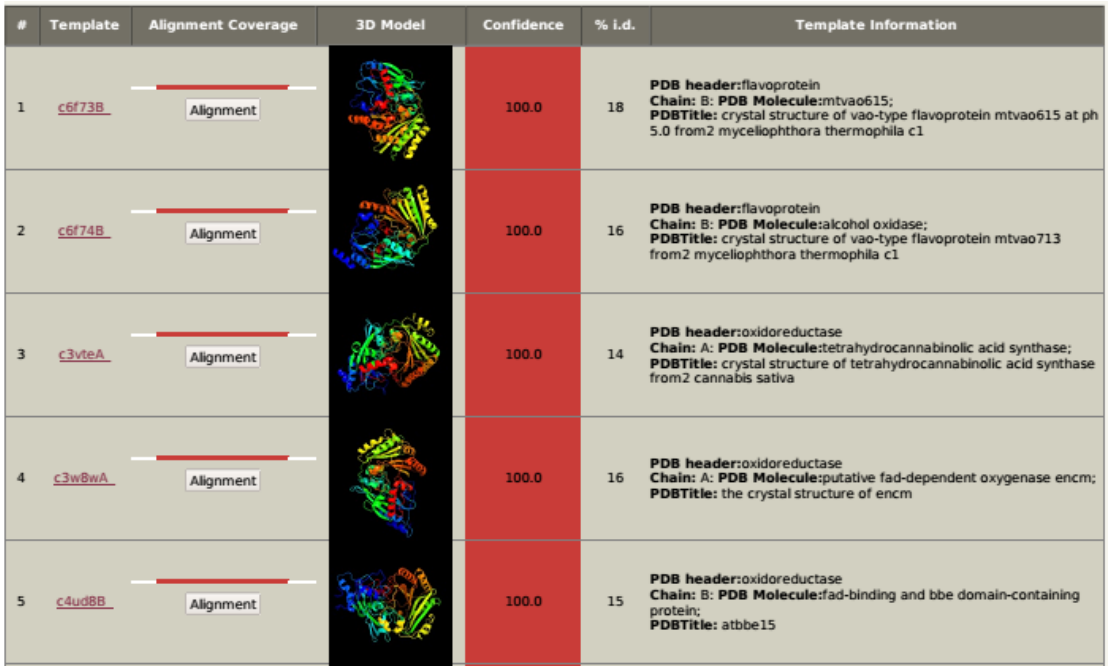

#	Template	Alignment Coverage	3D Model	Confidence	% i.d.	Template Information
1	c6f73B	Alignment		100.0	18	**PDB header:**flavoprotein **Chain:** B: **PDB Molecule:**mtvao615; **PDBTitle:** crystal structure of vao-type flavoprotein mtvao615 at ph 5.0 from2 myceliophthora thermophila c1
2	c6f74B	Alignment		100.0	16	**PDB header:**flavoprotein **Chain:** B: **PDB Molecule:**alcohol oxidase; **PDBTitle:** crystal structure of vao-type flavoprotein mtvao713 from2 myceliophthora thermophila c1
3	c3vteA	Alignment		100.0	14	**PDB header:**oxidoreductase **Chain:** A: **PDB Molecule:**tetrahydrocannabinolic acid synthase; **PDBTitle:** crystal structure of tetrahydrocannabinolic acid synthase from2 cannabis sativa
4	c3w8wA	Alignment		100.0	16	**PDB header:**oxidoreductase **Chain:** A: **PDB Molecule:**putative fad-dependent oxygenase encm; **PDBTitle:** the crystal structure of encm
5	c4ud8B	Alignment		100.0	15	**PDB header:**oxidoreductase **Chain:** B: **PDB Molecule:**fad-binding and bbe domain-containing protein; **PDBTitle:** atbbe15

Phyre2 results showed that ElcE is most similar to berberine bridge enzyme-like oxidases (BBLOs) or the vanillyl alcohol oxidases (VAOs), which are known to have a covalently linked flavin cofactor. There are not many homology crystal structures in the PDB database but all the top hits belong to the same family of oxidases. The first two hits are from the thermophilic fungus *Myceliopthora thermophila*.[31] The exact substrate for these two enzymes are unclear but ricinoleic acid was identified as a poor substrate for mtvao713 MtVAO713. The third hit is the well-characterised THC (Tetrahydrocannabinolic Acid) synthase from *Cannabis sativa*, which is known to catalyze an intramolecular C-C bond formation via a hydride transfer mechanism

Figure S8. LC-DAD-MS analysis of pYFAC-CH-7/9

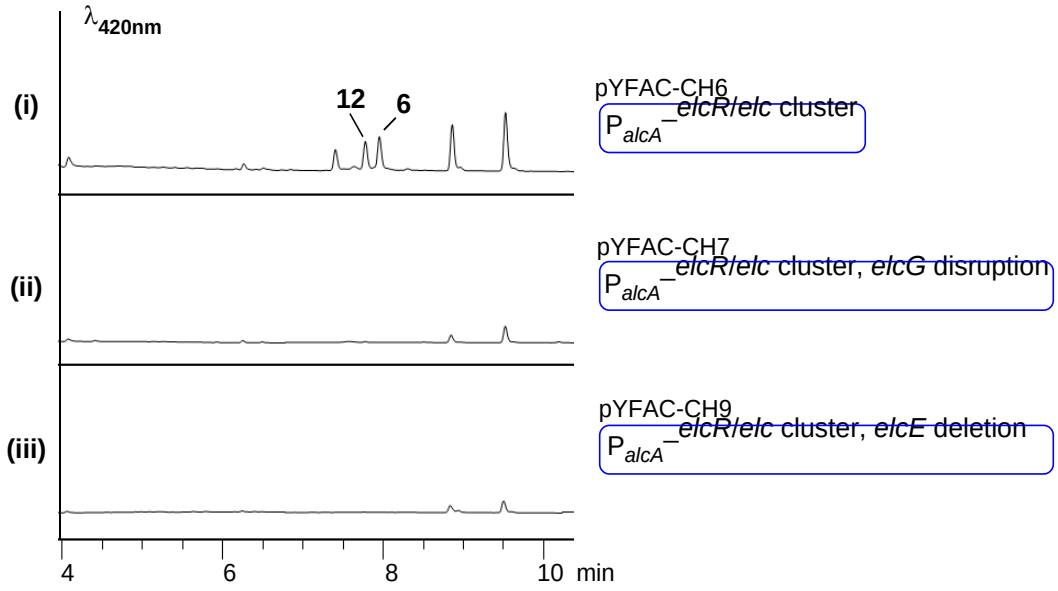

Figure S9. HRMS of 13, 14, 15, 16, 19, 20 and their corresponding UV-vis spectra

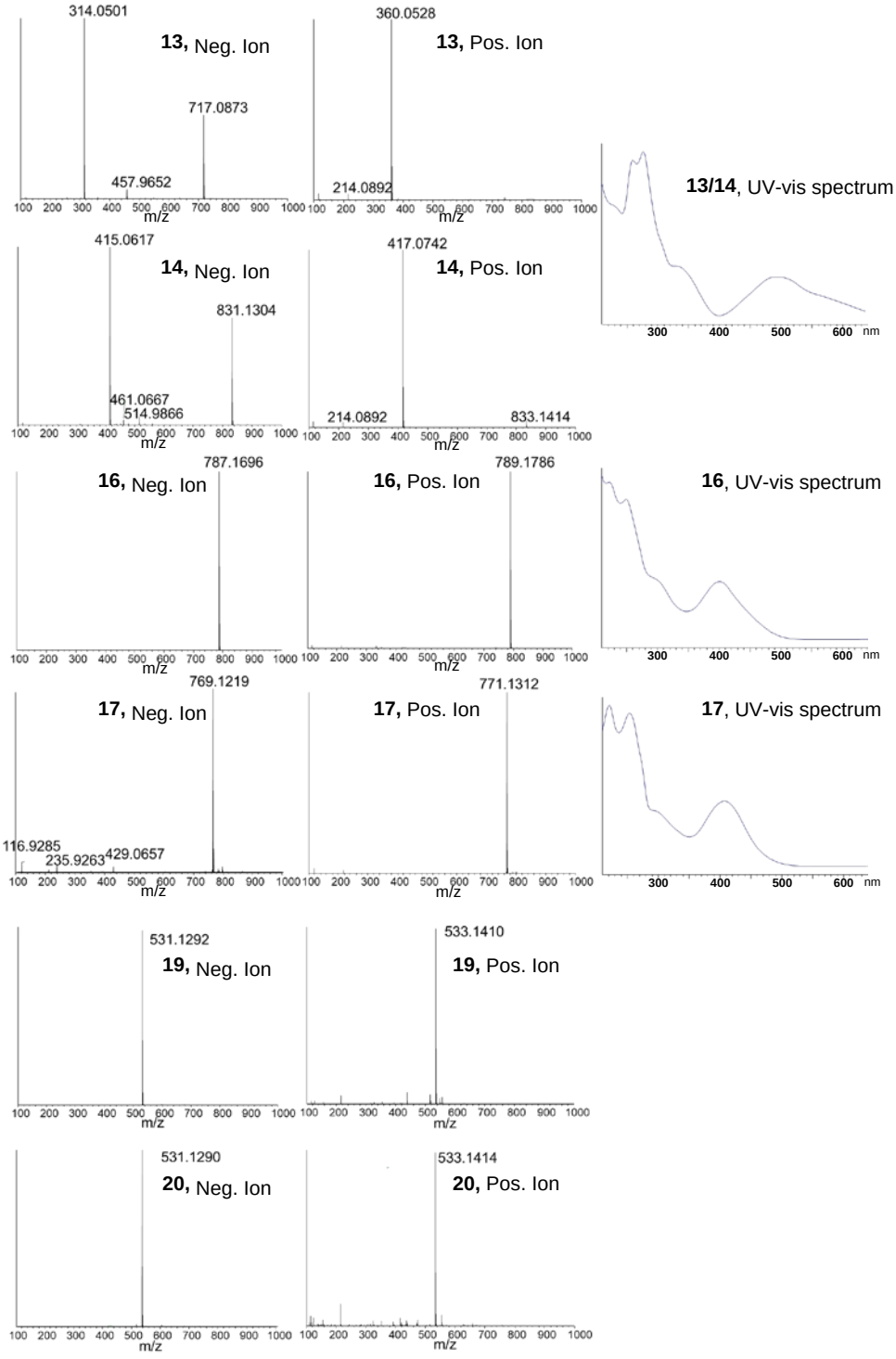

Figure S10. Extra metabolite profiling data from pathway reconstruction

(A) extra chromatogram data for other gene combinations not detailed in main manuscript. (B) Different replicates for combination of *elcA/B/D/E/G*. (C) UV-spectra of **15, 15'** and **18**.

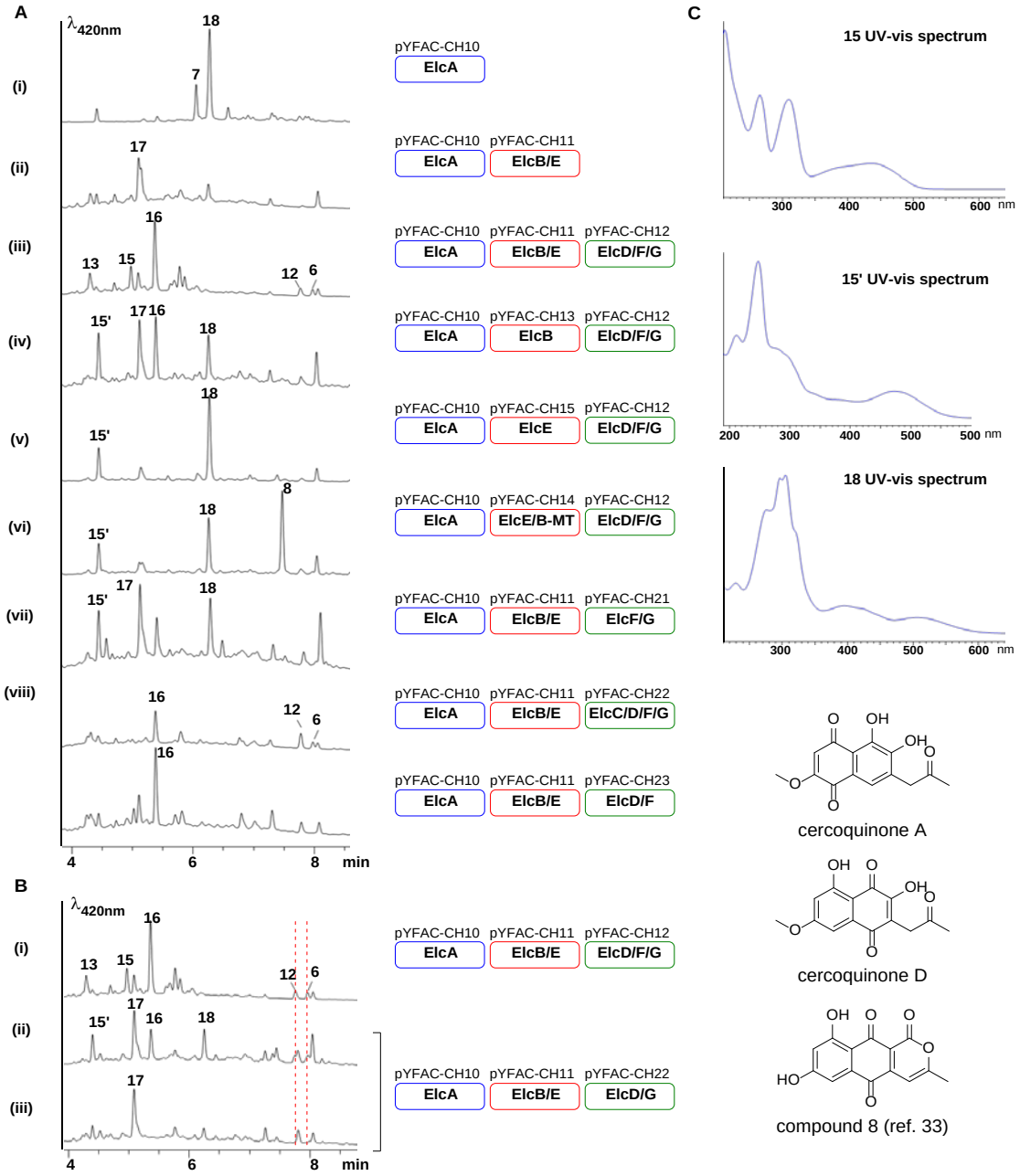

Compound **15** with *m/z* of 277 $[M+H]^+$was hypothesized to be related to cercoquinone A-D,[32] while **15'** has an *m/z* of 275$[M+H]^+$ and possessed an UV-spectra similar to the naphthoquinone derivative of nor-toralactone **6** identified by Newman and Townsend (labeled as compound 8 in the study).[32] Unfortunately, we were unable to isolate sufficient quantities for NMR characterization due to low yield and stability. *A. nidulans* expressing the combination *elcA/B/E* (without *elcD*) produced **17** with *m/z* of 771.1324$[M+H]^+$/769.1212$[M-H]^-$ (Figure S8) instead of **16**. The high resolution mass of **17** is consistent with $C_{42}H_{26}O_{15}$ (calculated m/z 771.1344 $[M+H]^+$/ 769.1199$[M-H]^-$). Unfortunately, **17** was unstable and

decomposed during isolation after repeated attempts. Thus, we were unable to obtain sufficient amount of the compound for NMR analysis. Nonetheless, the chemical formula $C_{42}H_{26}O_{15}$ suggests that **17** is a trimer like **16** and is of similar oxidation level, except lacking the methyl group introduced by ElcD on **16**. **18** was accumulated in prolonged culture of *A. nidulans* expressing *elcA* encoding the PKS only, but also in (iv) and (v) when either *elcE* or intact *elcB* is missing. Its UV-spectra is similar to that of **7** as shown in Figure S10. The compound possesses a strong UV absorbance at 280 nm, but our mass spectrum method failed to detect any mass peak within the range of *m/z* [100-1000]. It is hypothesized that **18** is formed from polymerization of **7**.

In the absence of *elcF*, the results varied. Here we showed the different replicates where the production of **12**/**6** is abolished for B-iii but not B-ii.

Figure S11. SignalP analysis of ElcE, ElcF, ElcG and ElcH.

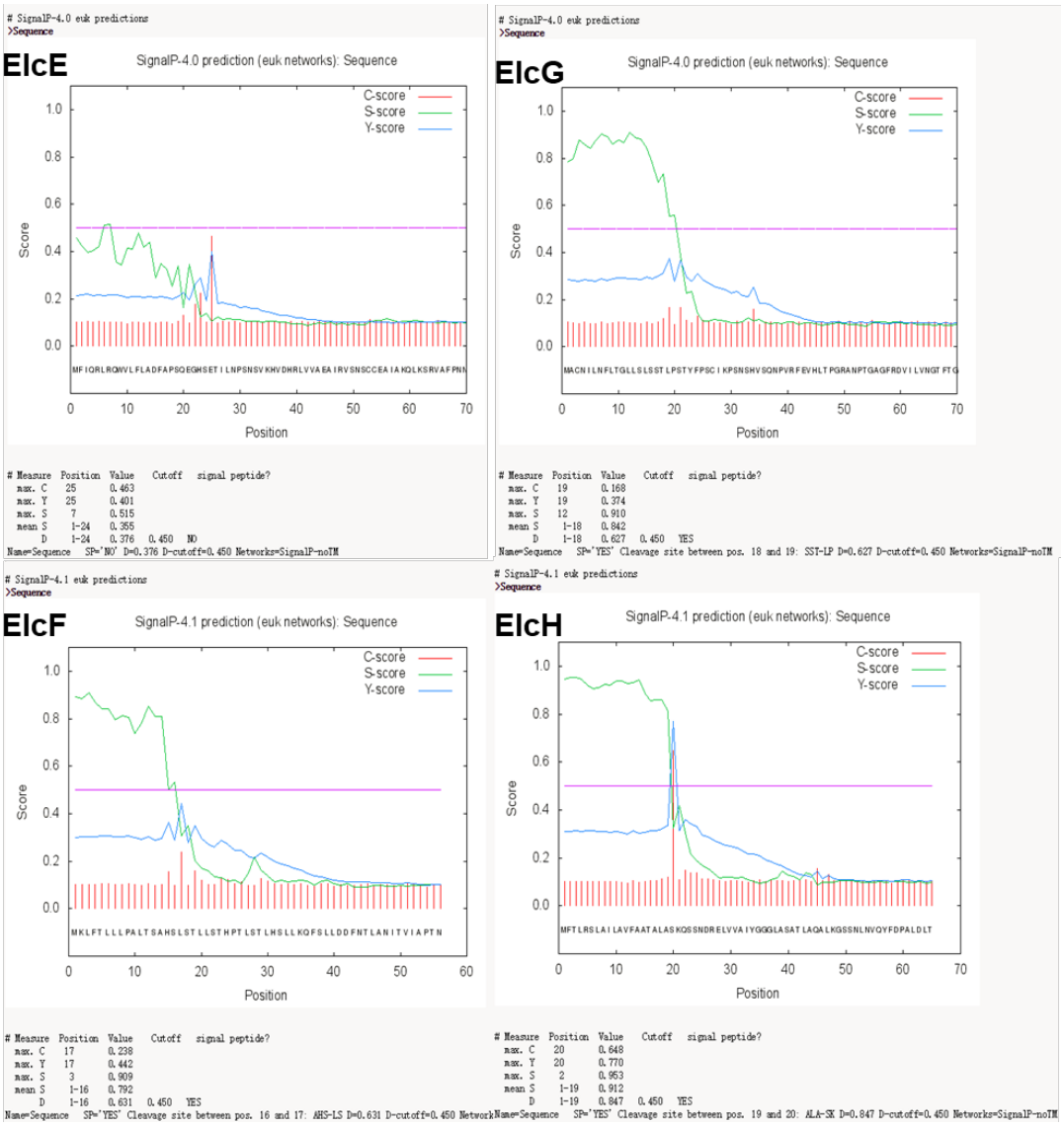

For enzyme complex to form, the enzymes must be occupying the same cellular space for them to interact. However, SignalP predicted a signal peptide at the N-terminus of ElcG suggesting that the protein is secreted. A closer inspection of the ElcE SignalP prediction result showed that although no signal peptide was predicted, the C- and Y- scores at the 25th amino acid residue from the N-terminal were just below the threshold. Likewise, the ElcF and ElcH was predicted to have an N-terminal signal peptide as well. Therefore, it is possible that these four proteins formed an extracellular complex as proposed by Frandsen et al. in aurofusarin biosynthesis.[33]

Curiously, the recently characterised laccase-like multicopper oxidase MCE from *Talaromyces pinophilus* that involved in oxidative coupling of napthopyranones was also predicted to have an N-terminus signal peptide by SignalP and that the Edman degradation sequence started exactly after the predicted cleavage site.[34] However, the authors reported no catalytic activity was present in the culture filtrate and the enzyme was isolated from mycelial fraction of the culture.

Therefore, it is possible that these biosynthetic proteins with N-terminus signal peptide might be transported to a sub-cellular compartment via endoplasmic reticulum but not secreted or remained at the cell surface post-secretion. The subcellular localisation of these enzymes is currently under investigation.

Figure S12. Gibbs free-energy reaction profile for the aldol reaction (i) and the two-step atropisomerization process (ii) ($\Delta G_{298,aq}$, DSD-PBEP86/Def2-TZVPP, kJ mol^{-1}).

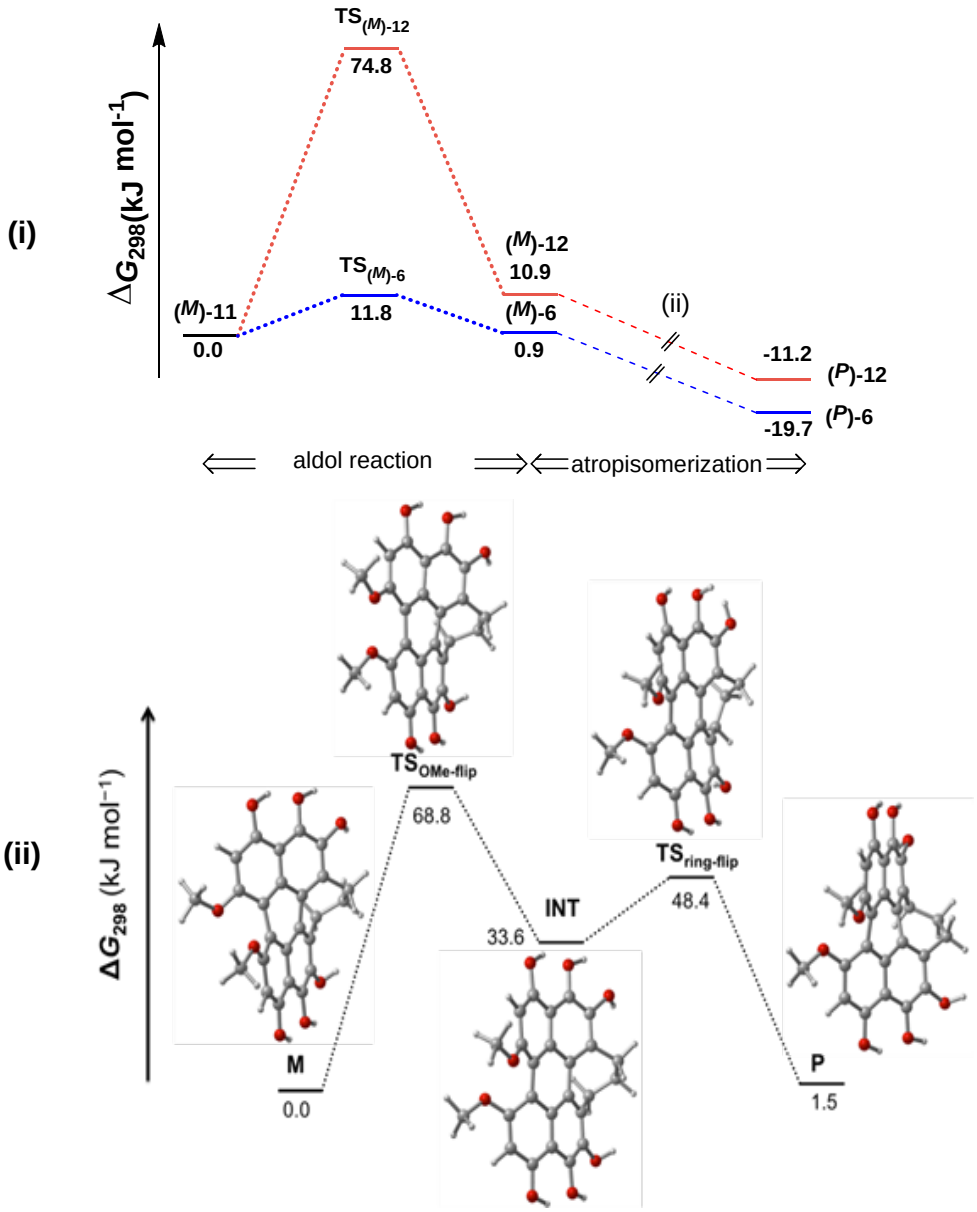

Double-hybrid density functional theory (DHDFT) calculations using the spin-component-scaled DSD-PBEP86 exchange-correlation functional was performed in a simulated aqueous environment in order to explore the potential energy surface (PES) for the conversion of the precursor (*M*)-**11** to hypocrellins (*P*)-**6** and (*P*)-**12**. Our DHDFT simulations supported that this is a multistep reaction, which involves an aldol reaction of (*M*)-**11** to (*M*)-**6** and (*M*)-**12** followed by an atropisomerization step to yield the corresponding (*P*)-**6** and (*P*)-**12** products.

In (i), if the C(O)Me group of (*M*)-**11** points above the plane of the molecule during the electrophonic attack it will lead to the formation of the (*M*)-**6** intermediate (via $TS_{(M)\text{-}6}$). Alternatively, if points below the plane, it will lead to the formation of the (*M*)-**12** intermediate (via $TS_{(M)\text{-}12}$). DHDFT simulations show that

$TS_{(M)\text{-}\mathbf{6}}$ has a significantly lower reaction barrier height for the aldol reaction, lies 11.8 kJ mol^{-1} above the reactant (*M*)-**11**, whereas, $TS_{(M)\text{-}\mathbf{12}}$ lies 74.8 kJ mol^{-1} above. Inspection of the transition structures reveals that the length of the forming C•••C bond in $TS_{(M)\text{-}\mathbf{6}}$ is 1.916 Å, whereas in $TS_{(M)\text{-}\mathbf{12}}$ the length increases to 2.129 Å due to larger steric repulsion between the two C(O)Me side chains. Thus, the difference between the two activation energies is attributed to the longer C•••C bond length in $TS_{(M)\text{-}\mathbf{12}}$. However, it is important to stress that these reaction barrier heights indicate that both transition structures are accessible at that at the temperature at which the experiments were carried out (namely, 30° C). Similarly, the formed C–C bond in the *(M)*-**6** intermediate (1.618 Å) is shorter than that in the *(M)*-**12** intermediate (1.643 Å). The energy difference between the products of the aldol condensation reaction (*(M)*-**6** and *(M)*-**12**) is largely attributed to this difference in the length of the formed C–C bond. Although both transition structures are assessable at the experimental temperature, we cannot completely rule out that endogenous enzyme in *A. nidulans* could be responsible for the aldol reaction especially that one of the hypocrellin products, (*P*)-**12**, has higher energy barrier and it has never been reported previously.

The aldol condensation step results in the *(M)*-**6** and *(M)*-**12** intermediates (i), which lie 0.9 and 10.9 kJ mol^{-1}, respectively, above the energy of the *(M)*-11 reactant. These intermediates are high-energy atropisomers of the experimentally observed *(P)*-**6** and *(P)*-**12** products. In particular, the *(P)*-**6** and *(P)*-**12** products lie 19.7 and 11.2 kJ mol^{-1} below the energy of the *(M)*-**11** reactant, respectively.

It has been shown experimentally that the presence of a 7-membered in perylenequinones can lower the barrier for atropisomerization.[35, 36] However, to the best of our knowledge, this process has not been investigated computationally. It is worthwhile examining the possible reaction mechanism of the atropisomerization step. For reasons of computational efficiency, we have examined this process using a smaller model system in which the functional groups on the 7-membered ring were replaced by hydrgens. We find that atropisomerization can proceed via a two-step mechanism. In the first step the OMe groups on the one side of the molecule flip, and in the second step the conformation of the 7-membered ring changes to allow for the atropisomerization to be completed (ii). The Gibbs-free energy surface for the proposed two-step mechanism is shown in Figure S1 of the Supporting Information. The reaction barrier for the first step is 68.8 kJ mol^{-1}, whilst the reaction barrier for the second step is 48.4 kJ mol^{-1}. These results indicate that the atropisomerization is kinetically accessible at room temperature.

Figure S13. Atropisomerization of 12 and 6 at room temperature.

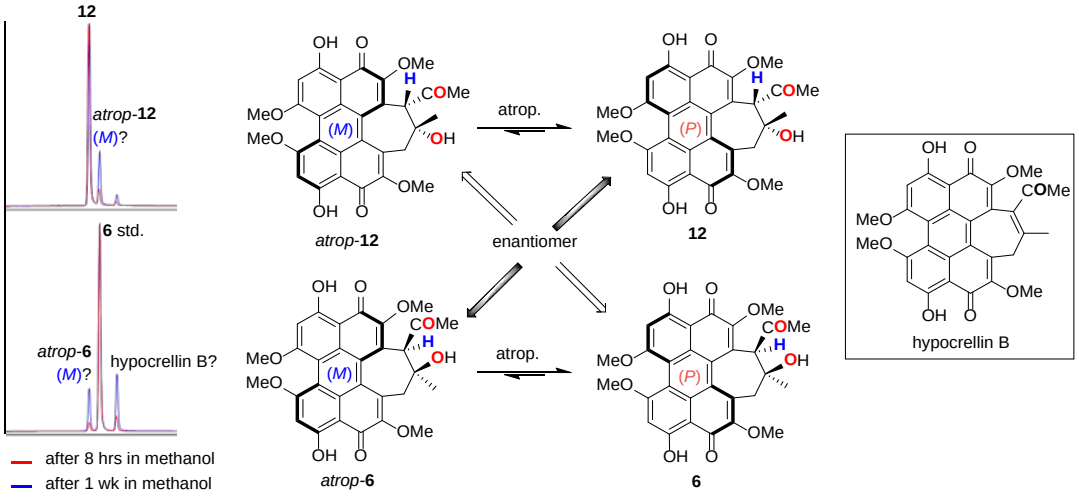

To test whether **12** and **6** could interconvert between their two atropisomeric forms, the purified compounds (dried) were individually dissolved in methanol and let them sit at room temperature to equilibrate over time. We took a small amount of sample for LC-DAD-MS after 8 hrs and then a week later. The LC-DAD-MS showed that, in the 8-hrs sample, a small peak was present in the **12** sample that corresponded to the t_R of **6**. Likewise, a small peak with the t_R corresponded to **12** can be found in the **6** sample. This two small peaks increased in ratio after one week. The two new peaks have identical UV-vis spectra and mass to **12** and **6**. It is highly likely that they correspond to the atropisomer of **12** and **6**, respectively, given that *atrop*-**6** is an enantiomer of **12** while *atrop*-**12** is an enantiomer of **6**, their t_R is expected to overlap.

Within the week, the ratio of the **12** against its putative atropisomer have gone from about 13:1 to approximately 4:1, while the ratio of **6** against its putative atropisomer have gone from approximately 30:1 to 5:1. The final ratio for **6** versus *atrop*-***6*** after a week is similar to what was previously reported.[35, 37] Therefore, the above results is strong evidence that supports our proposed atropisomerisation. Besides the conversion to atropisomer, in sample **6**, we also see an increase in ratio of another peak at a later t_R, which based on mass and UV-vis spectrum could be hypocrellin B (derivative of **6** formed by elimination of water, in box).

Figure S14. ^{1}H NMR spectrum (600 MHz) of 12 in $CDCl_3$-*d*

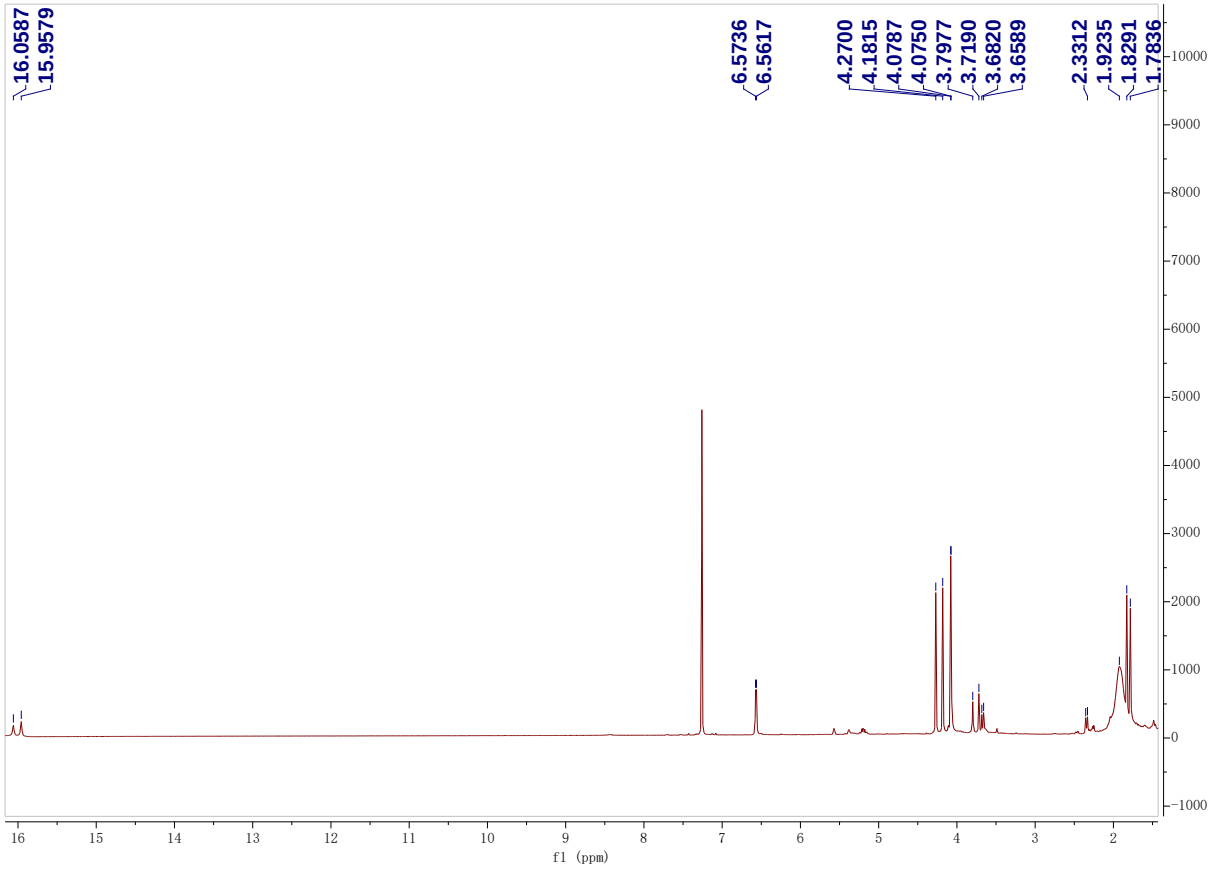

Figure S15. ^{13}C NMR spectrum (150 MHz) of 12 in $CDCl_3$-*d*

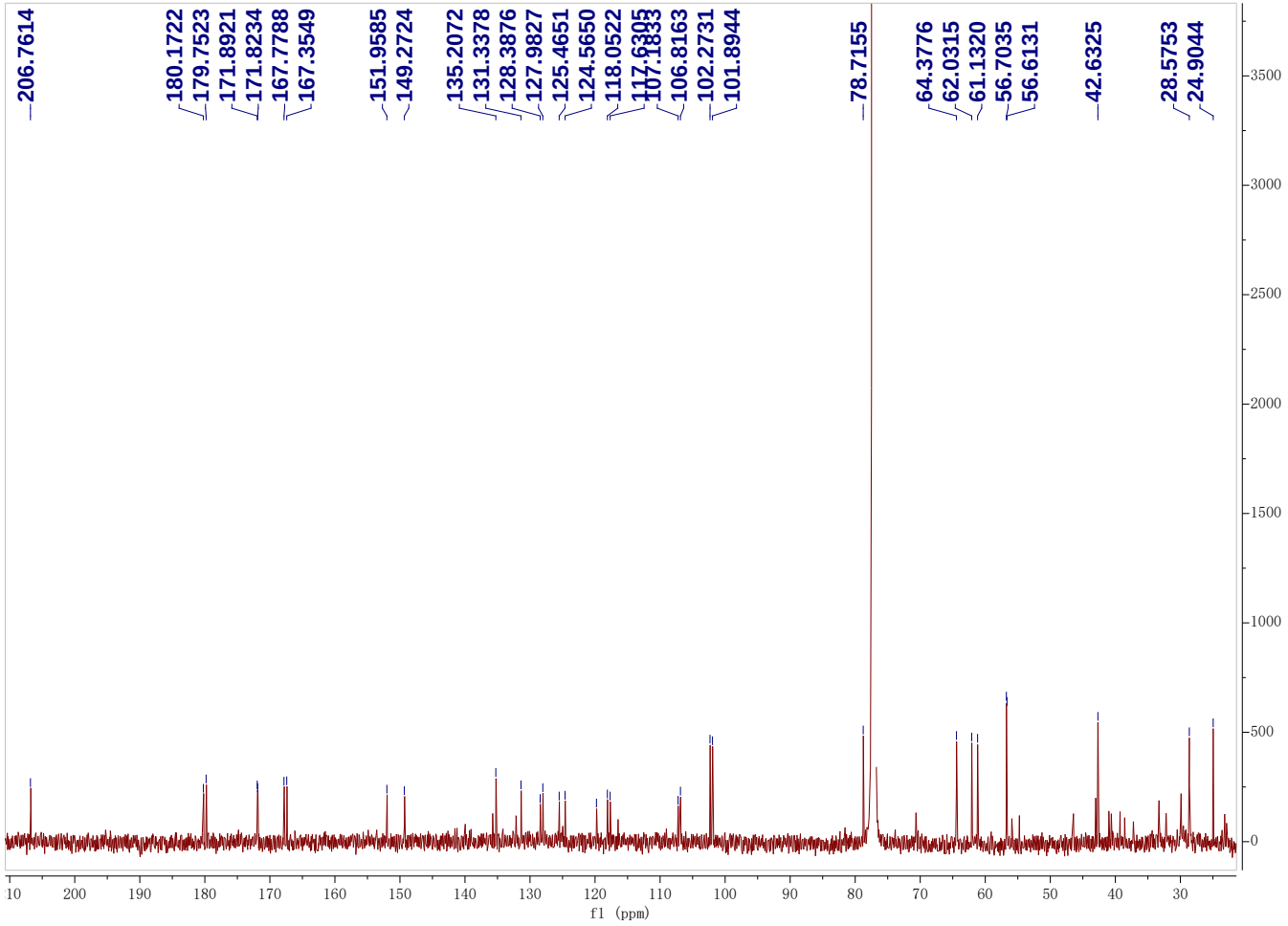

Figure S16. ^{1}H-^{1}H gCOSY NMR spectrum (600 MHz) of 12 in $CDCl_3$-*d*

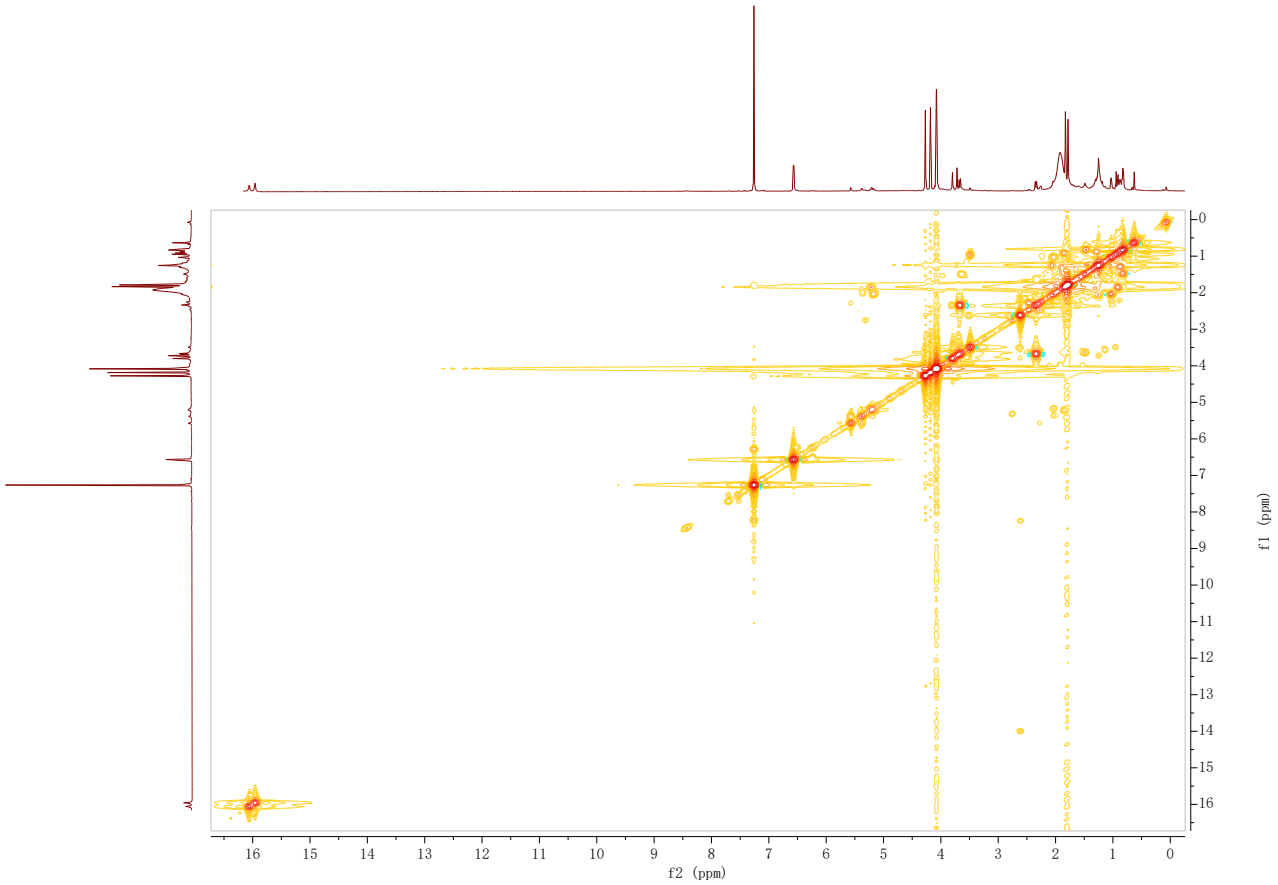

Figure S17. HSQC NMR spectrum (600 MHz) of 12 in $CDCl_3$-*d*

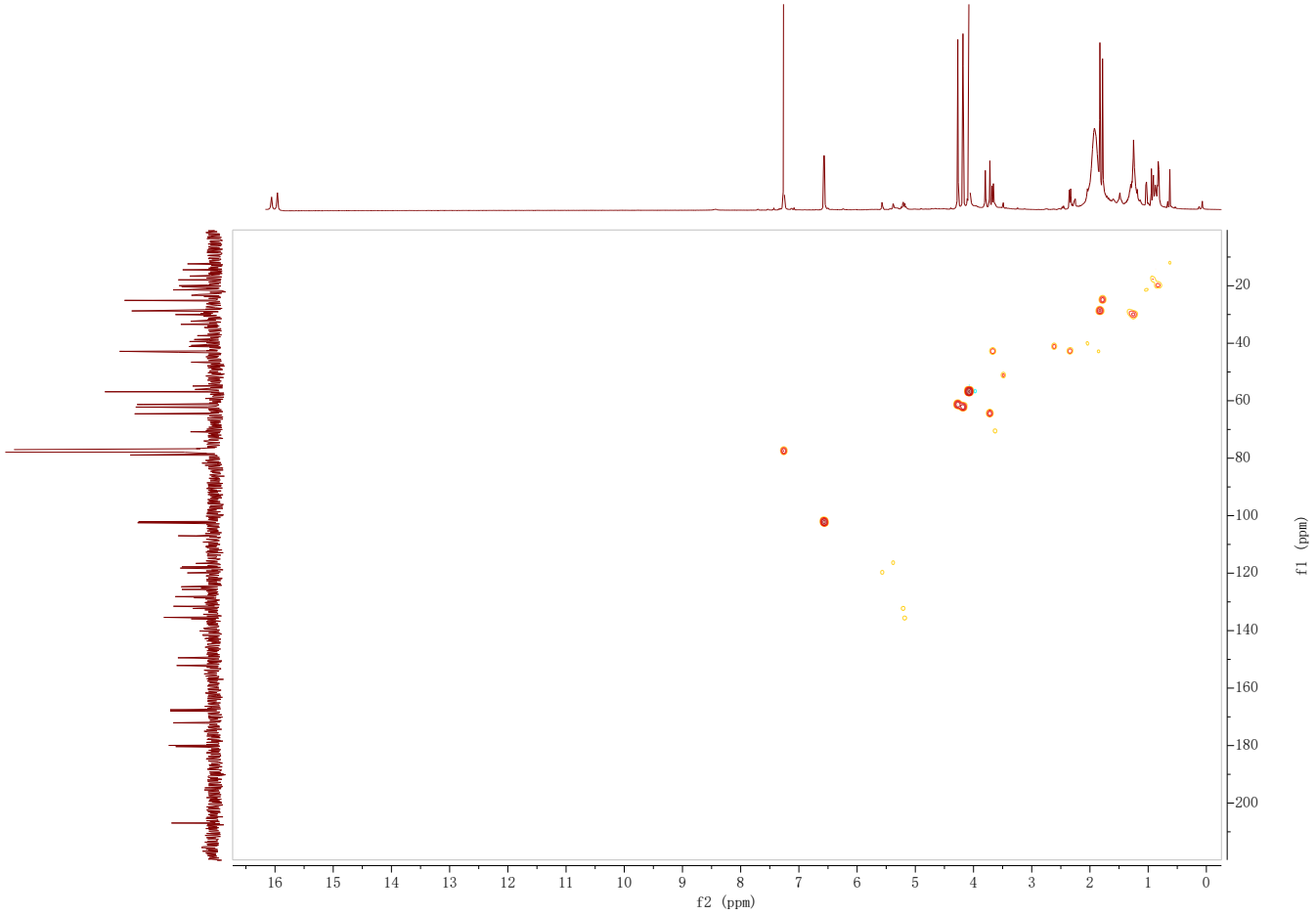

Figure S18. HMBC NMR spectrum (600 MHz) of 12 in $CDCl_3$-*d*

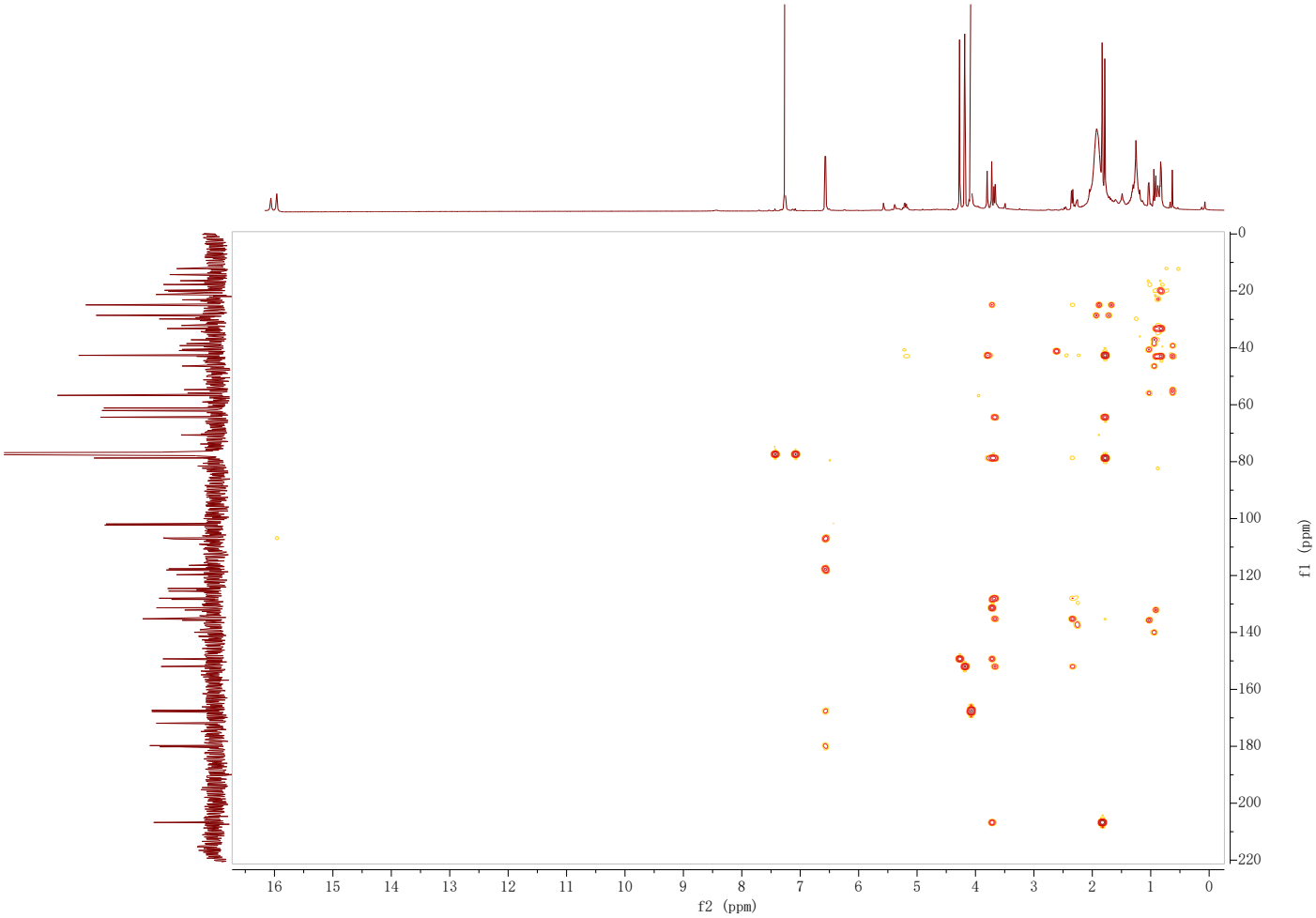

Figure S19. 1D ^{1}H-NOESY NMR spectrum (600 MHz) of 12 in $CDCl_3$-*d*

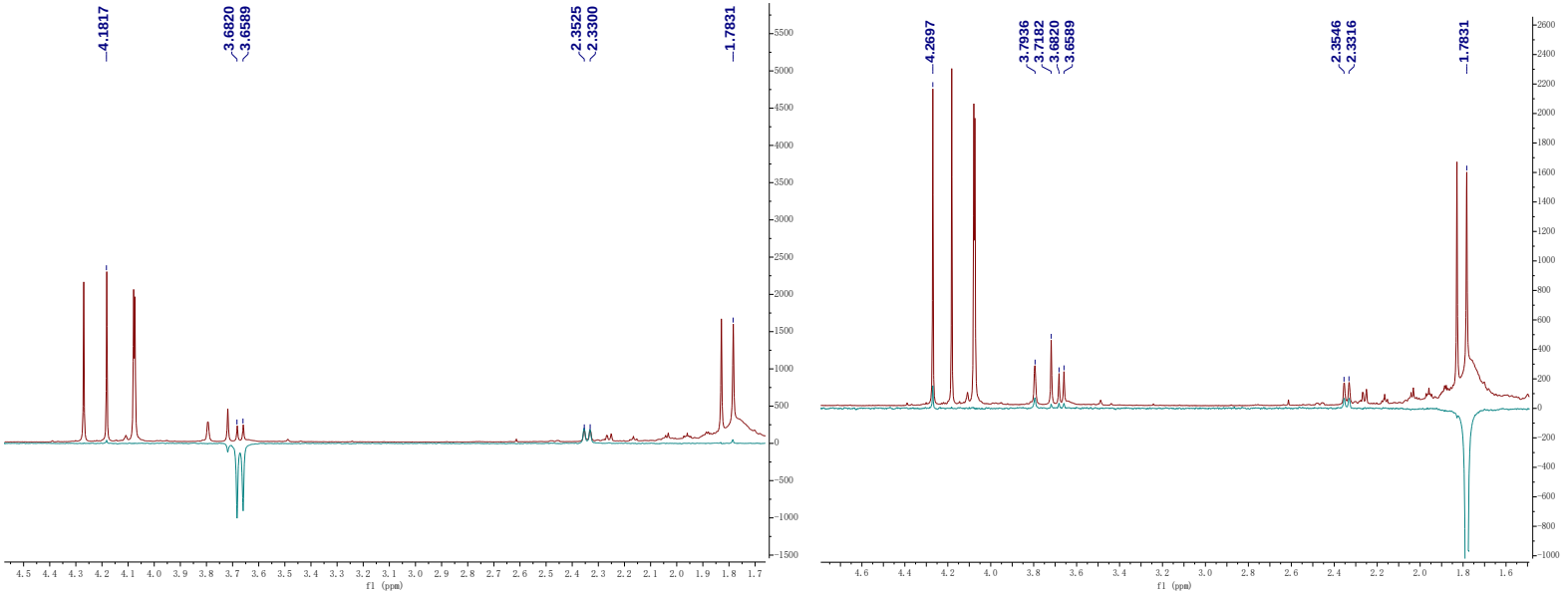

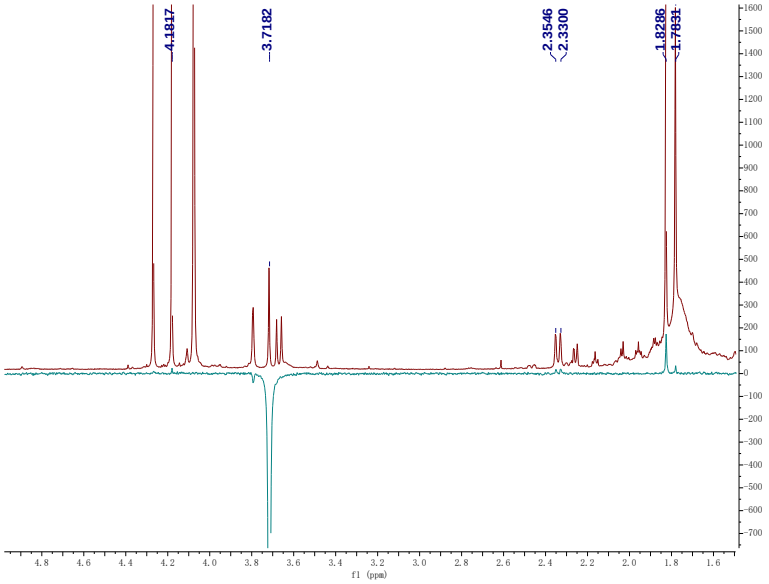
4.1817
3.7182
2.3546
2.3300
1.8286
1.7831
f1 (ppm)

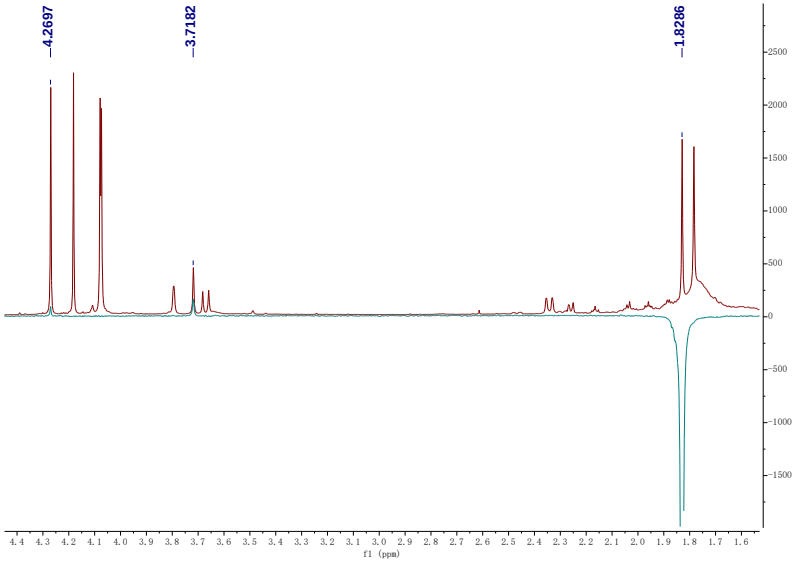
4.2697
3.7182
1.8286
f1 (ppm)

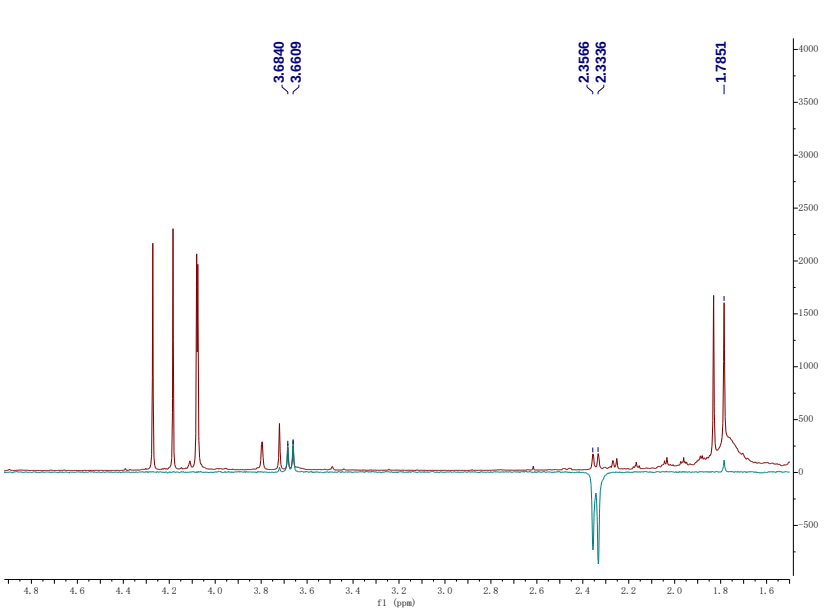
3.6840
3.6609
2.3566
2.3336
1.7851
f1 (ppm)

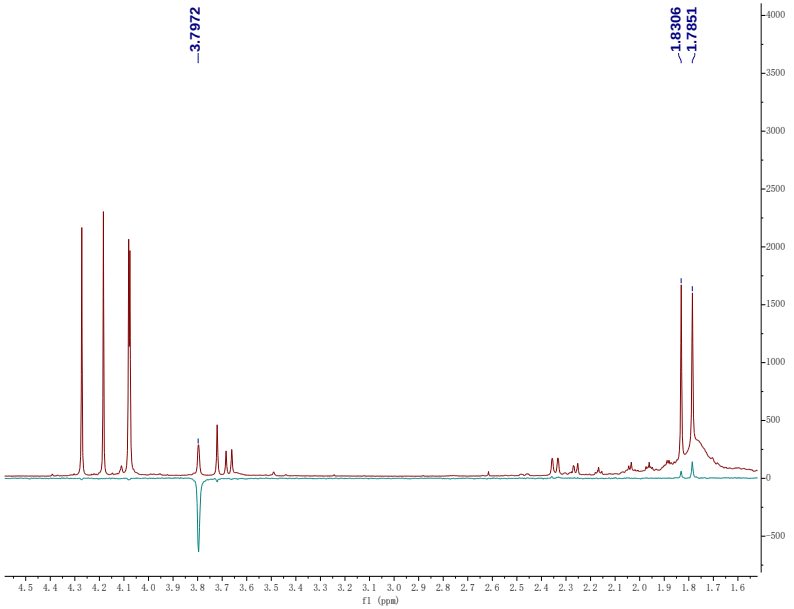
3.7972
1.8306
1.7851
f1 (ppm)

Figure S20. ^{1}H NMR spectrum (600 MHz) of 6 in $CDCl_3$-*d*

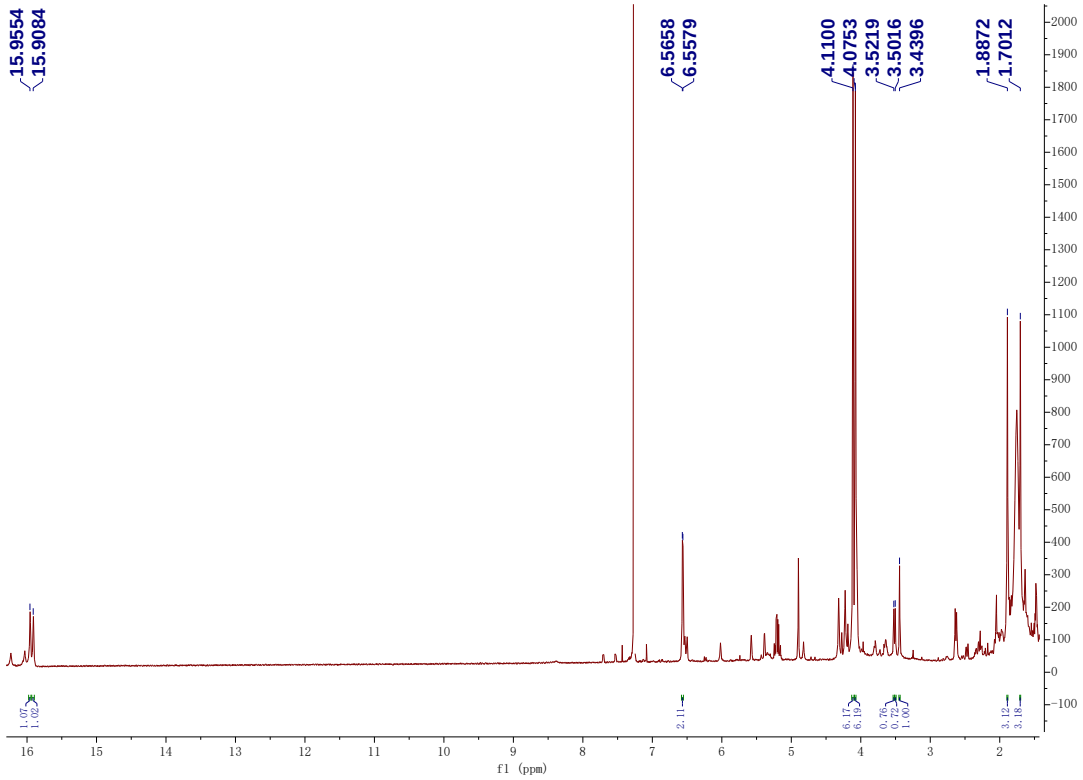

Figure S21. ^{1}H NMR spectrum (600 MHz) of hypocrellin A in $CDCl_3$-*d*.

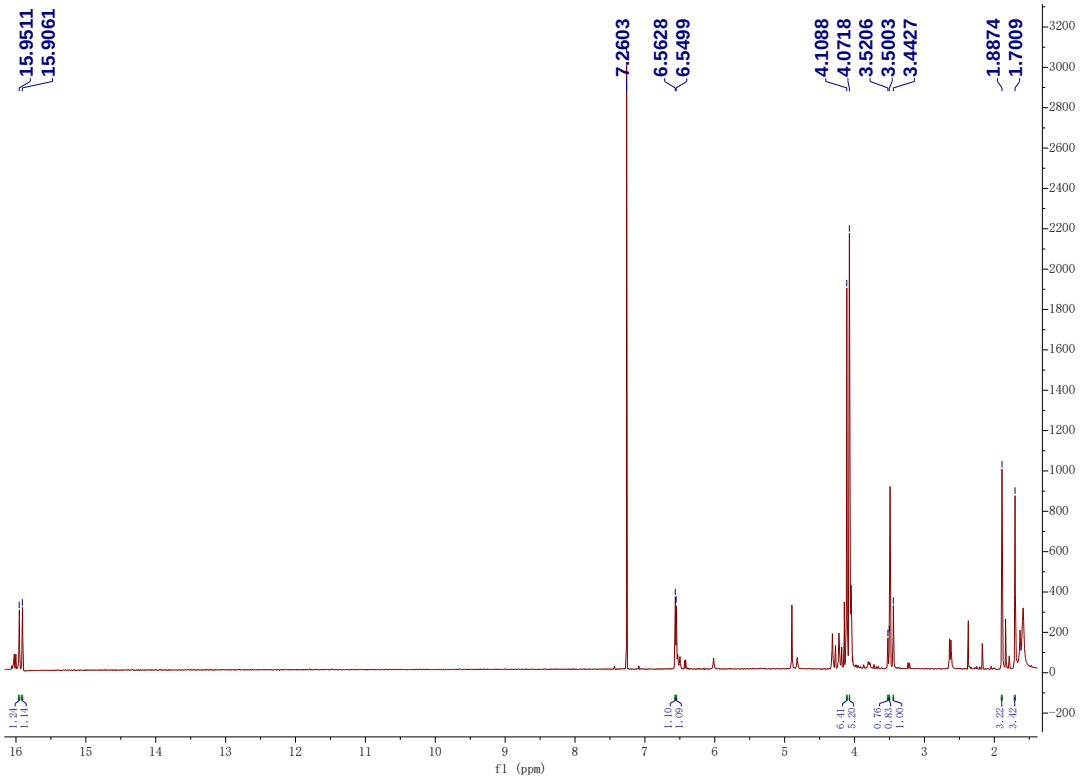

Figure S22. ^{1}H NMR spectrum (600 MHz) of elsinochrome A (1) in $CDCl_3$-*d*

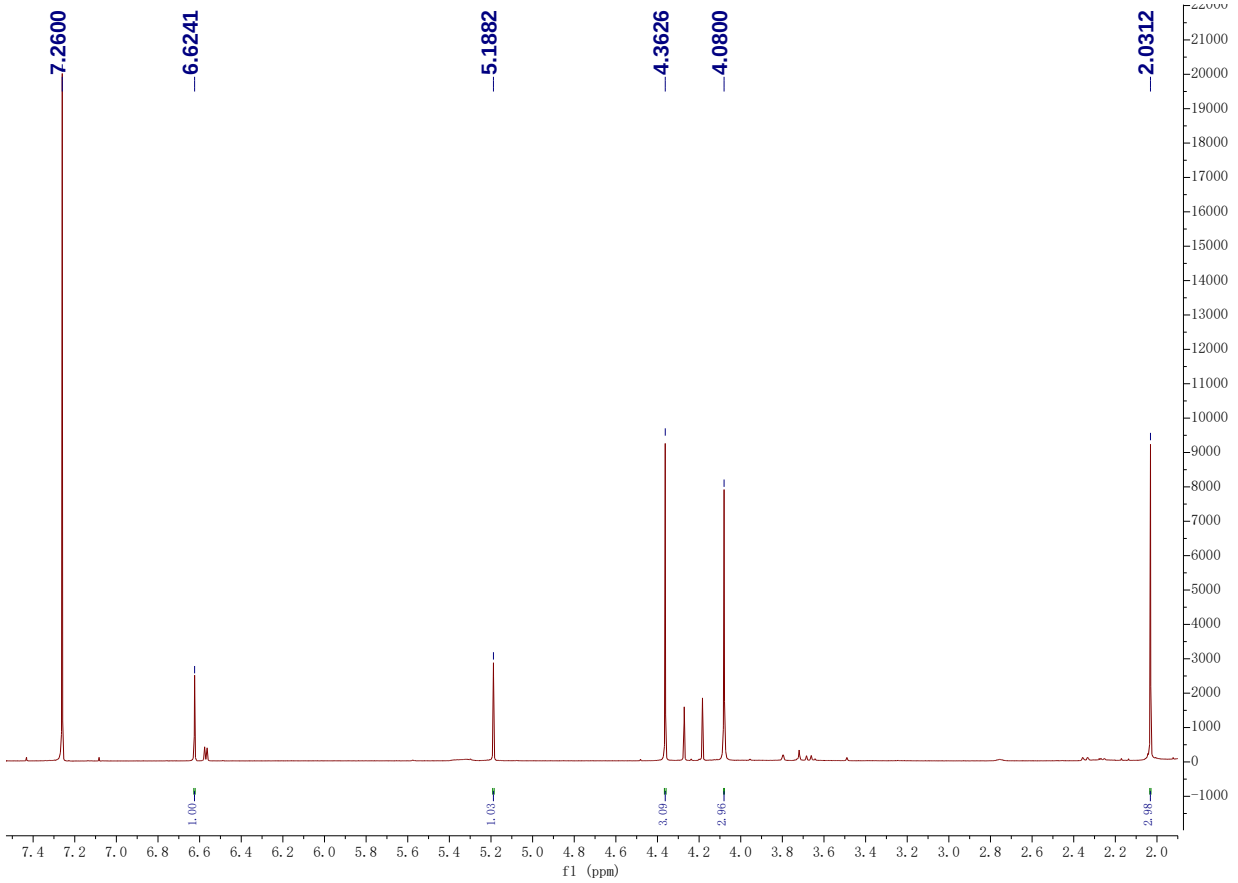

Figure S23. ^{13}C NMR spectrum (150 MHz) of elsinochrome A (1) in $CDCl_3$-*d*

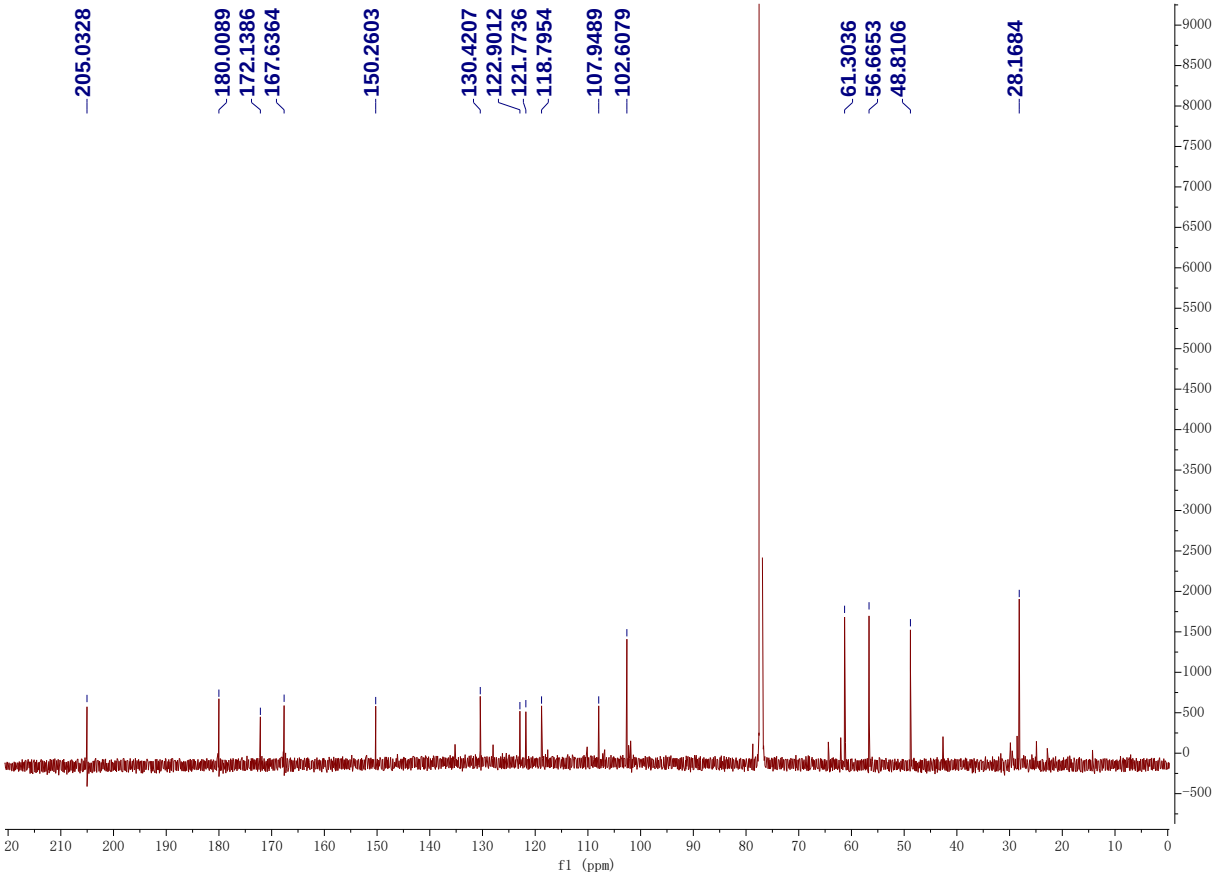

Figure S24. HSQC NMR spectrum (600 MHz) of elsinochrome A (1) in $CDCl_3$-*d*

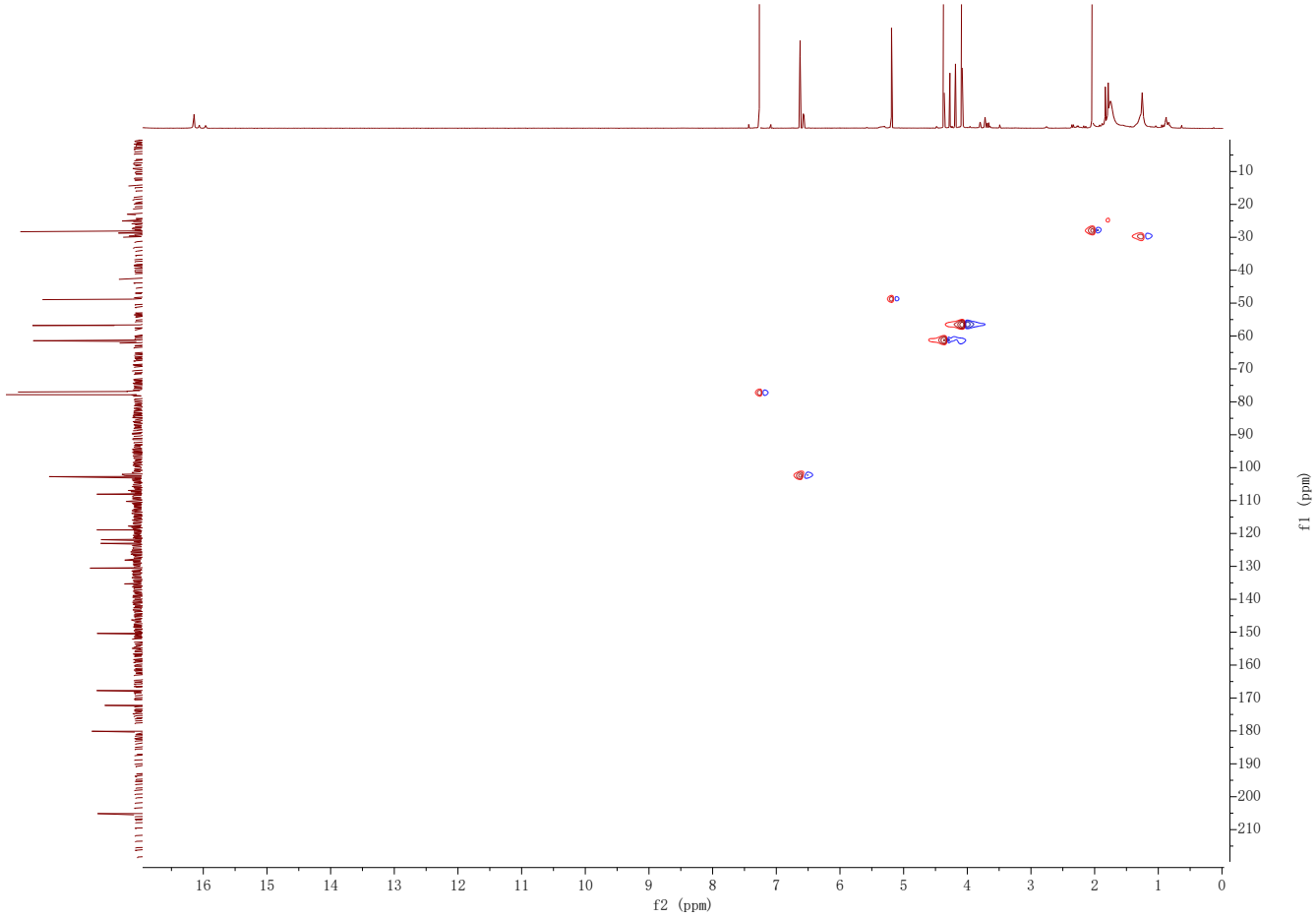

Figure S25. HMBC NMR spectrum (600 MHz) of elsinochrome A (1) in $CDCl_3$-*d*

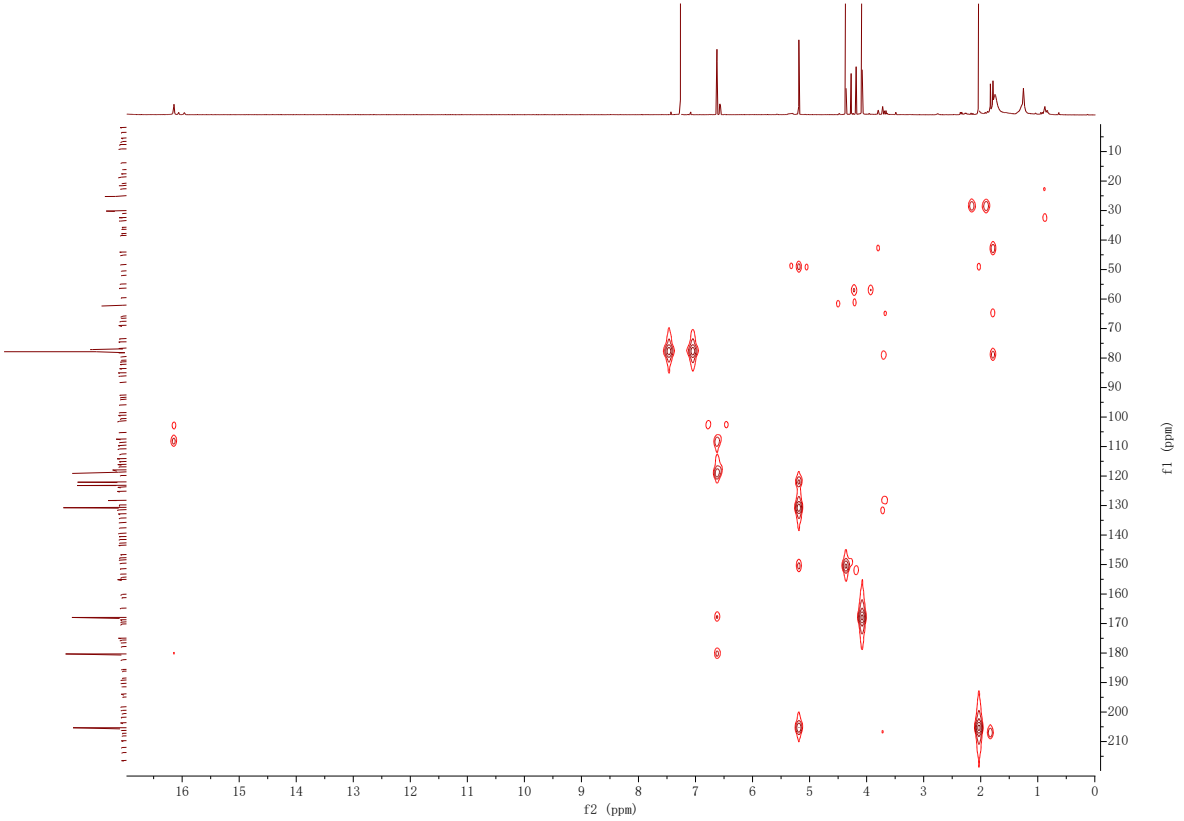

Figure S26. ^{1}H NMR spectrum (500 MHz) of toralactone (8) in $CDCl_3$-*d*.

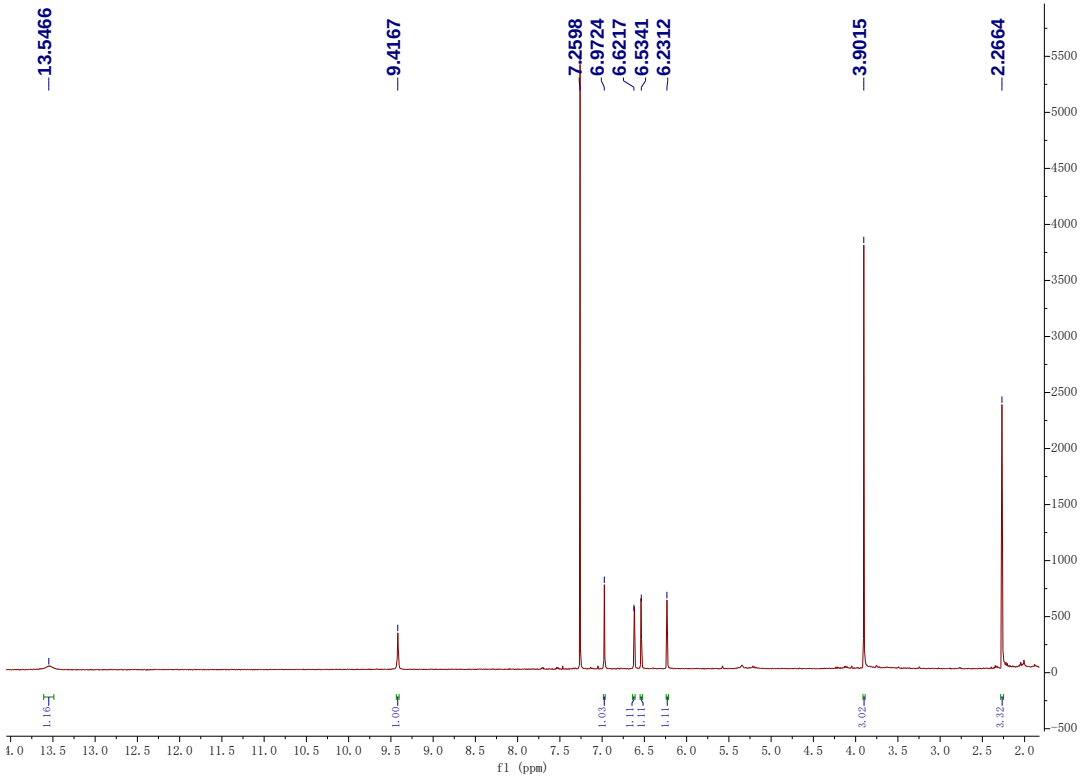

Figure S27. ^{1}H NMR spectrum (500 MHz) of 13 in D_2O

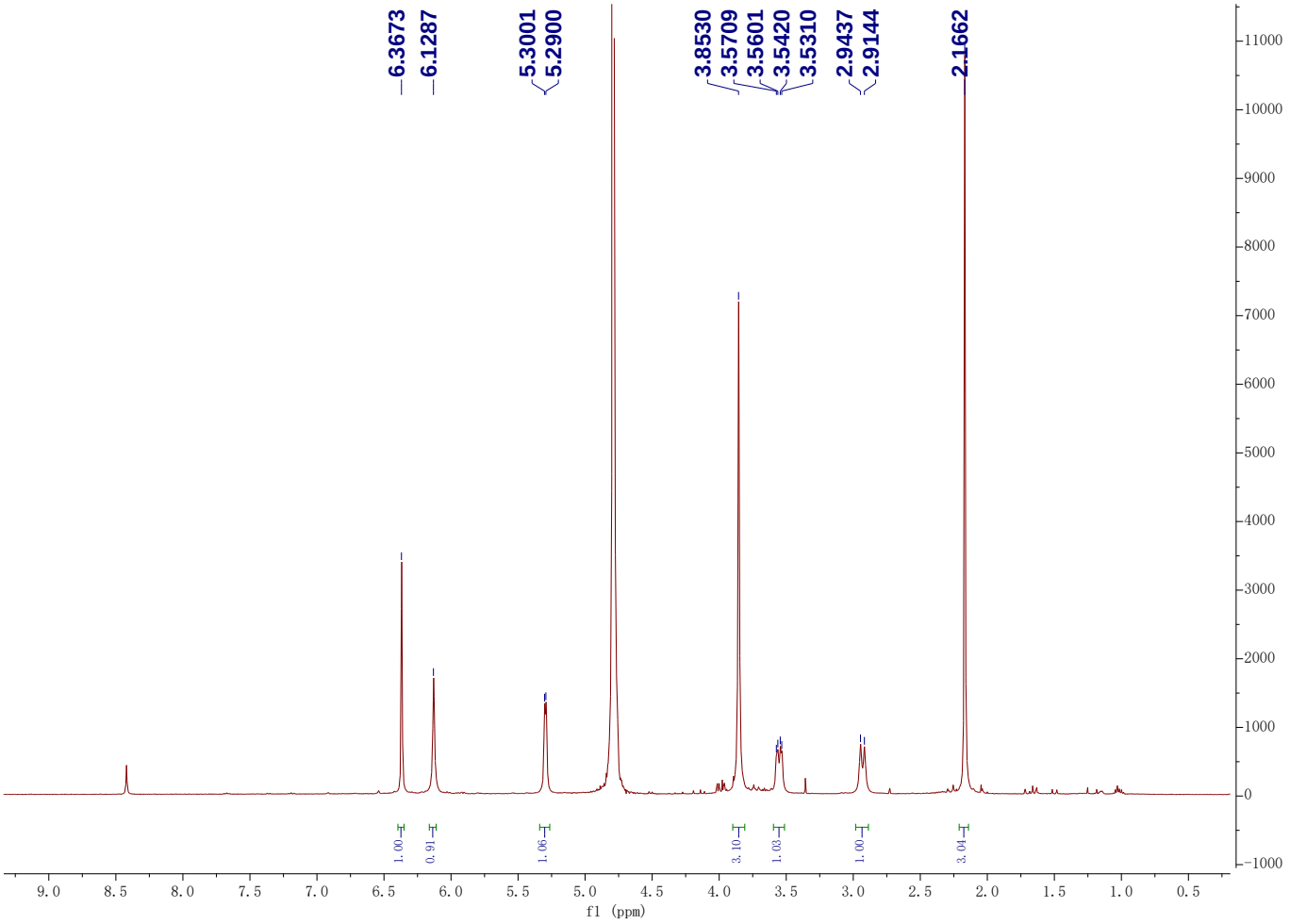

Figure S28. ^{13}C NMR spectrum (125 MHz) of 13 in D_2O

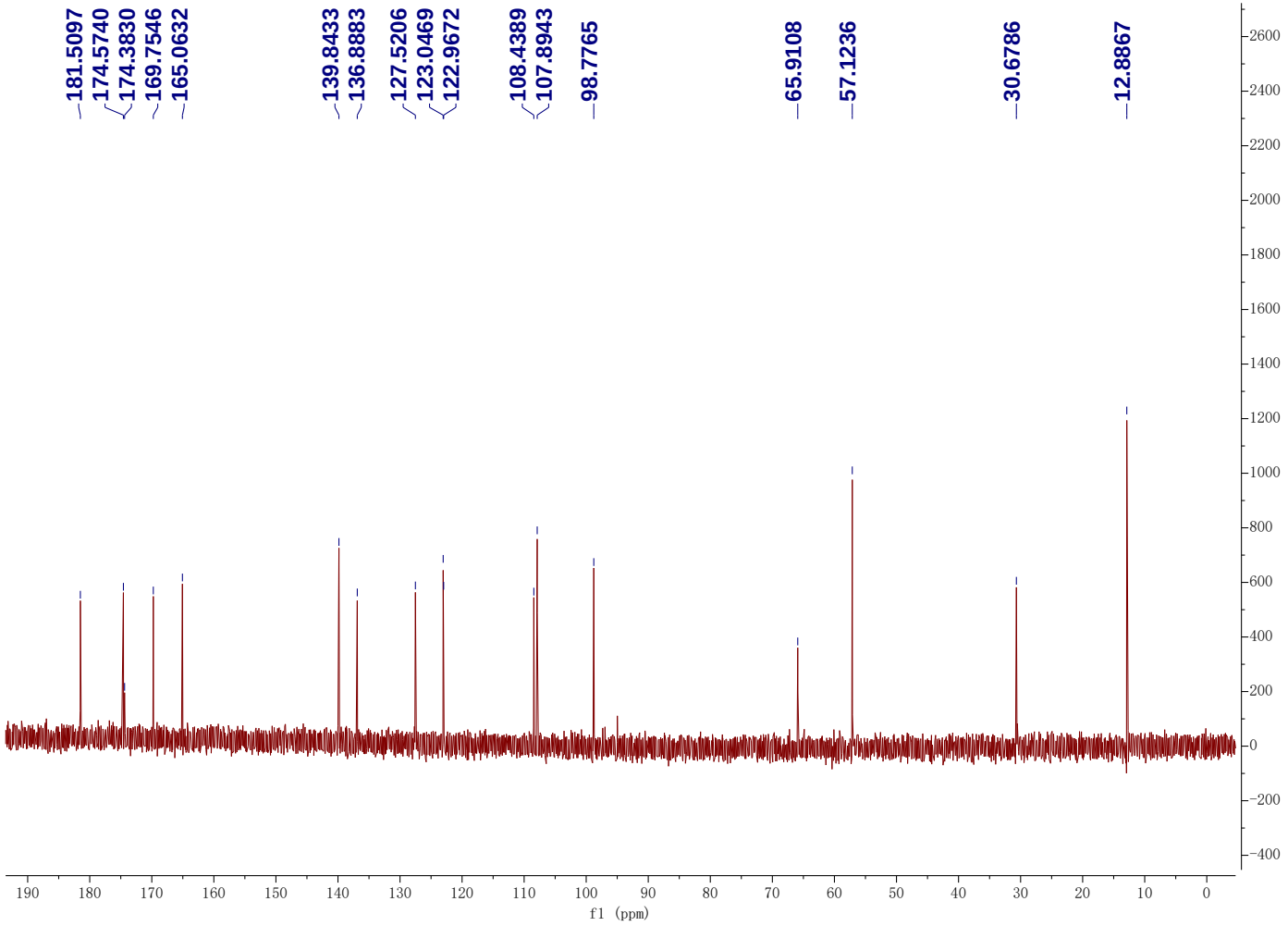

Figure S29. ^{1}H-^{1}H gCOSY NMR spectrum (500 MHz) of 13 in D_2O

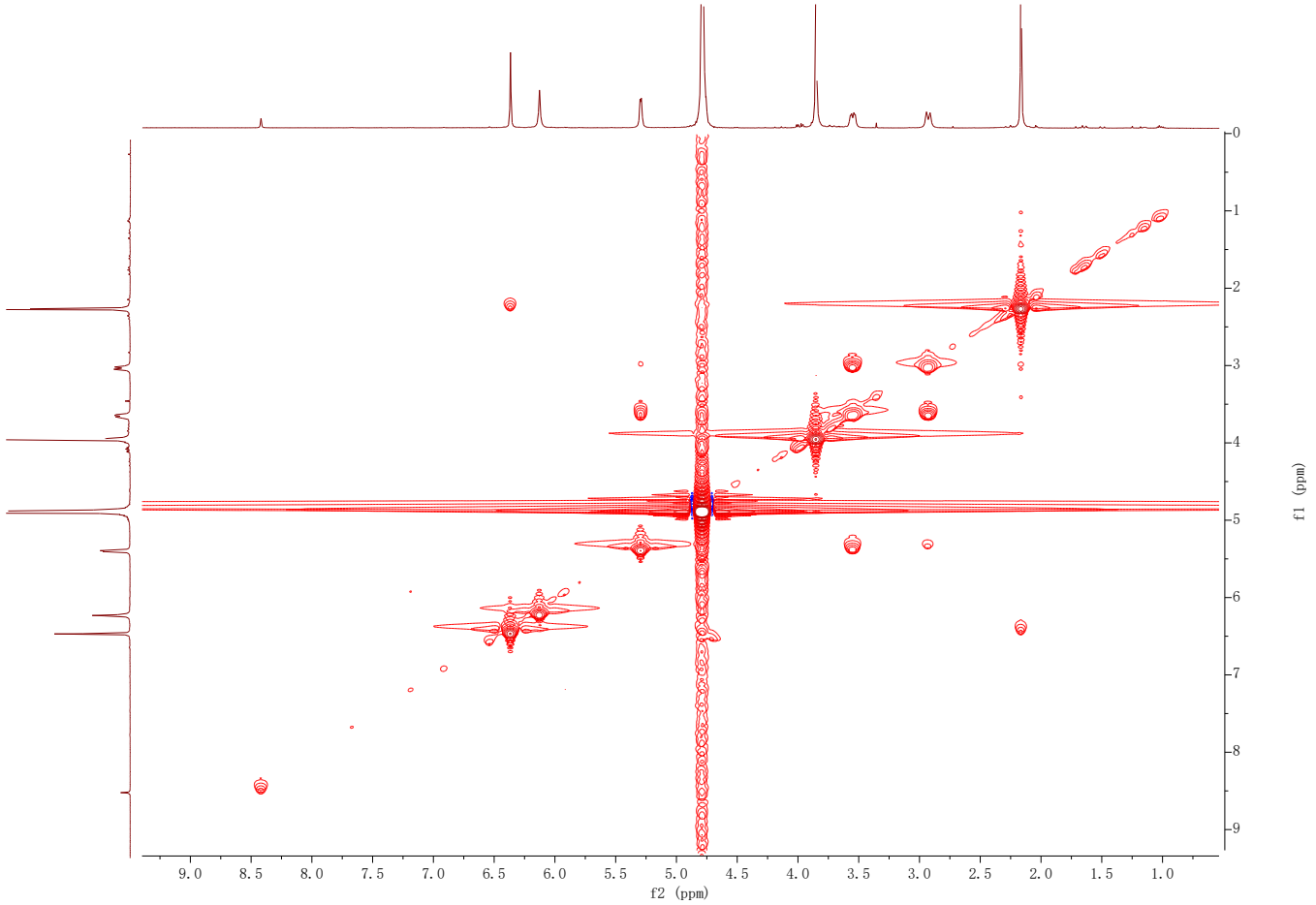

Figure S30. HSQC NMR spectrum (500 MHz) of 13 in D_2O

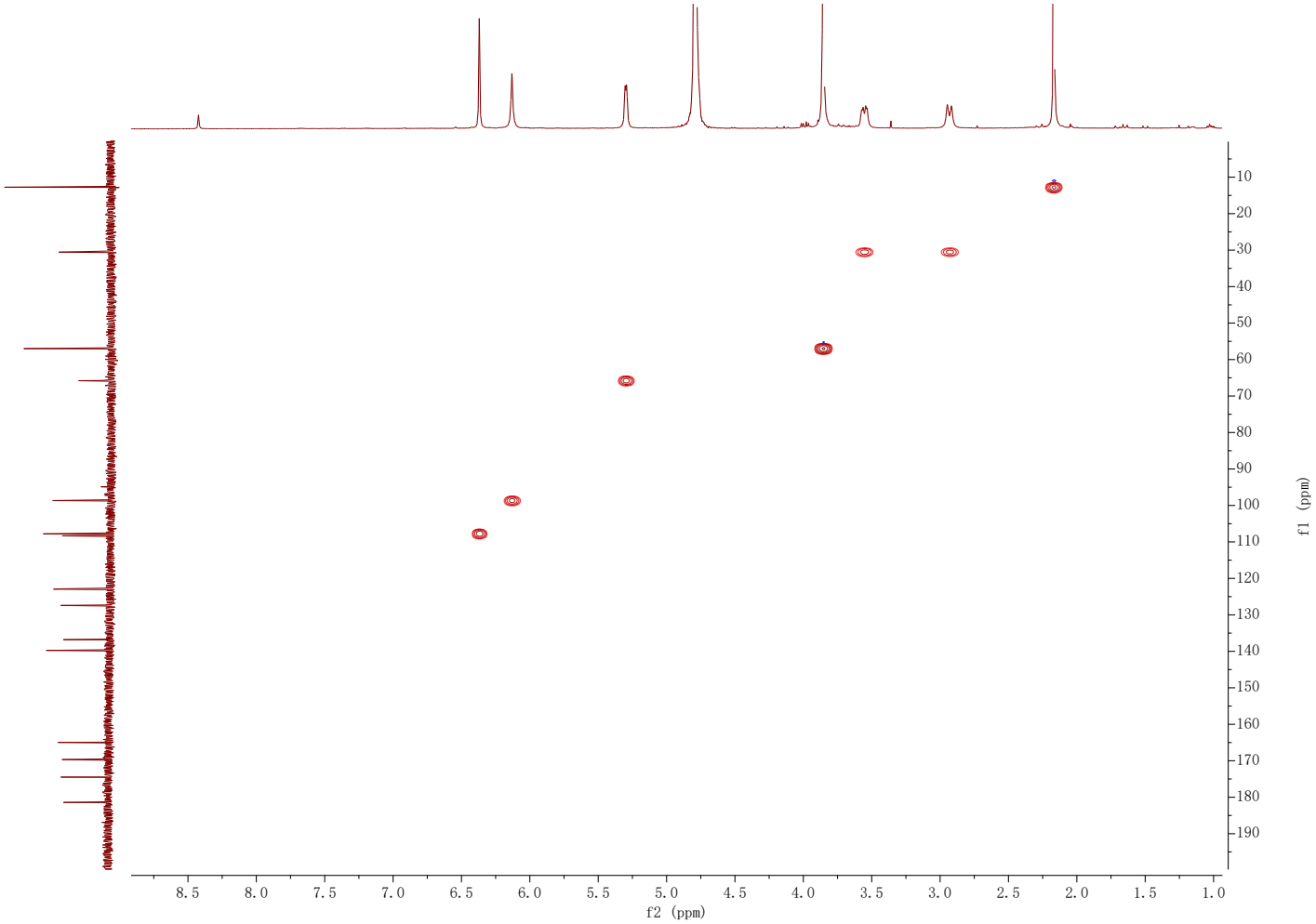

Figure S31. HMBC NMR spectrum (500 MHz) of 13 in D_2O

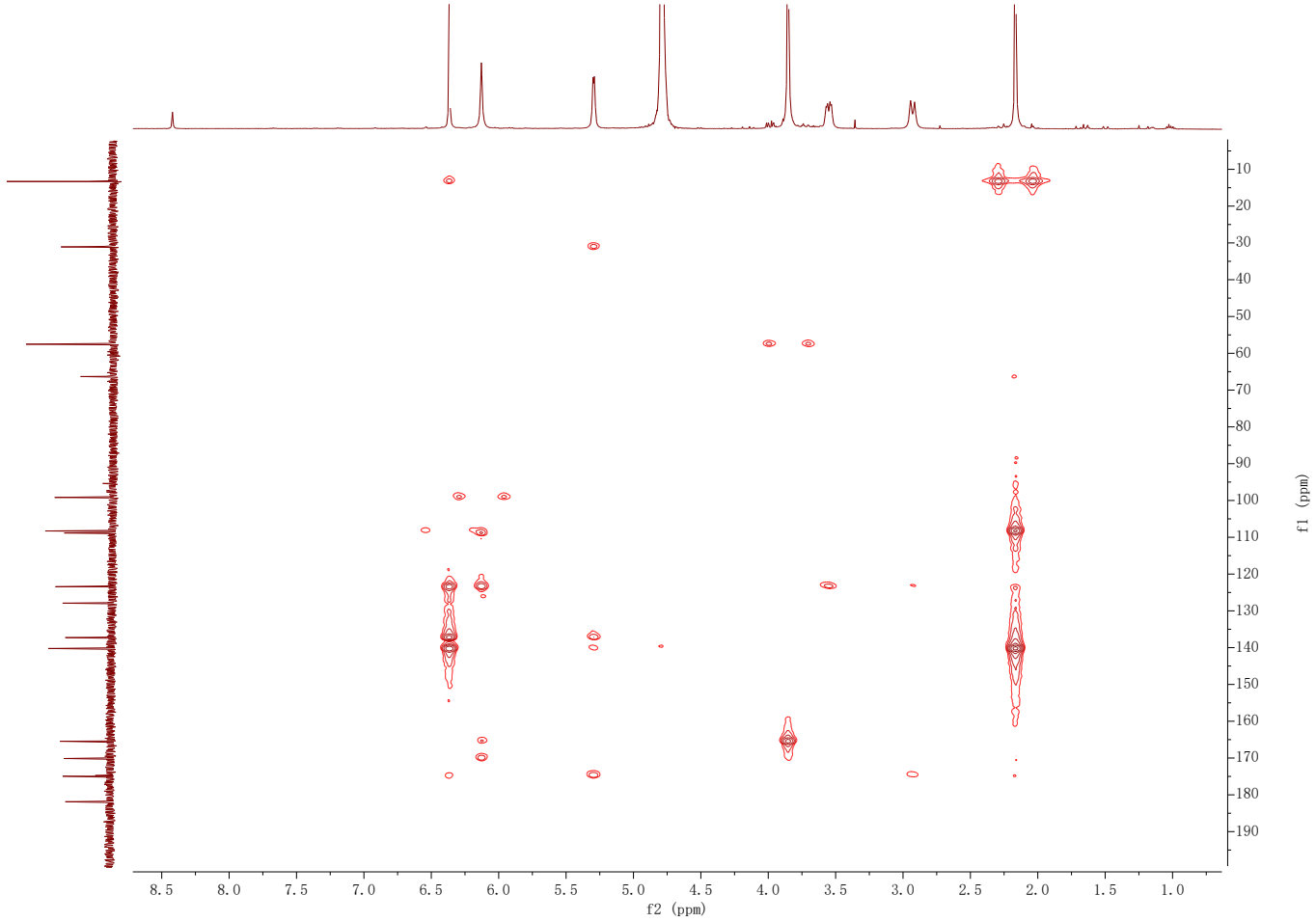

Figure S32. ^{1}H NMR spectrum (500 MHz) of 14 in DMSO-d_6

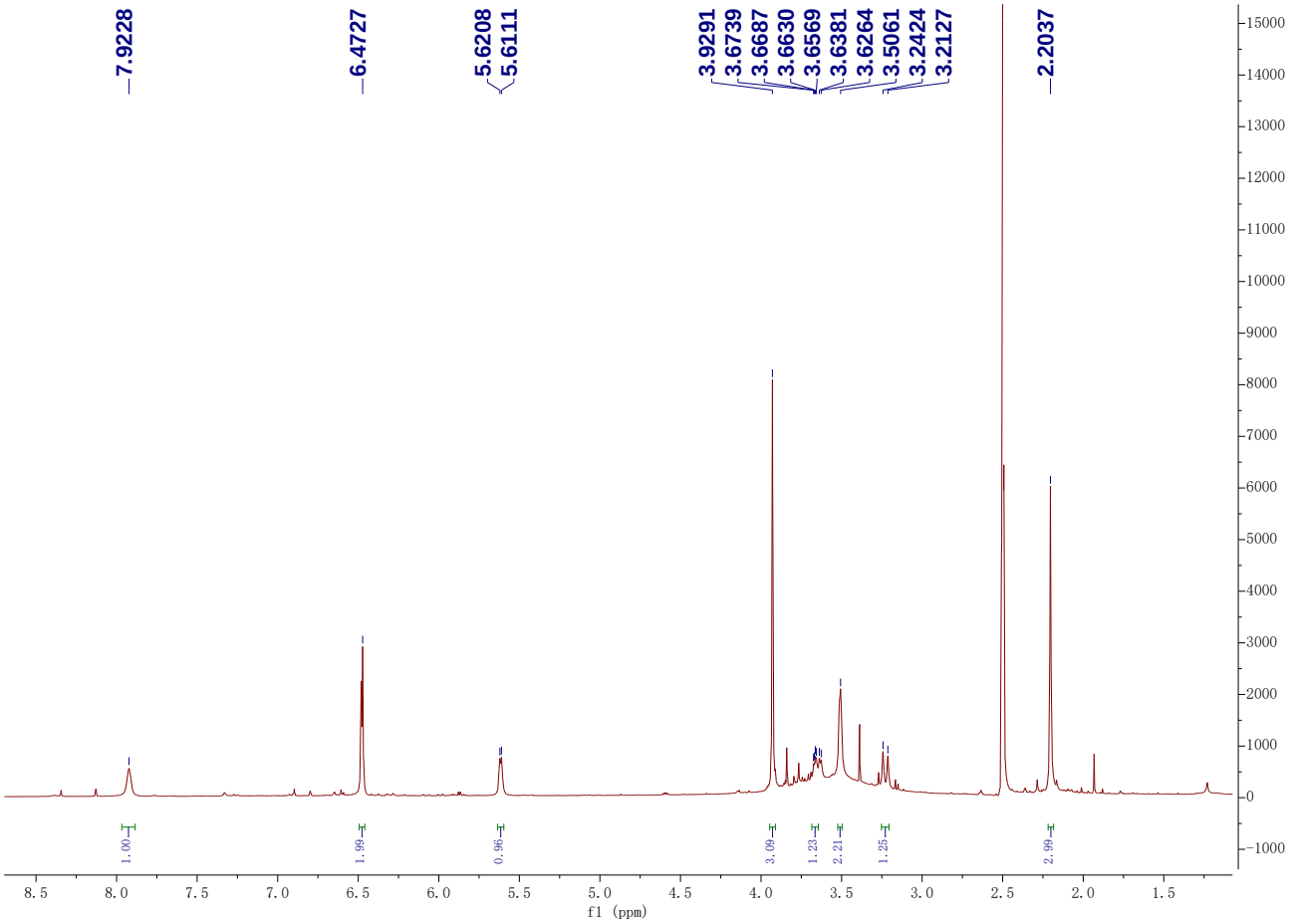

Figure S33. ^{13}C NMR spectrum (125 MHz) of 14 in DMSO-d_6

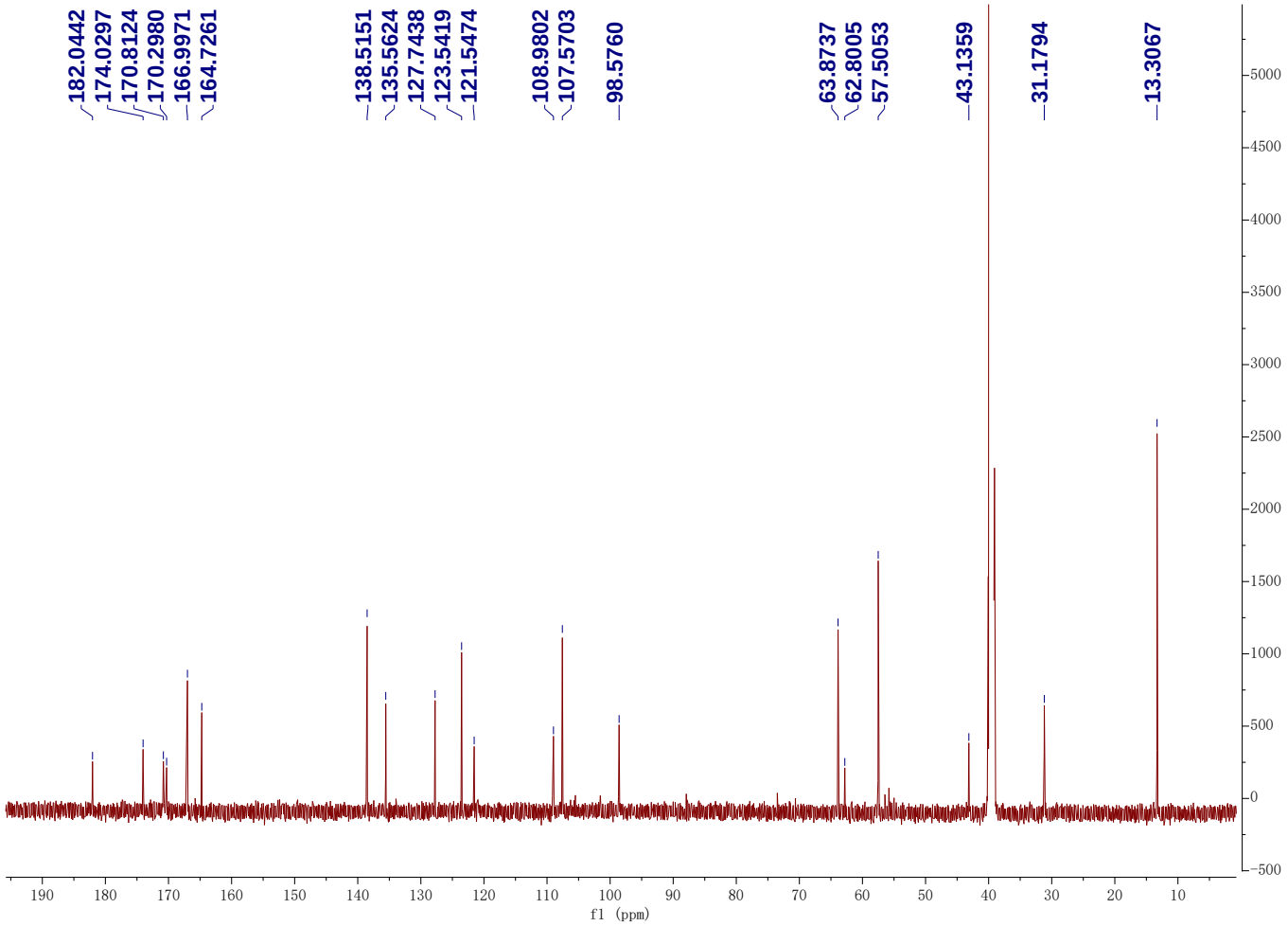

Figure S34. DEPT-135 ^{13}C NMR spectrum (125 MHz) of 14 in DMSO-d_6

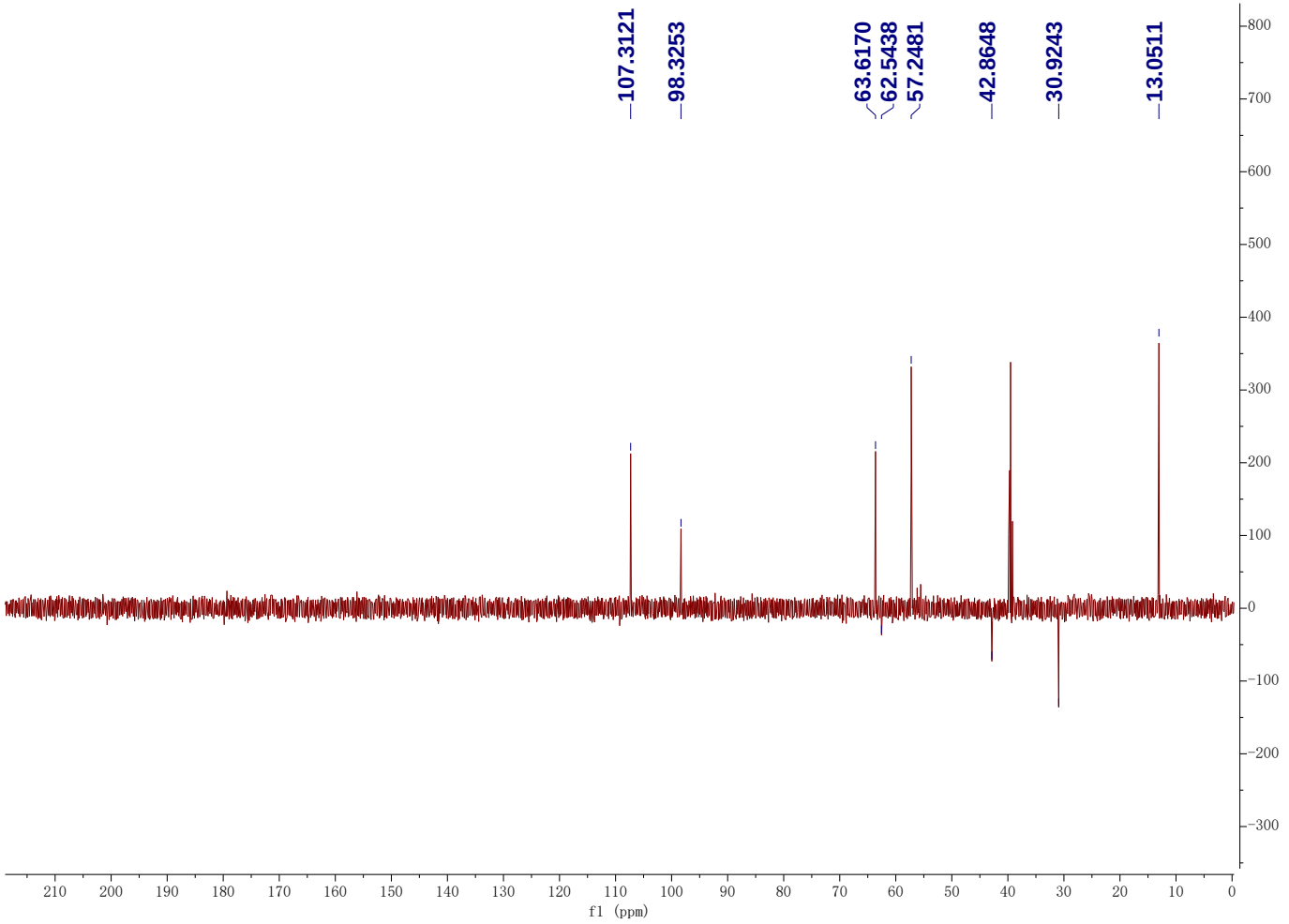

Figure S35. ^{1}H-^{1}H gCOSY NMR spectrum (500 MHz) of 14 in DMSO-d_6

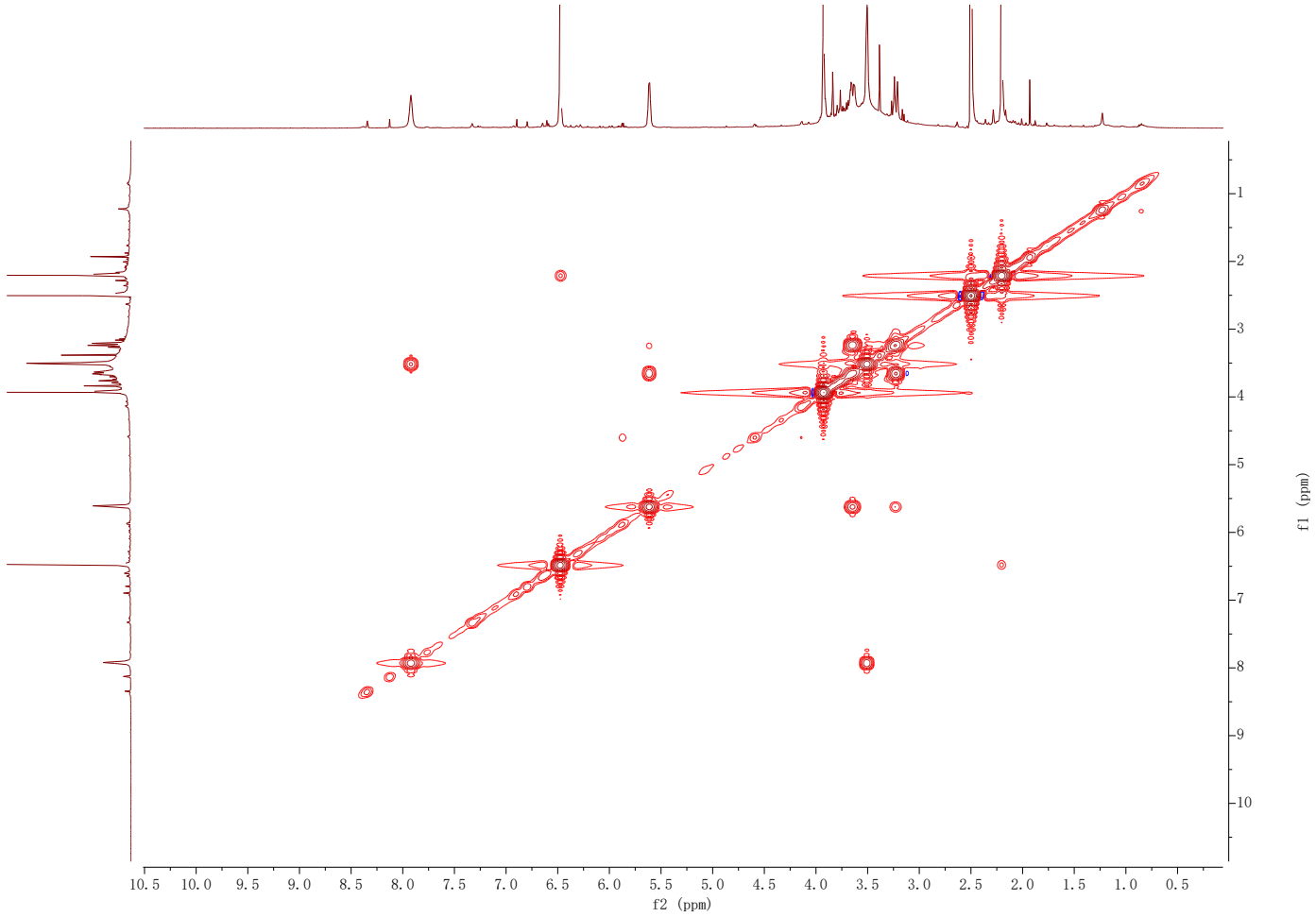

Figure S36. HSQC NMR spectrum (500 MHz) of 14 in DMSO-d_6

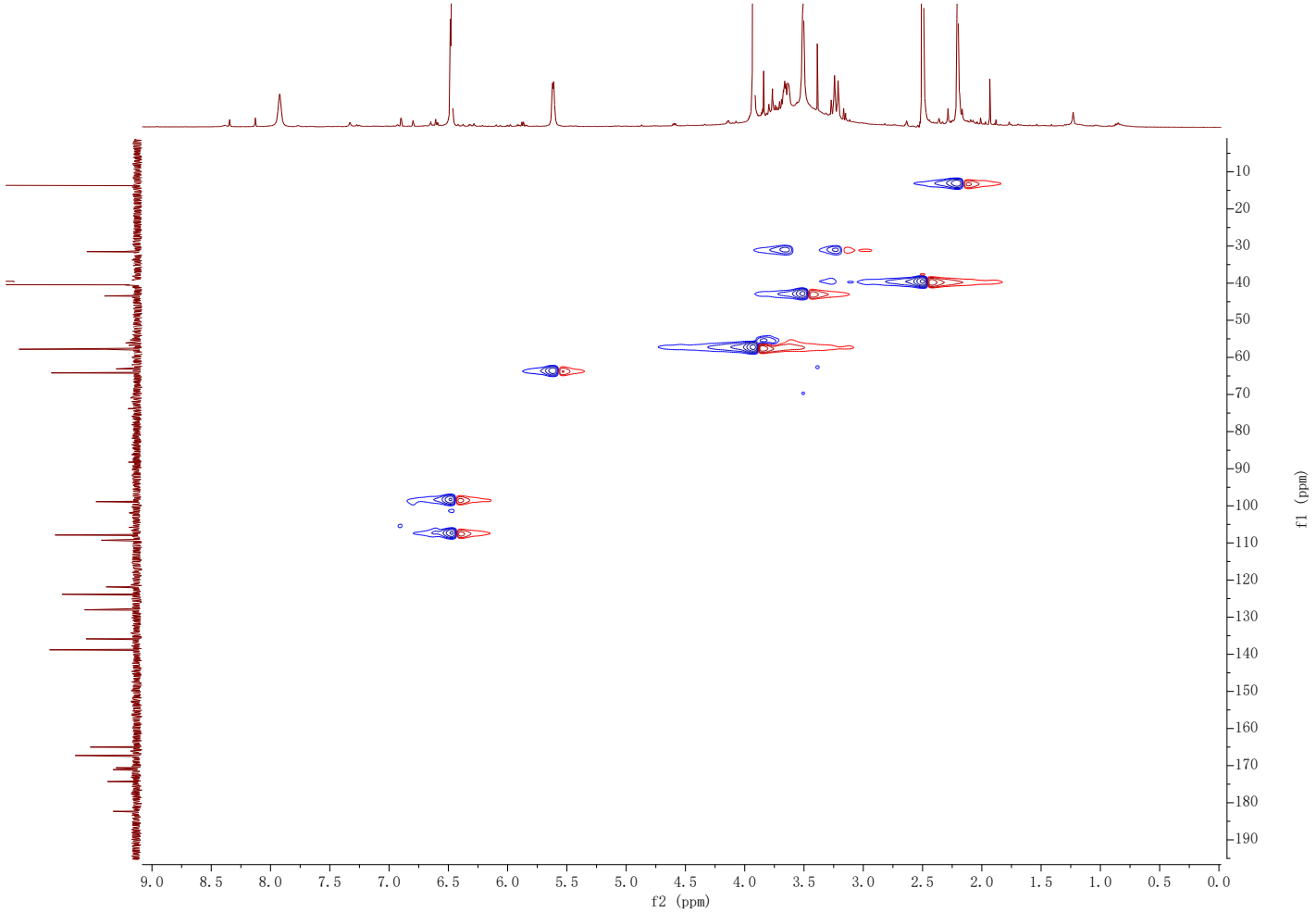

Figure S37. HMBC NMR spectrum (500 MHz) of 14 in DMSO-d_6

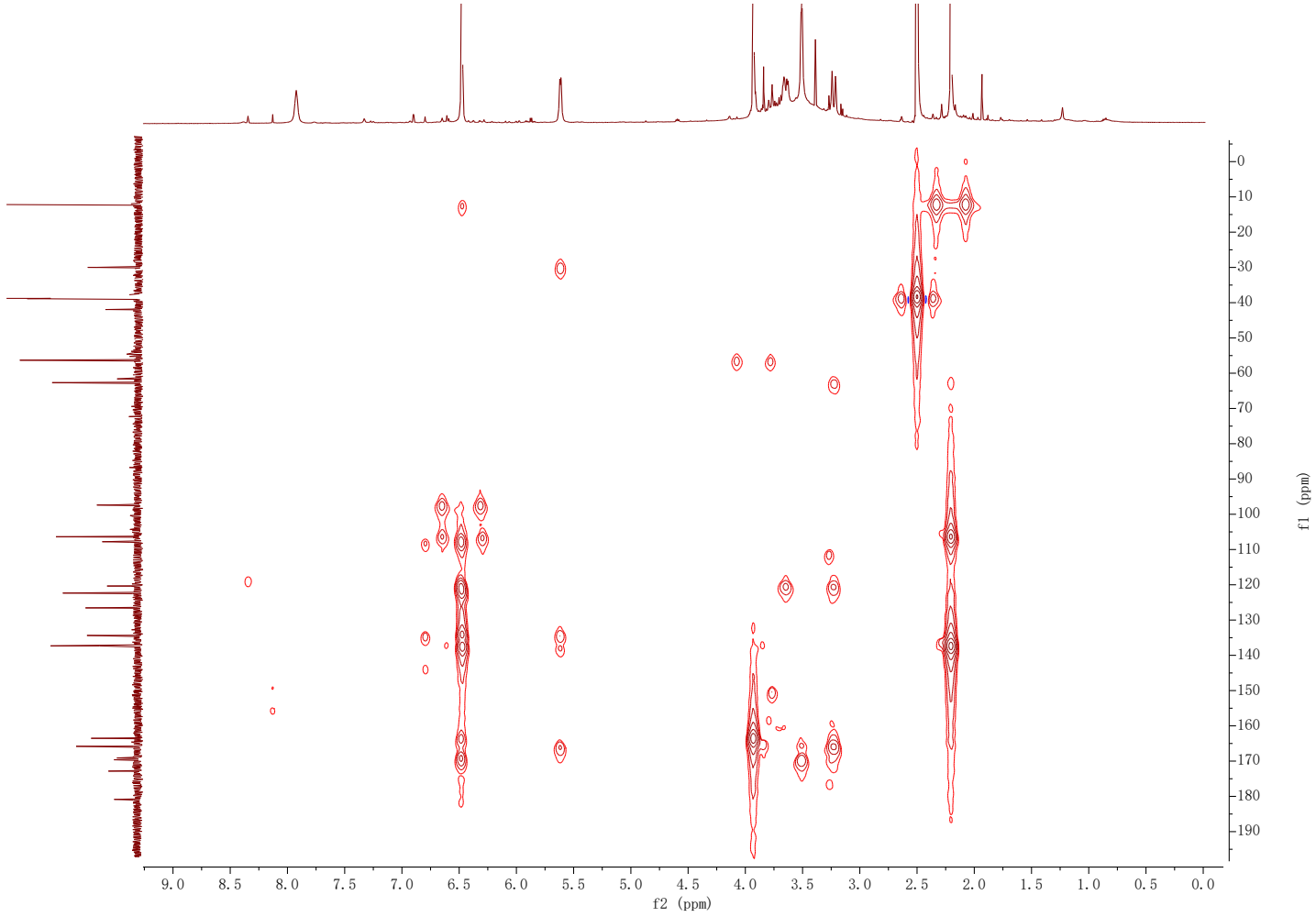

Figure S38. ^{1}H NMR spectrum (600 MHz) of 16 in DMSO-d_6

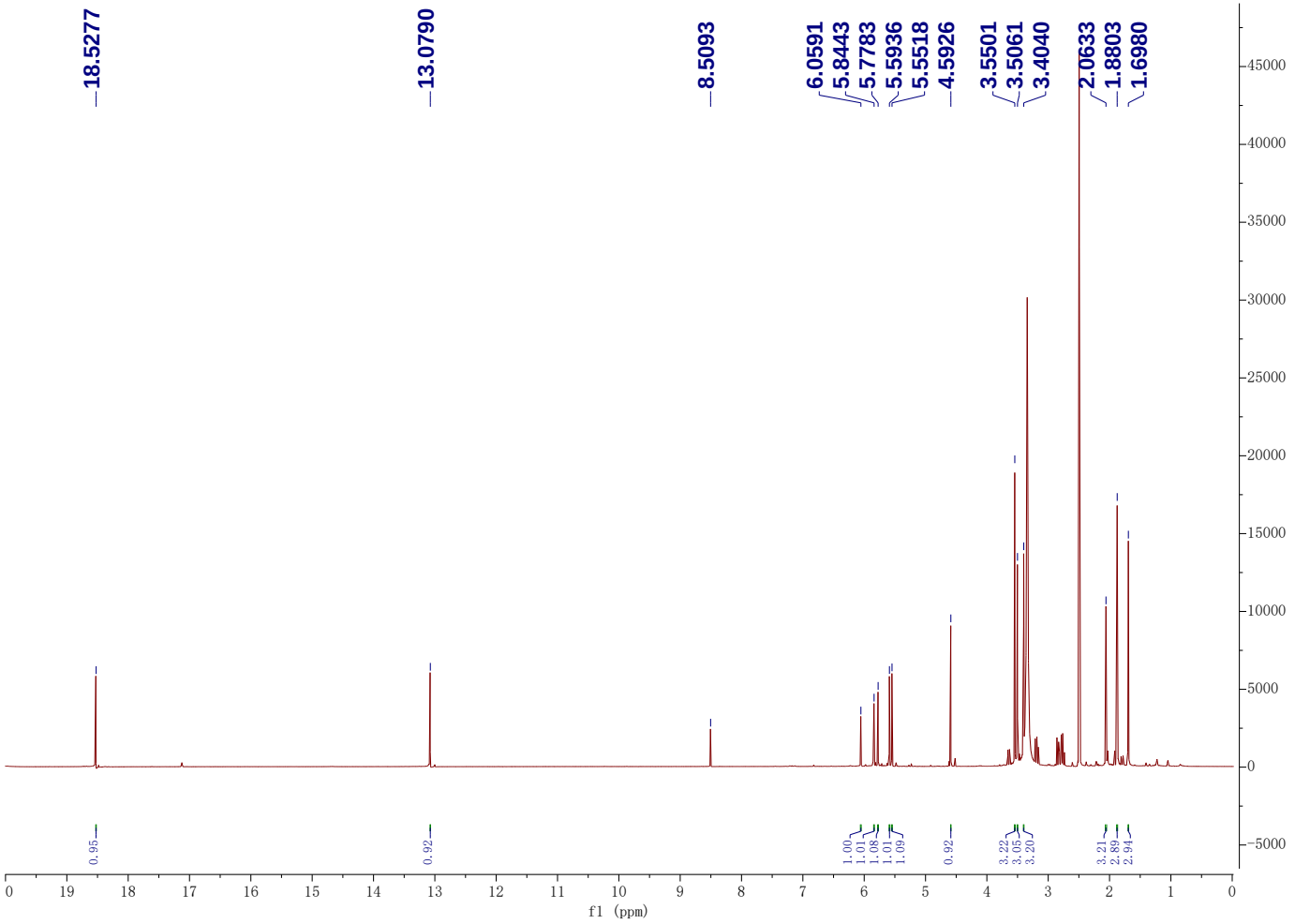

Figure S39. ^{13}C NMR spectrum (150 MHz) of 16 in DMSO-d_6

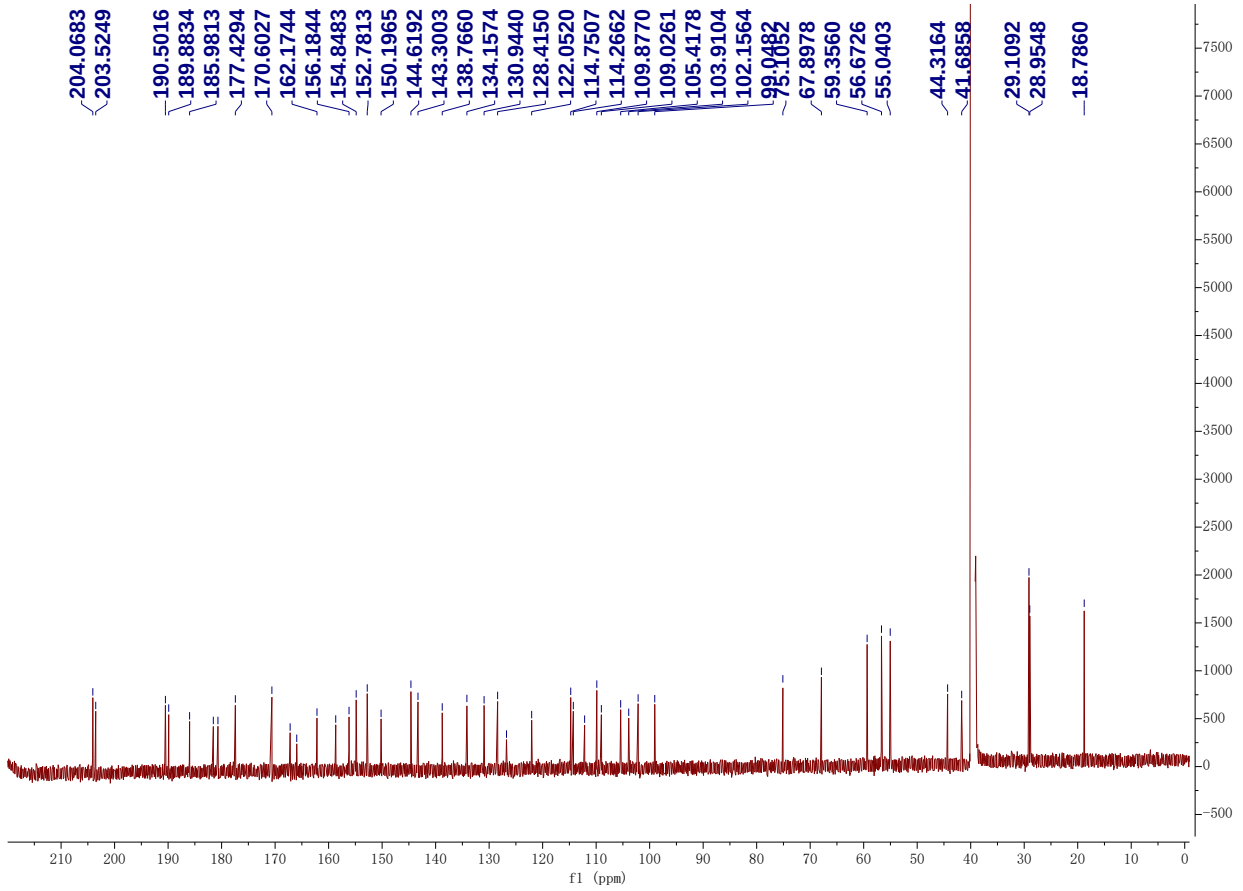

Figure S40. ^{1}H-^{1}H gCOSY NMR spectrum (600 MHz) of 16 in DMSO-d_6

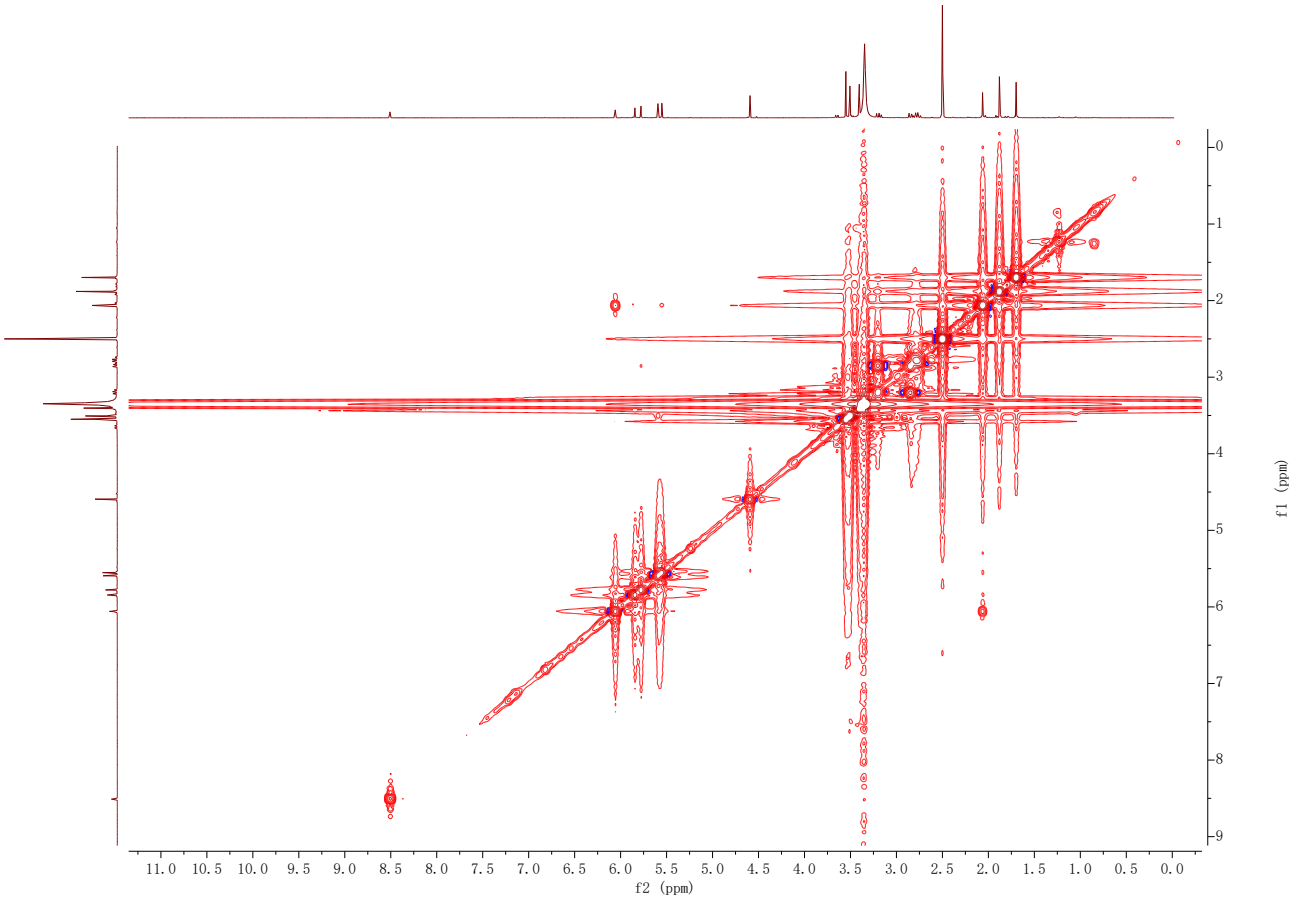

Figure S41. DEPT-135 and DEPT-90 ^{13}C NMR spectrum (150 MHz) of 16 in DMSO-d_6

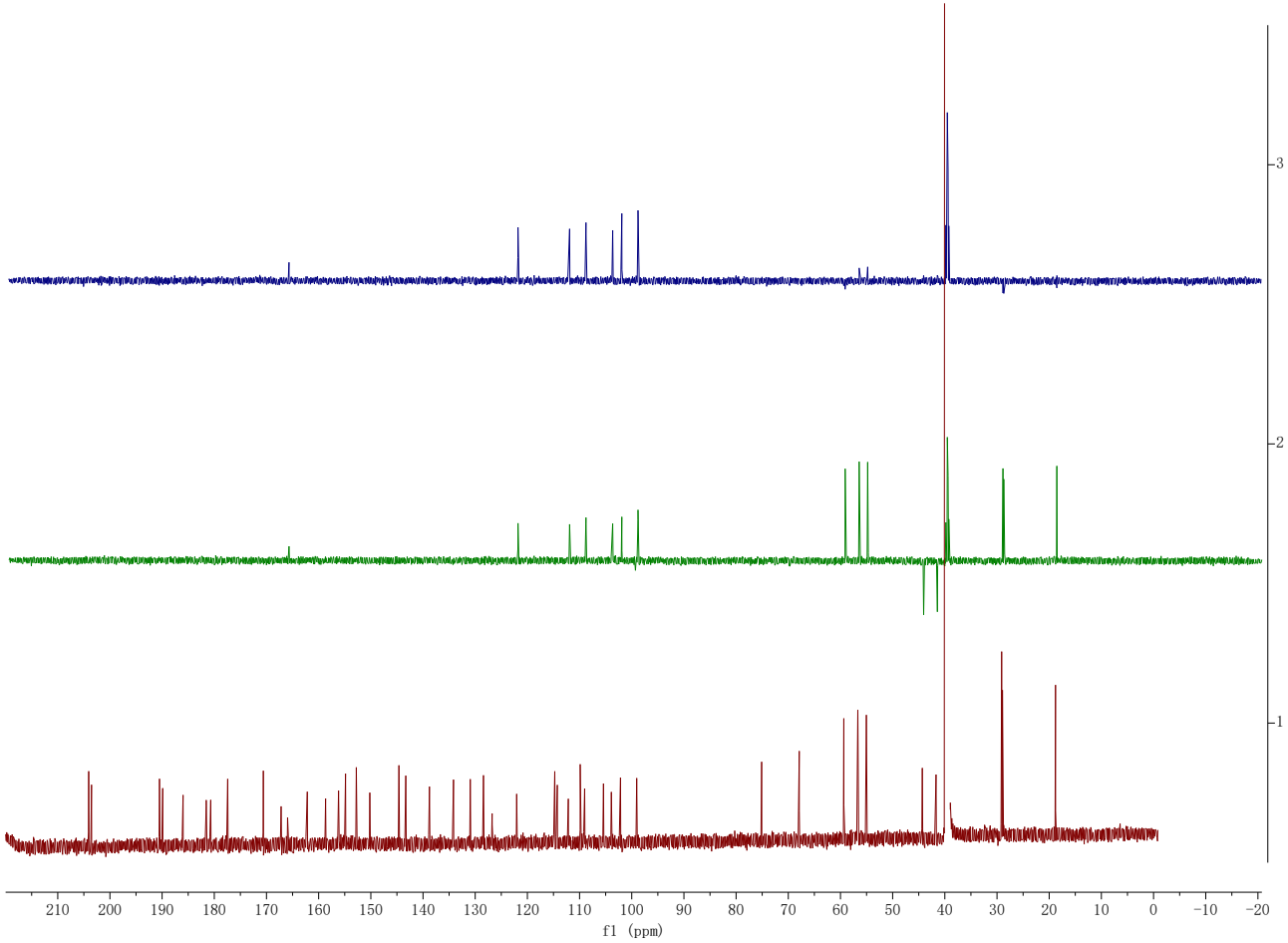

Figure S42. HSQC NMR spectrum (600 MHz) of 16 in DMSO-d_6

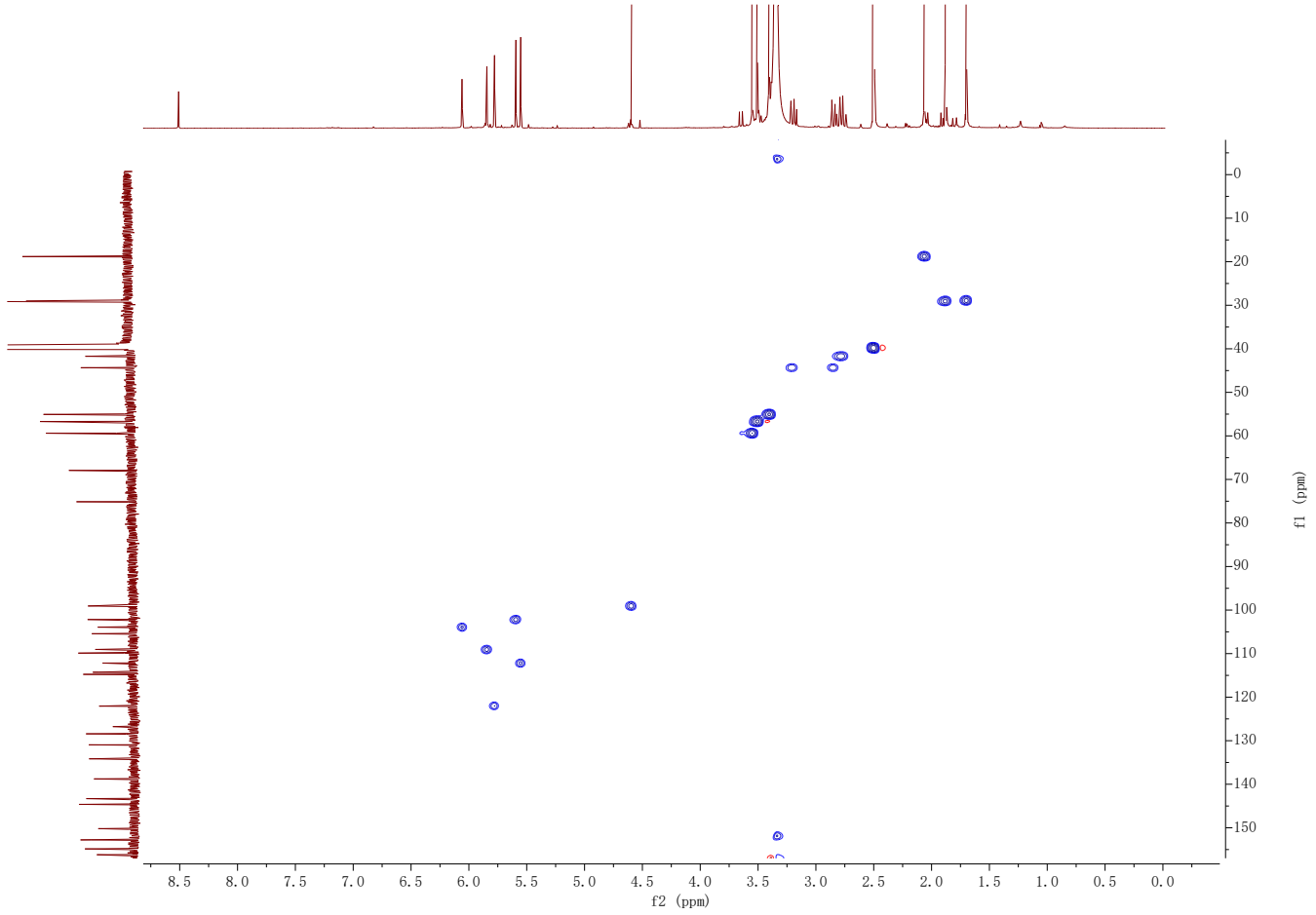

Figure S43. HMBC NMR spectrum (600 MHz) of 16 in DMSO-d_6

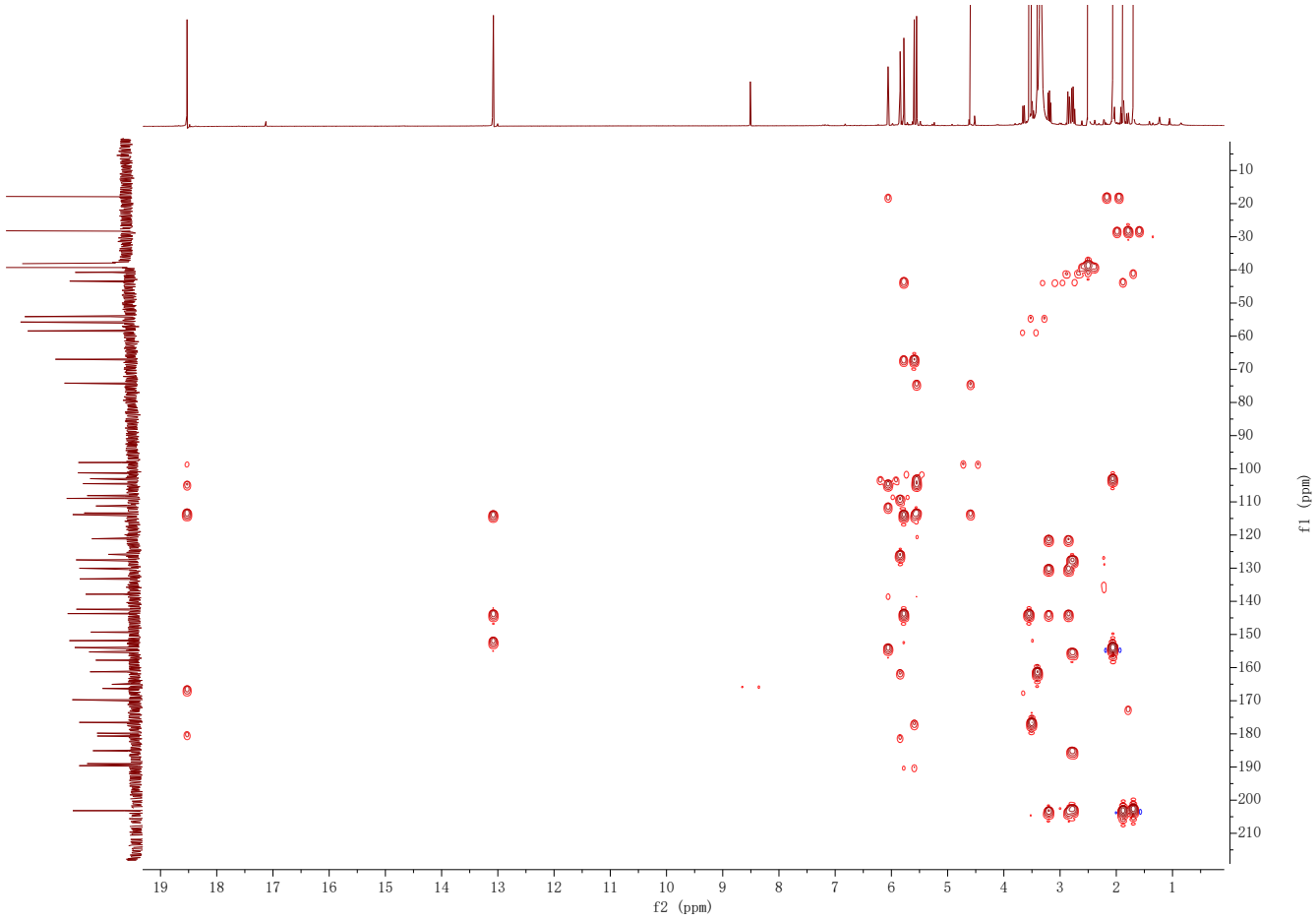

Figure S44. ^{1}H NOESY NMR spectrum (600 MHz) of 16 in DMSO-d_6

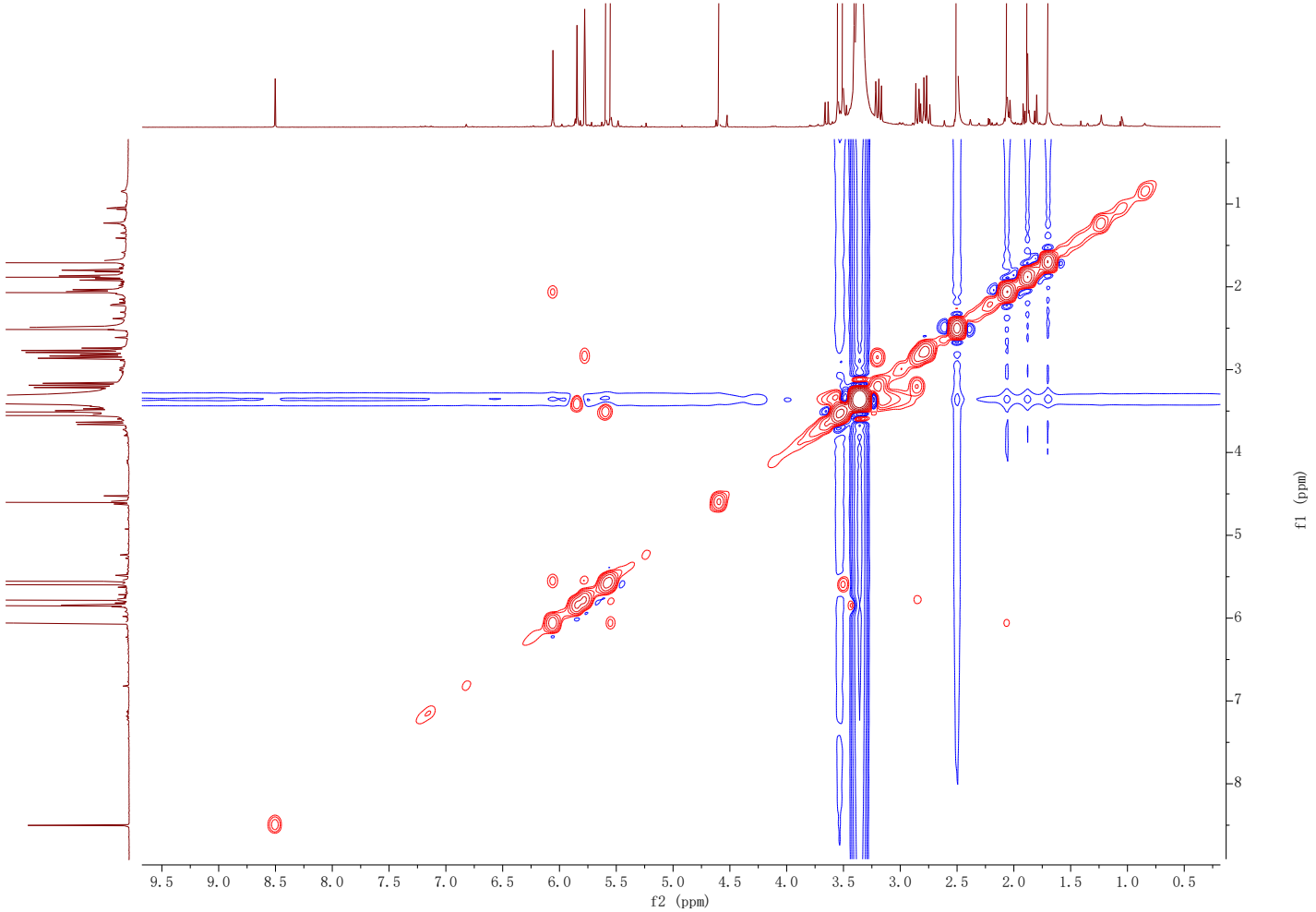

Figure S45. ^{1}H NMR spectrum (500 MHz) of 16 in D_2O

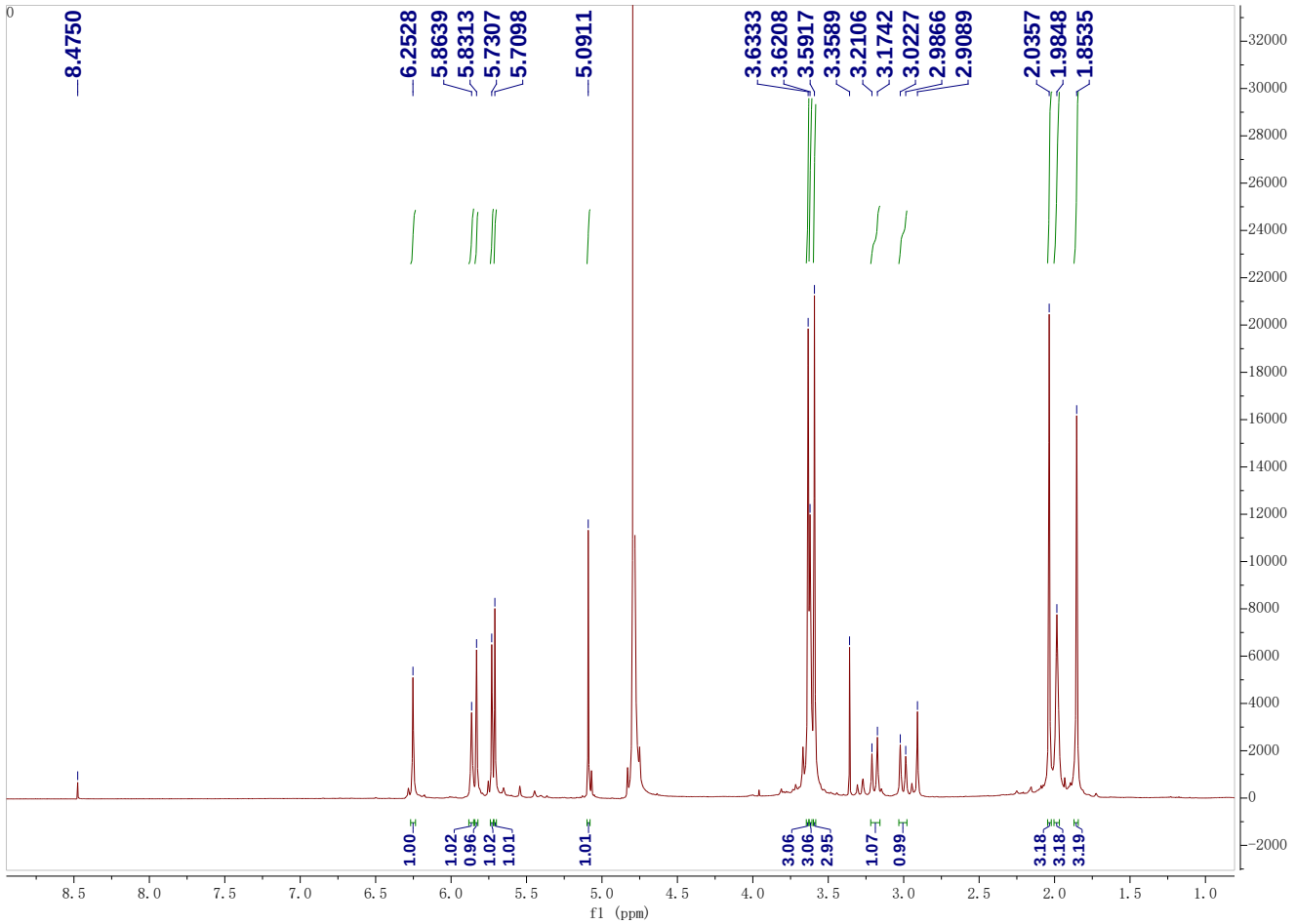

Figure S46. ^{13}C NMR spectrum (125 MHz) of 16 in D_2O

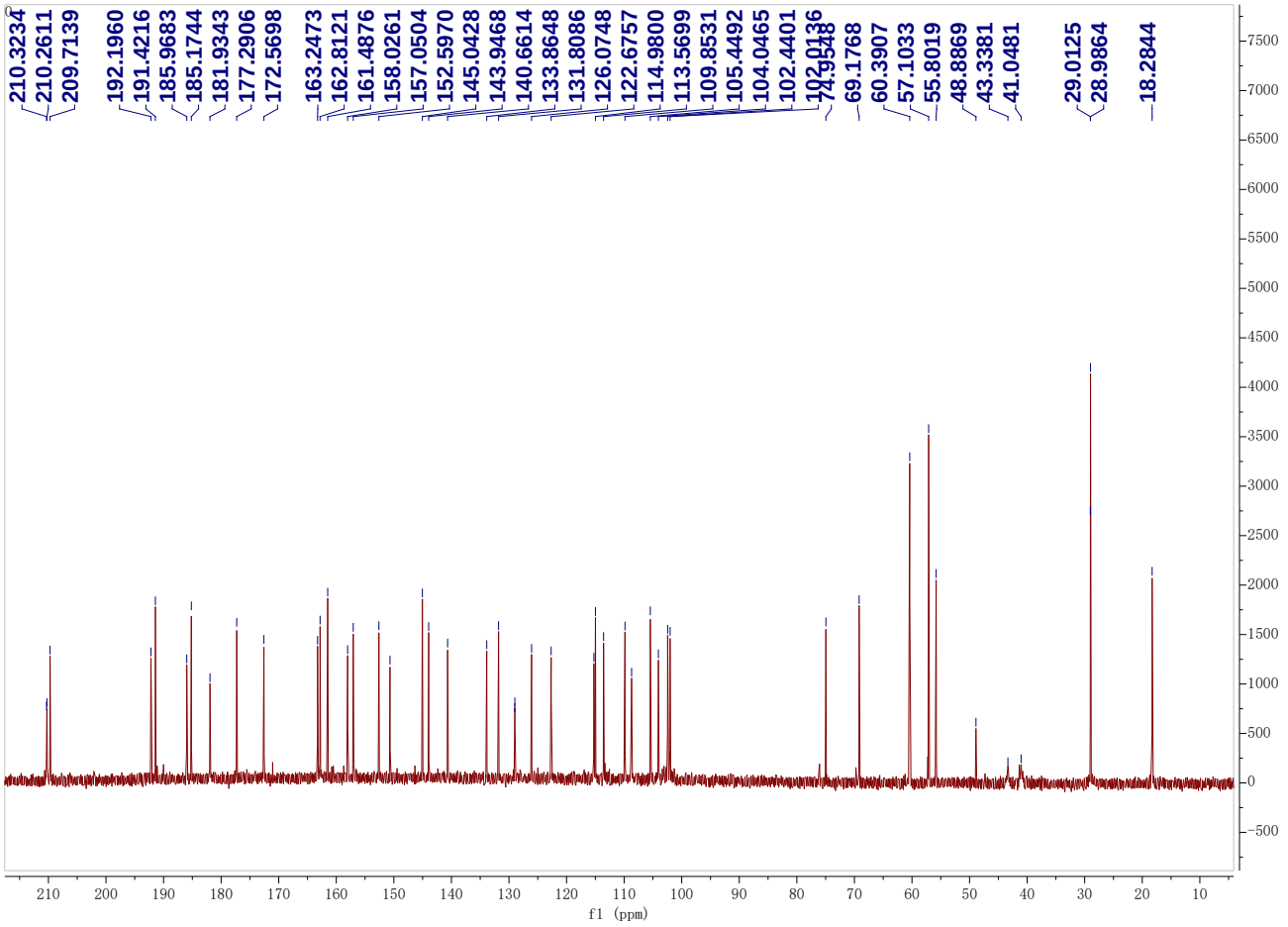

Figure S47. ^{1}H-^{1}H gCOSY NMR spectrum (500 MHz) of 16 in D_2O

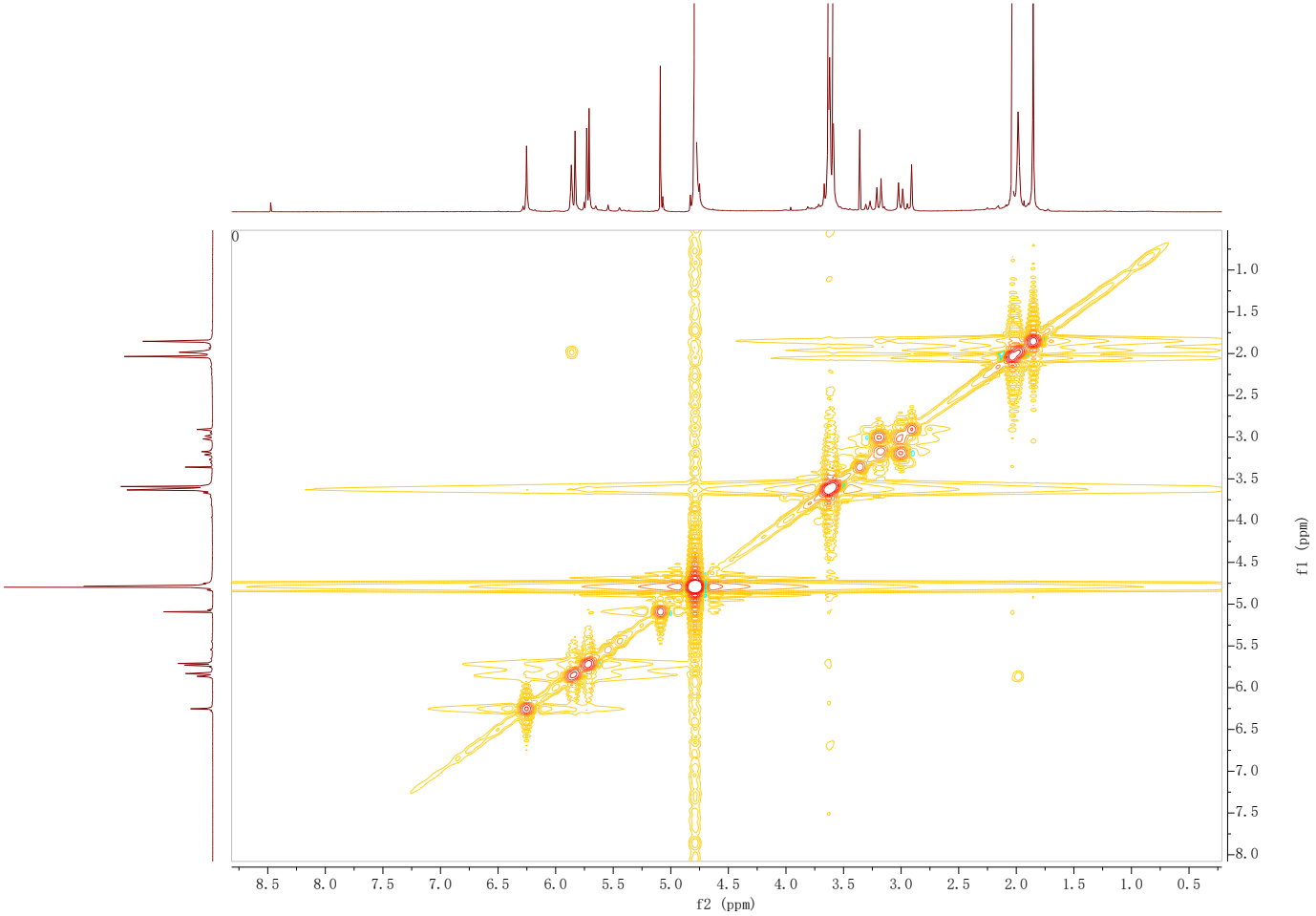

Figure S48. DEPT-135 and DEPT-90 ^{13}C NMR spectrum (125 MHz) of 16 in D_2O

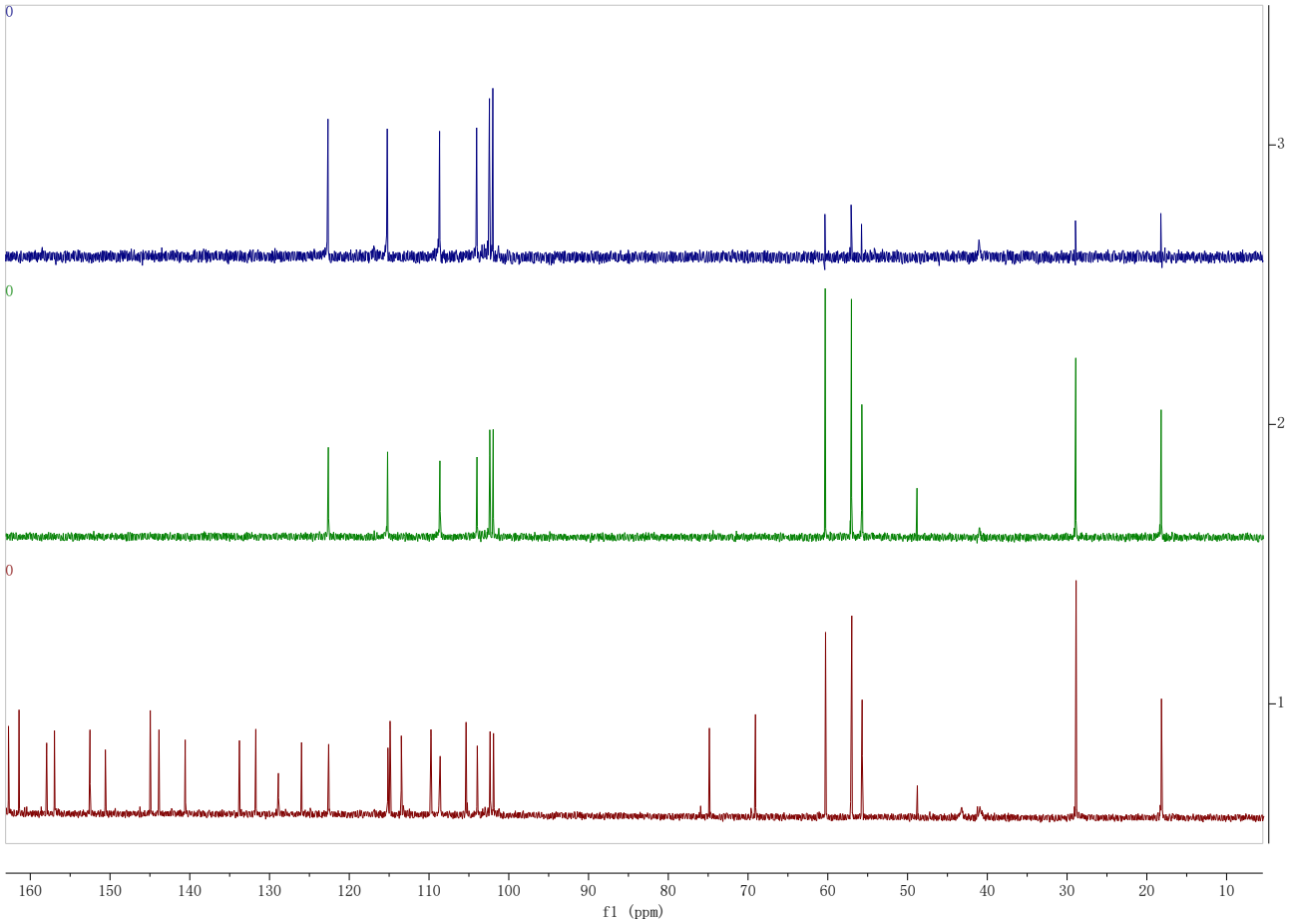

Figure S49. HSQC NMR spectrum (500 MHz) of 16 in D_2O

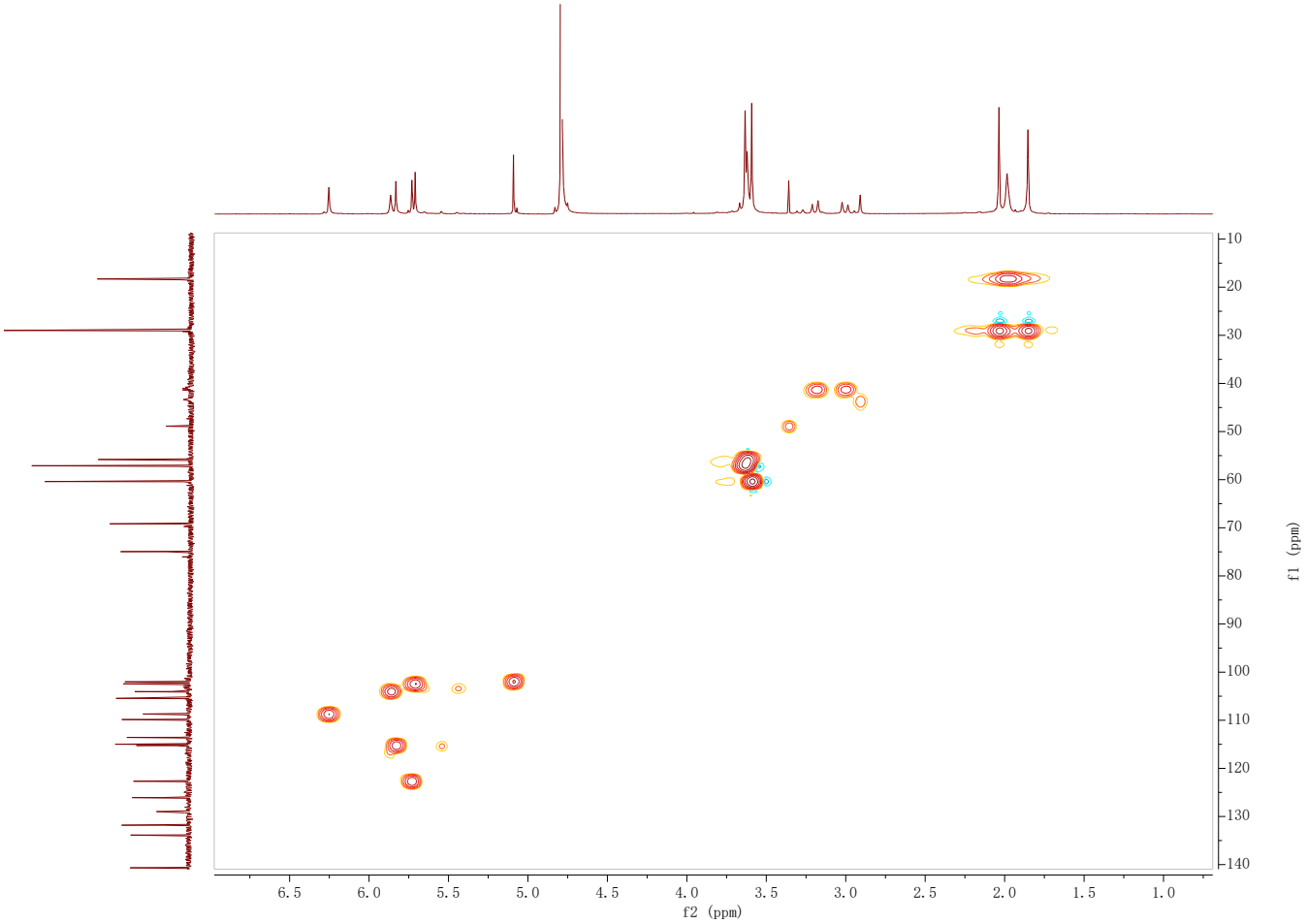

Figure S50. HMBC NMR spectrum (500 MHz) of 16 in D_2O

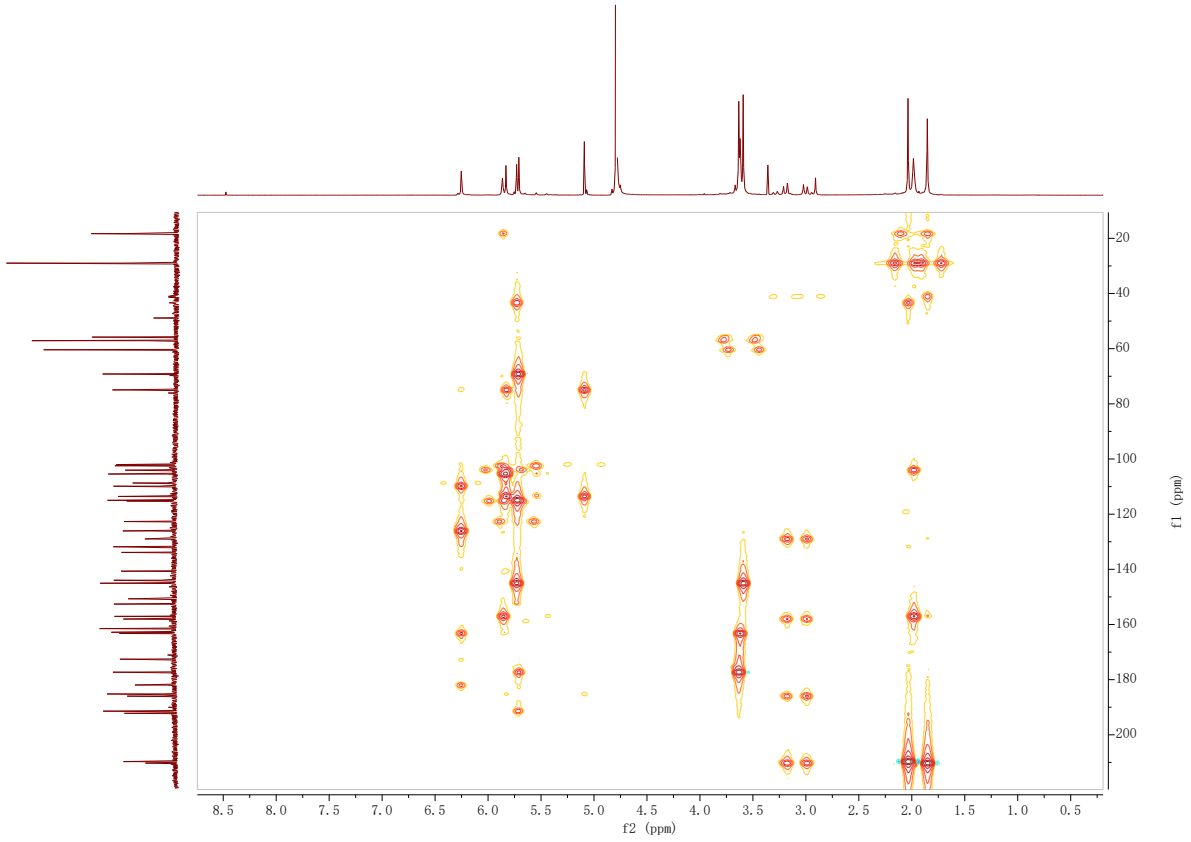

Figure S51. ^{1}H NMR spectrum (600 MHz) of 19 in $CDCl_3$-*d*

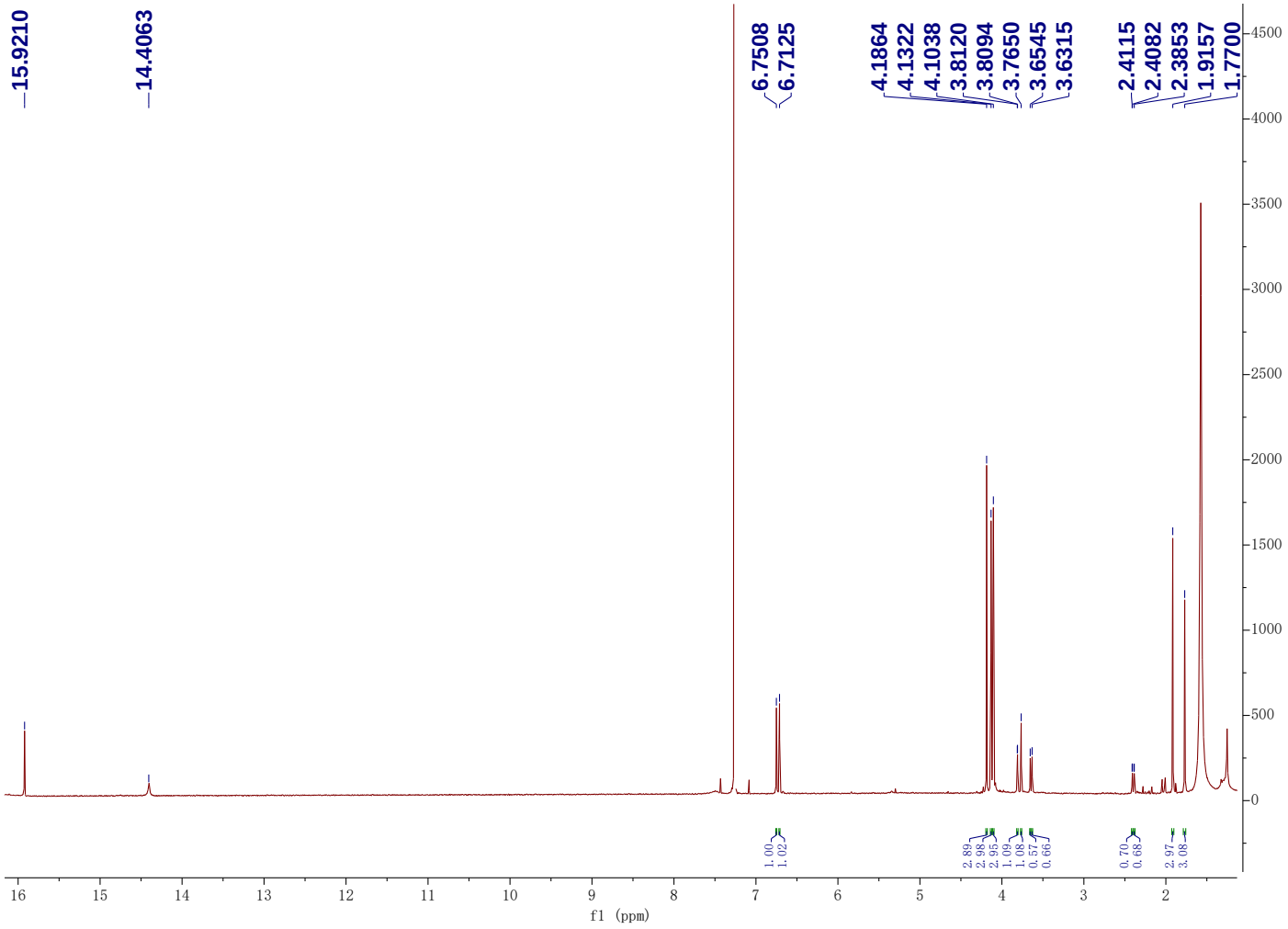

Figure S52. ^{13}C NMR spectrum (150 MHz) of 19 in $CDCl_3$-*d*

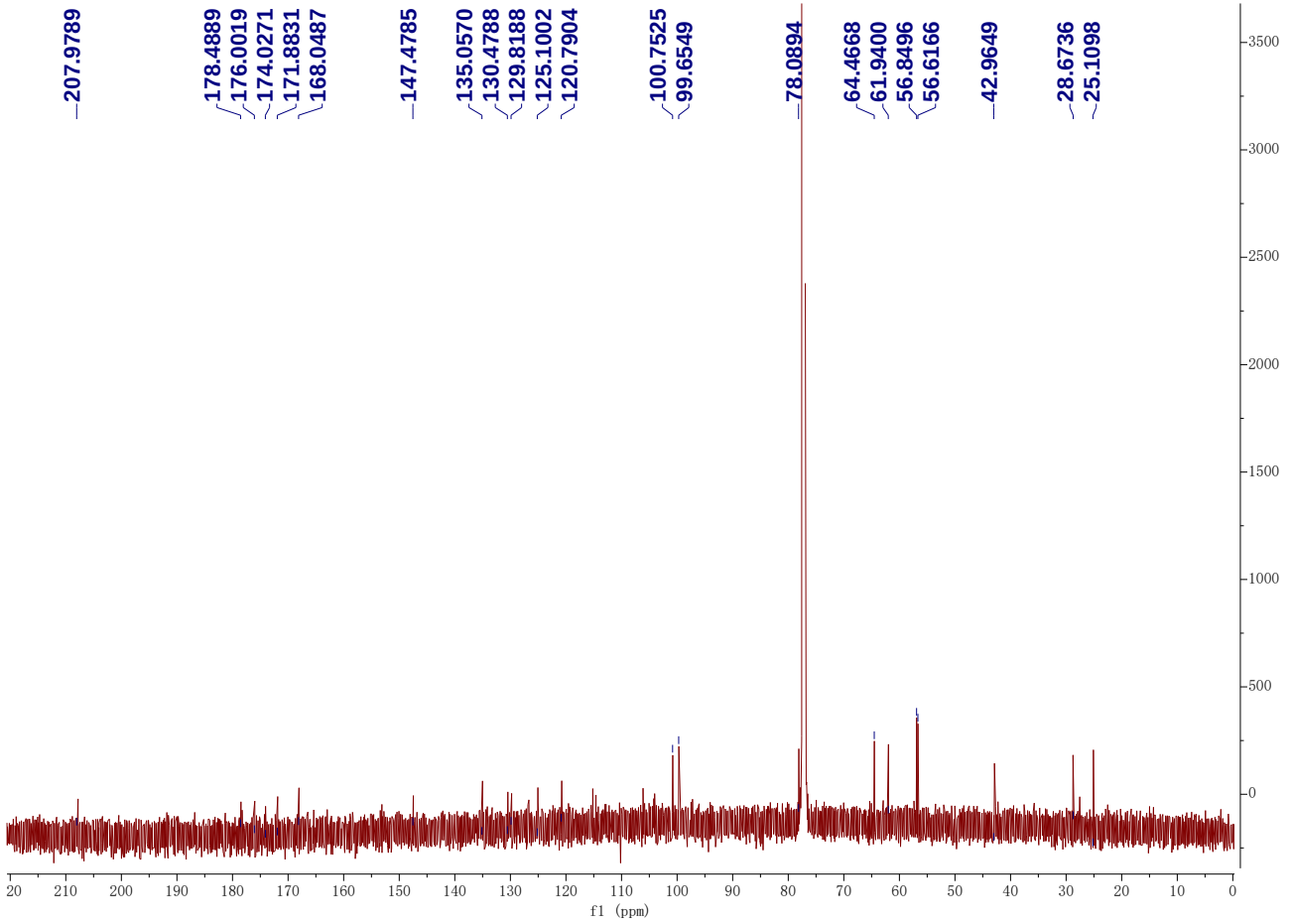

Figure S53. HSQC NMR spectrum (600 MHz) of 19 in $CDCl_3$-*d*

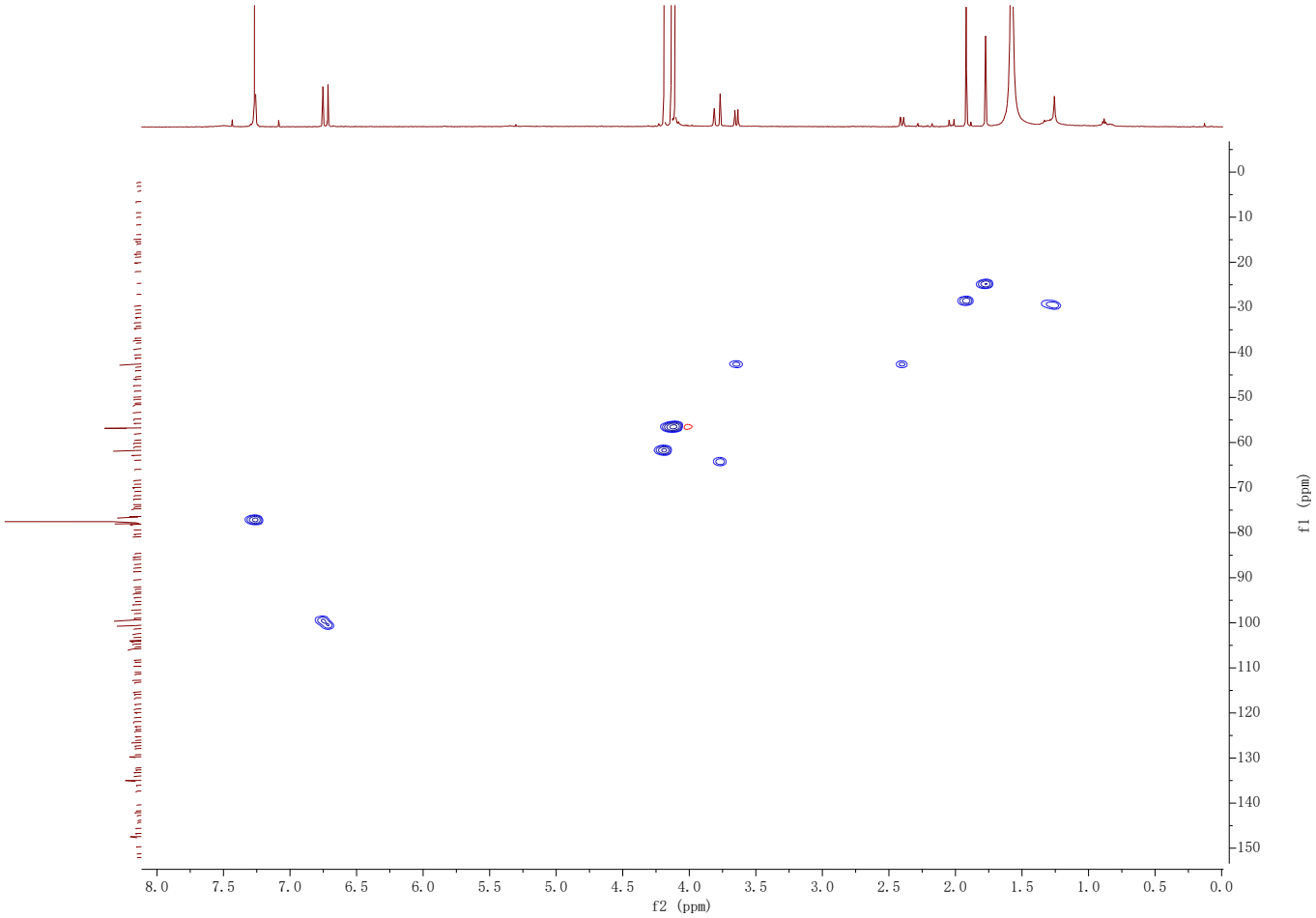

Figure S54. HMBC NMR spectrum (600 MHz) of 19 in $CDCl_3$-*d*

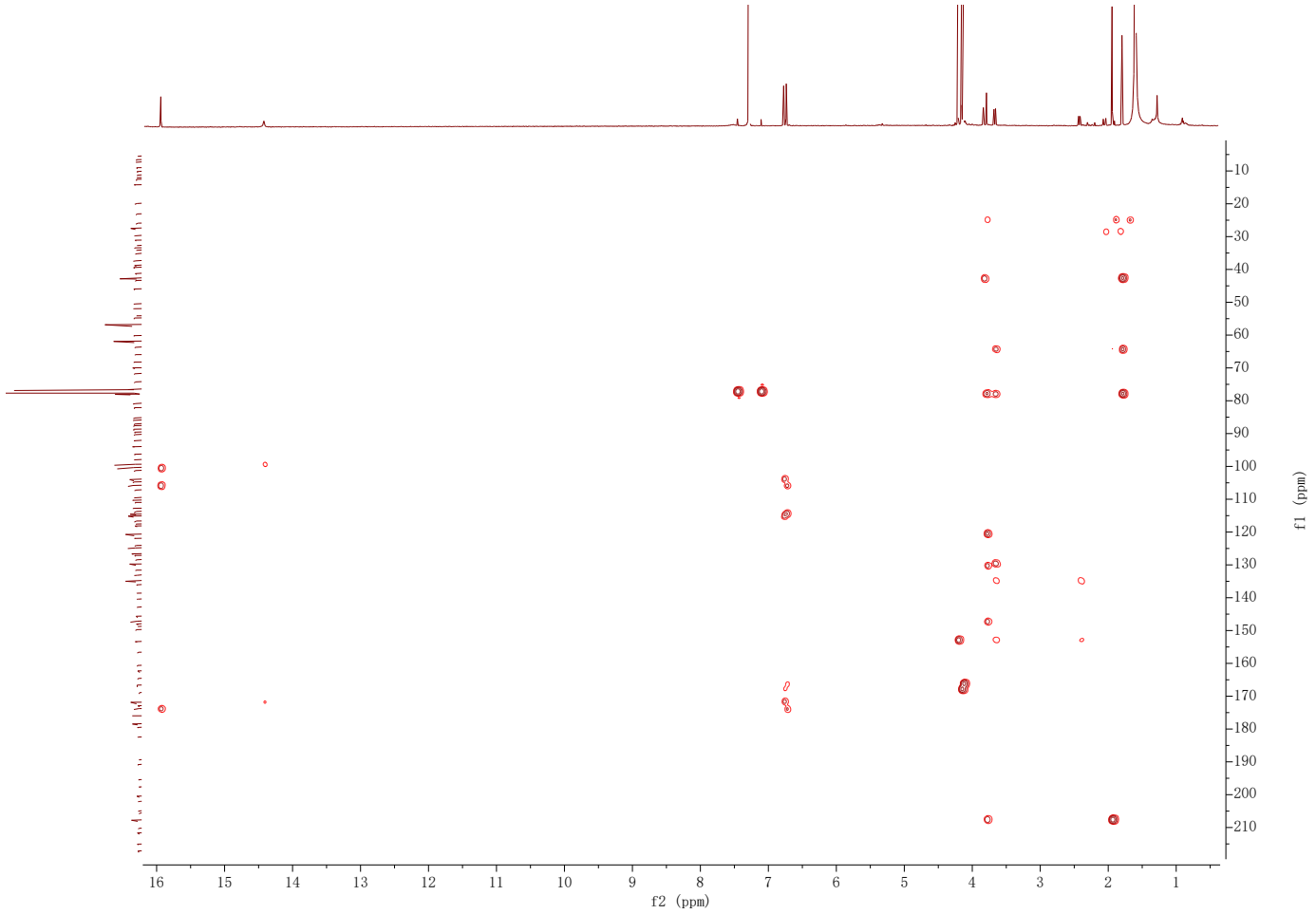

Figure S55. ^{1}H NMR spectrum (600 MHz) of 20 in $CDCl_3$-*d*

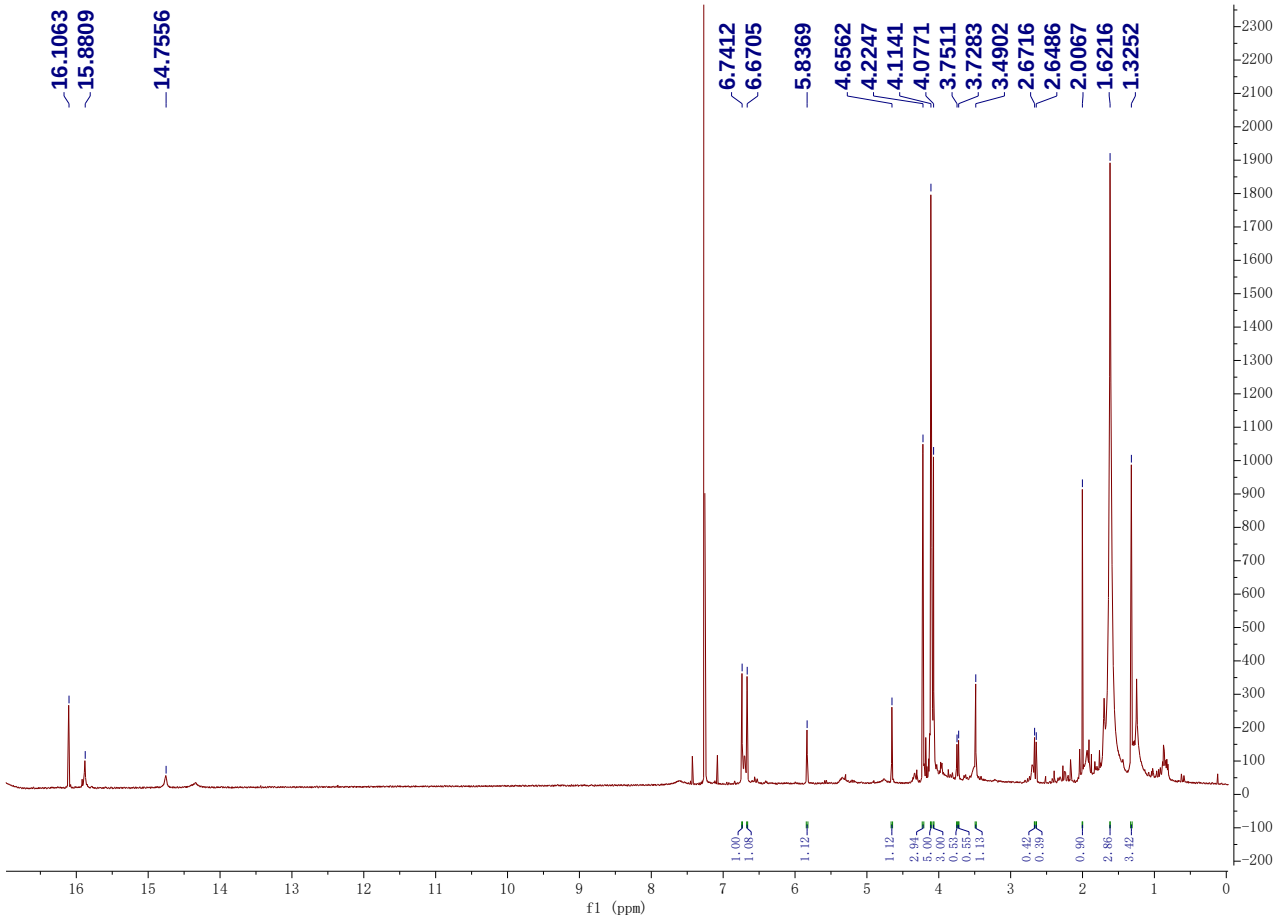

Figure S56. ^{13}C NMR spectrum (150 MHz) of 20 in $CDCl_3$-*d*

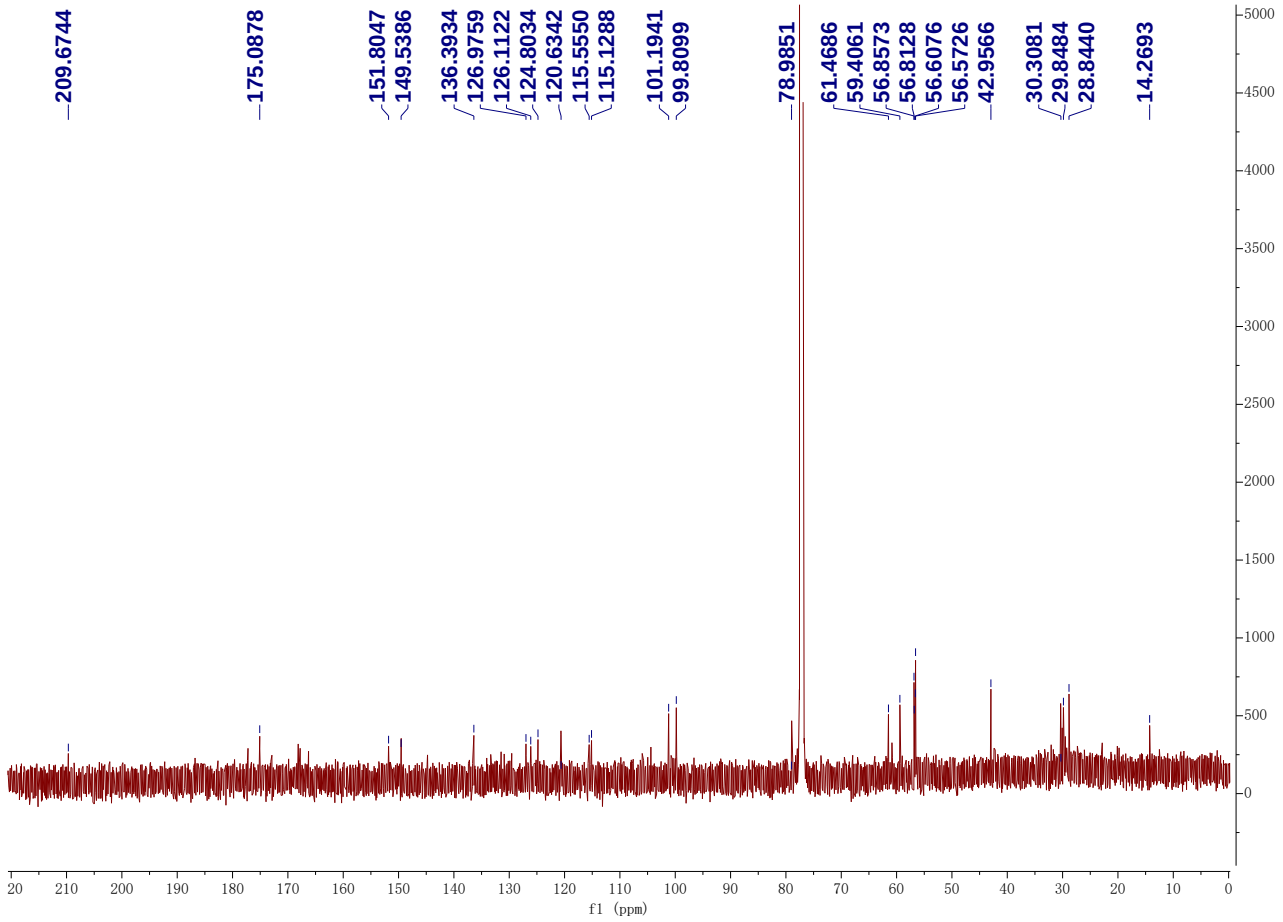

Figure S57. HSQC NMR spectrum (600 MHz) of 20 in $CDCl_3$-*d*

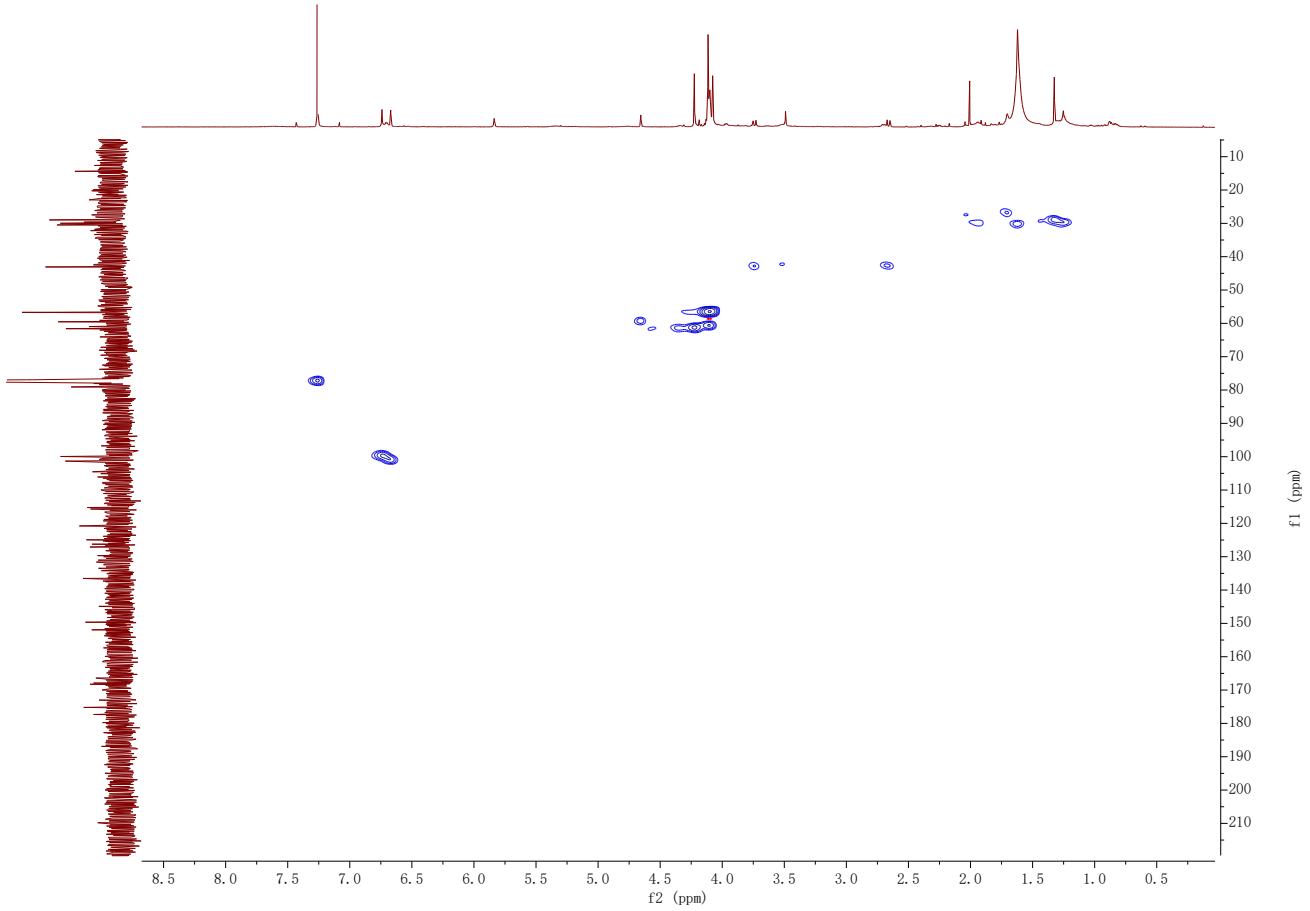

Figure S58. HMBC NMR spectrum (600 MHz) of 20 in $CDCl_3$-*d*

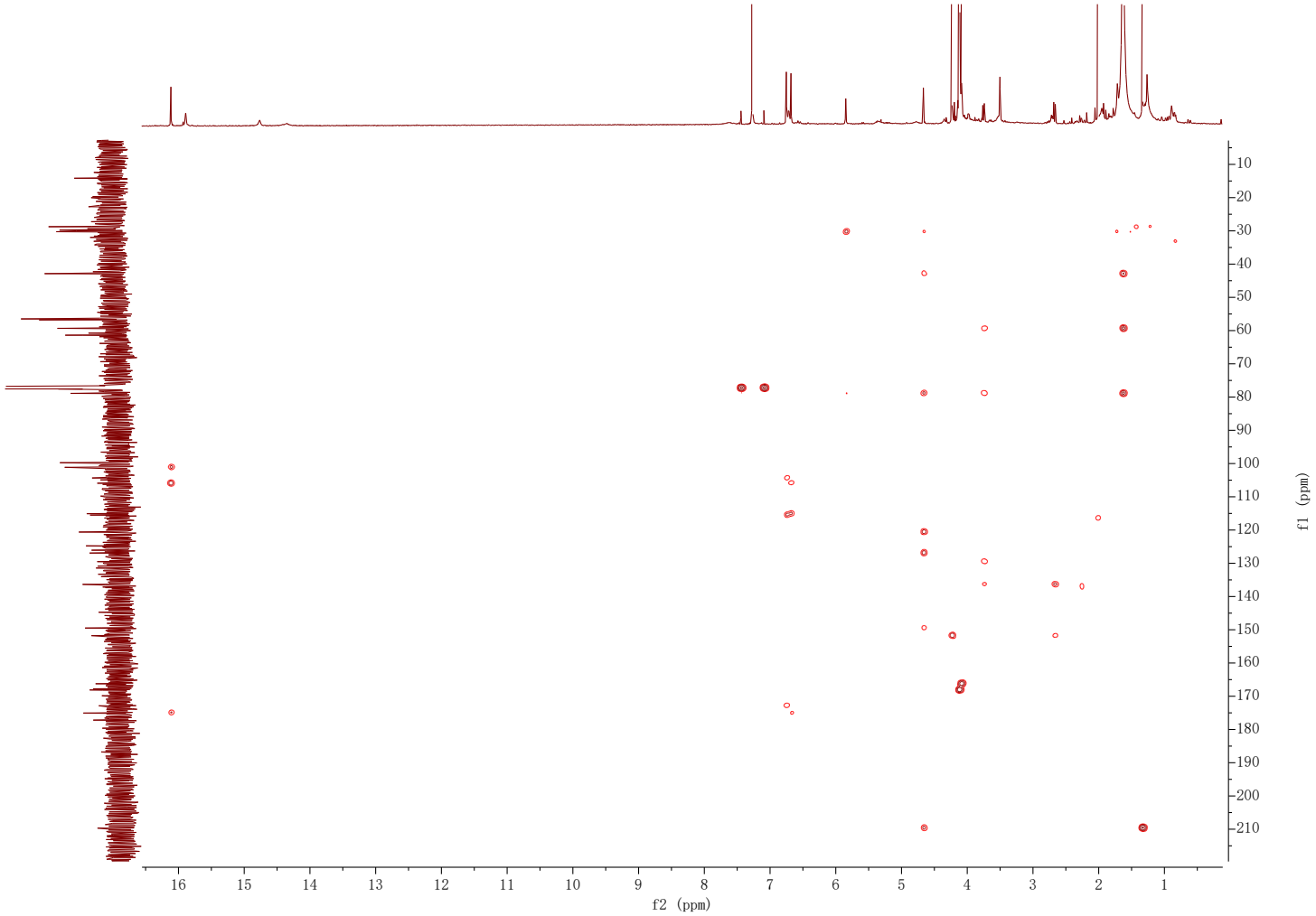

References

1. Y. M. Chiang, M. Ahuja, C. E. Oakley, R. Entwistle, A. Asokan, C. Zutz, C. C. Wang and B. R. Oakley, *Angew. Chem.*, 2016, **128**, 1694-1697.
2. Y. H. Chooi, G. Zhang, J. Hu, M. J. Muria‐Gonzalez, P. N. Tran, A. Pettitt, A. G. Maier, R. A. Barrow and P. S. Solomon, *Environ. Microbiol.*, 2017, **19**, 1975-1986.
3. F. Y. Lim, J. F. Sanchez, C. C. Wang and N. P. Keller, *Methods Enzymol.*, 2012, **517**, 303.
4. M. Kearse, R. Moir, A. Wilson, S. Stones-Havas, M. Cheung, S. Sturrock, S. Buxton, A. Cooper, S. Markowitz and C. Duran, *Bioinformatics*, 2012, **28**, 1647-1649.
5. L. A. Kelley, S. Mezulis, C. M. Yates, M. N. Wass and M. J. Sternberg, *Nat. Protoc.*, 2015, **10**, 845.
6. Y. Tsunematsu, N. Ishikawa, D. Wakana, Y. Goda, H. Noguchi, H. Moriya, K. Hotta and K. Watanabe, *Nat. Chem. Biol.*, 2013, **9**, 818.
7. Y.-H. Chooi, M. J. Muria-Gonzalez, O. L. Mead and P. S. Solomon, *Appl. Environ. Microbiol.*, 2015, **81**, 5309-5317.
8. J. E. DiCarlo, J. E. Norville, P. Mali, X. Rios, J. Aach and G. M. Church, *Nucleic Acids Res.*, 2013, **41**, 4336-4343.
9. TURBOMOLE V7.1 2016, a development of University of Karlsruhe and Forschungszentrum Karlsruhe GmbH, 1989-2007, TURBOMOLE GmbH, since 2007. Available from http://www.turbomole.com
10. C. Lee, W. Yang and R. G. Parr, *Phys. Rev. B*, 1988, **37**, 785.
11. A. D. Becke, *J. Chem. Phys.*, 1993, **98**, 5648-5652.
12. P. Stephens, *J. Phys. Chem.*, 1994, **98**, 11623.
13. M. Frisch, G. Trucks, H. B. Schlegel, G. Scuseria, M. Robb, J. Cheeseman, G. Scalmani, V. Barone, B. Mennucci and G. Petersson, *Inc., Wallingford, CT*, 2009, **200**.
14. A. D. Becke and E. R. Johnson, *J. Chem. Phys.*, 2005, **123**, 154101.
15. S. Grimme, *Wiley Interdiscip. Rev.: Comput. Mol. Sci.*, 2011, **1**, 211-228.
16. L. Goerigk and S. Grimme, *Wiley Interdiscip. Rev.: Comput. Mol. Sci.*, 2014, **4**, 576-600.
17. S. Kozuch and J. M. Martin, *J. Comput. Chem.*, 2013, **34**, 2327-2344.
18. S. Kozuch and J. M. Martin, *Phys. Chem. Chem. Phys.*, 2011, **13**, 20104-20107.
19. A. Karton, A. Tarnopolsky, J.-F. Lamére, G. C. Schatz and J. M. Martin, *J. Phys. Chem. A*, 2008, **112**, 12868-12886.
20. A. Karton, R. J. O'Reilly and L. Radom, *J. Phys. Chem. A*, 2012, **116**, 4211-4221.
21. L. Goerigk, A. Karton, J. M. Martin and L. Radom, *Phys. Chem. Chem. Phys.*, 2013, **15**, 7028-7031.
22. A. Karton and L. Goerigk, *J. Comput. Chem.*, 2015, **36**, 622-632.
23. L.-J. Yu, F. Sarrami, R. J. O'Reilly and A. Karton, *Chem. Phys.*, 2015, **458**, 1-8.
24. F. Weigend and R. Ahlrichs, *Phys. Chem. Chem. Phys.*, 2005, **7**, 3297-3305.
25. Y. Zhao, N. E. Schultz and D. G. Truhlar, *J. Chem. Theory Comput.*, 2006, **2**, 364-382.
26. A. V. Marenich, C. J. Cramer and D. G. Truhlar, *J. Phys. Chem. B*, 2009, **113**, 6378-6396.
27. J. DiCarlo, J. Norville, P. Mali, X. Rios, J. Aach and G. Church, *Nucleic Acids Res.*, 2013, **41**, 4336-4343.
28. P. B. Ouwerkerk and A. H. Meijer, in *Plant Reverse Genetics*, Springer, 2011, pp. 211-227.
29. M. W. Shen, F. Fang, S. Sandmeyer and N. A. Da Silva, *Yeast*, 2012, **29**, 495-503.
30. S. Mazzini, L. Merlini, R. Mondelli and L. Scaglioni, *J. Chem. Soc., Perkin Trans. 2*, 2001, 409-416.
31. A. R. Ferrari, H. J. Rozeboom, A. S. Vugts, M. J. Koetsier, R. Floor and M. W. Fraaije, *Mol.*, 2018, **23**, 111.
32. A. G. Newman and C. A. Townsend, *J. Am. Chem. Soc.*, 2016, **138**, 4219-4228.
33. R. J. Frandsen, C. Schütt, B. W. Lund, D. Staerk, J. Nielsen, S. Olsson and H. Giese, *J. Biol. Chem.*, 2011, **286**, 10419-10428.
34. M. Kawaguchi, T. Ohshiro, M. Toyoda, S. Ohte, J. Inokoshi, I. Fujii and H. Tomoda, *Angew. Chem.*, 2018.
35. E. M. O'Brien, B. J. Morgan, C. A. Mulrooney, P. J. Carroll and M. C. Kozlowski, *J. Org. Chem.*, 2009, **75**, 57-68.
36. G. Nasini, L. Merlini, G. D. Andreetti, G. Bocelli and P. Sgarabotto, *Tetrahedron*, 1982, **38**, 2787-2796.
37. E. M. O'Brien, B. J. Morgan and M. C. Kozlowski, *Angew. Chem.*, 2008, **120**, 6983-6986.